CHALMERS
UNIVERSITY OF TECHNOLOGY

Simulation of transient heat and mass flows in a supermarket

Master of Science Thesis

KAROL MARCINIAK

Department of Civil and Environmental Engineering
Division of Building Technology
CHALMERS UNIVERSITY OF TECHNOLOGY
Gothenburg, Sweden BOMX02-16-134

REPORT NO. BOMX02-16-134

Simulation of transient heat and mass flows in a supermarket

KAROL MARCINIAK

Department of Civil and Environmental Engineering
Division of Building Technology
CHALMERS UNIVERSITY OF TECHNOLOGY
Gothenburg, Sweden 2016

Simulation of transient heat and mass flows in a supermarket
KAROL MARCINIAK

Master thesis no. BOMX02-16-134
Department of Civil and Environmental Engineering
Chalmers University of Technology
SE-412 96 Göteborg
Sweden
Telephone +46 (0)31-772 1000

Chalmers Reproservice
Göteborg , Sweden 2016

Simulation of transient heat and mass flows in a supermarket
KAROL MARCINIAK
Department of Civil and Environmental Engineering
Division of Building Technology
Chalmers University of Technology

ABSTRACT

This thesis concerns heat and mass flows in a supermarket. In the recent years progress in refrigeration and lighting technology has occurred leading to decrease in supermarkets' energy demand. It was the reason to conduct this work, where hygrothermal flows within a modernly designed supermarket are analyzed and a transient computer model of these flows is introduced.

A real supermarket located in Hanover, Germany, was a basis for model design. Its construction and equipment features were reflected in the model based on building plans, technical documentation and internet database collecting measurements from sensors. However, these information were limited, so some additional assumptions had to be made. Hourly values of outside temperature, humidity and solar radiation (last one obtained from program Meteonorm) for the whole year 2015 were input data for the created program. Results of the simulation included temperature and humidity of two zones, which the supermarket was divided into, with the resolution higher than one hour for better accuracy. They were subject of validation with real supermarket's performance. Moreover, the program was capable of calculating values of particular heat and moisture flows. Testing under forced conditions is a way of model's verification.

The main problem with modelling supermarket's inside air regarded high level of relative humidity during warm period and therefore three methods of decreasing it are presented: controllable fresh air supply, adjustable inside temperature and mechanical dehumidification. They allowed to reduce inside humidity to the level corresponding to real conditions in the supermarket. Better convergence is obtained for simulated temperature than humidity particularly in hourly perspective.

Created model and obtained conclusions could help in the process of designing supermarkets or help to improve computer models of supermarkets.

Keywords: model, transient, hydrothermal, heat, mass, moisture, flows, supermarket

Table of contents

List of symbols:

A	area [m^2]
c	specific heat capacity [$Jkg^{-1}K^{-1}$]
C	heat capacity per area [$JK^{-1}m^{-2}$]
d	depth
E	solar irradiance [Wm^{-2}]
h	specific enthalpy [Jkg^{-1}]
H	enthalpy [J]
k	thermal conductivity [$Wm^{-2}K^{-1}$]
L	length [m]
m	mass [kg]
$\dot{m}$	mass flow [kgs^{-1}]
n_p	number of people [-]
N	number of [-]
$\dot{Q}$	heat flow [W]
R	thermal resistance [KW^{-1}]
S	height [m]
t	temperature [^oC]
T	temperature [K]
$\dot{V}$	volumetric flow [m^3s^{-1}]
x	absolute humidity of air [$kgkg^{-1}$]

Greek:

α	absorptance factor [-]
β	solar altitude [^{o}]
τ	time [s]
Σ	surface tilt angle [^{o}]
γ	surface-solar azimuth angle [^{o}]
ϕ	solar azimuth [^{o}]
ψ	surface azimuth [^{o}]
δ	thickness [m]
θ	angle of incidence [^{o}]
ρ	density [kgm^{-3}]

Subscriptions:

1	vertical doored medium-temperature refrigerated display cabinet
2	vertical doored low-temperature refrigerated display cabinet
3	horizontal doored medium-temperature refrigerated display cabinet
4	horizontal doored low-temperature refrigerated display cabinet
1person	one person
adj	adjacent zone
add_max	maximum additional fresh air
air	air in the zone
amb	ambient, outside
ASH	anti-sweat heaters
c	conduction
case	air temperature in a refrigerated display cabinet
C-lth	cooling load of a low-temperature glassed horizontal RDC
C-ltv	cooling load of a low-temperature glassed vertical RDC
C-mth	cooling load of a medium-temperature glassed horizontal RDC
C-mtv	cooling load of a medium-temperature glassed vertical RDC
cw	conduction through walls of refrigerated display cabinets
da	dry infiltration air
defrost	defrosting equipment
dehum	mechanical dehumidification
evap	evaporation
fa	fresh air
fans	fans recirculating air
floor	inside layer of the floor
H	shadow
hs-lth	heat sink in horizontal doored low-temperature refrigerated display cabinets
hs-ltv	heat sink in vertical doored low-temperature refrigerated display cabinets
hs-mth	heat sink in horizontal doored medium-temperature refrigerated display cabinets
hs-mtv	heat sink in vertical doored medium-temperature refrigerated display cabinets
HVAC	ventilation system
in	heat transfer between inside surface and inside air
inf	infiltration
int	internal gain
isurf	inside surface
isurf_sol	solar radiation incident on inside surface
LED	artificial LED lighting
light	artificial internal lighting
l-lth	latent heat load of a horizontal doored low-temperature RDC
l-ltv	latent heat load of a vertical doored low-temperature RDC
l-mth	latent heat load of a horizontal doored medium-temperature RDC
l-mtv	latent heat load of a vertical doored medium-temperature RDC
machinery	machinery room
mix	air mixing between zones

mix_i	air mixing with zone i
o	outside air
OH	overhang
osurf	outside surface
osurf_sol	solar radiation incident on outside surface
out	heat transfer between outside air and outside surface
p	periodic penetration
people	people
rad	radiation through opening
rc	refrigeration capacity
RDC	refrigerated display cabinet
rec	recirculation air
Rinf	infiltration through opening in refrigerated display cabinets
roof_in	inner layer of the roof
roof_out	outer layer of the roof
sa	supply air
s-inf	sensible part of infiltration heat load
SL	sun-lit
structure	structure (external walls, roof, floor, windows)
tc	thermal capacious elements
v	water vapour
w	water, condensate
w-lth	condensate in a horizontal doored low-temperature RDC
w-ltv	condensate in a vertical doored low-temperature RDC
w-mth	condensate in a horizontal doored medium-temperature RDC
w-mtv	condensate in a vertical doored medium-temperature RDC
wall_in	inner layer of the wall
wall_out	outer layer of the wall
win	window
win_sol	solar radiation transmitted through window
zone	considered zone
zonei	adjacent zone number i

1. Introduction

1.1. Background

Supermarkets are medium size self-service retail shops selling groceries, household products and other goods in high volumes at relatively low prices [26]. Average range of sales area of these stores is between 280 m^2 and 1400 m^2 [31]. A research carried out in Great Britain in 1360 supermarkets showed that annual electrical energy use of these shops ranges from about 500 kWh/m^2 of sales area per year to 2300 kWh/m^2. However the average electrical energy intensity drops from 1500 to 850 kWh/m^2 per year as the sales floor area increases from 280 to 1400 m^2 [31]. Reason for that is the change from food dominant sales operation to non-food dominant and a decrease in refrigeration energy demand per unit sales floor area. Moreover larger stores may provide bigger and more efficient refrigeration systems.

Reducing energy demand in supermarkets is important because of environmental concerns such as global warming due to indirect carbon dioxide equivalent emissions or refrigerant leakages. Furthermore it should provide money savings for the owner of the retail food store.

Two main factors contributing to electrical energy use within a supermarket are: refrigeration and artificial lighting (figure 1). They are followed by HVAC, external lighting, kitchen, bakery and other ancillary services in different order depending on the particular store – its sales area and applied technologies.

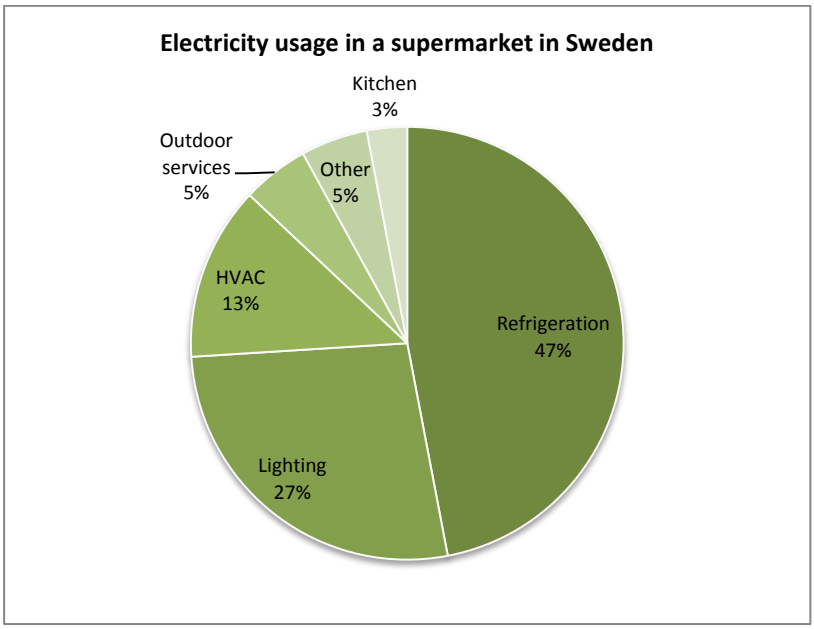

Figure 1. Electricity use sources in a supermarket in Sweden [1]

In the past few years a progress in refrigeration and lighting technology within supermarkets has occurred. Obsolete open refrigerated food cabinets are being replaced by much more efficient closed refrigerated display cabinets or retrofitted with glass doors. These improvements provide from 25% to 86% in electrical energy savings [16]. Moreover, the mass of condensate may be reduced by 88% [18] which means much lower dehumidification of supermarket's air. It helps to control inside air

conditions and reach an optimal for humans and products relative humidity between 30% and 65%. In such case an additional humidifier inside the air handling unit does not necessarily need to be installed.

Another breakthrough happens in terms of artificial lighting, because of swift development in energy-efficient LED technology [19]. Supermarkets replace incandescent and fluorescent bulbs illuminating store area [2] in order to save energy and modern generations of refrigerated display cabinets are equipped with LED lighting [19]. Longer lifetime together with lower energy demand result in money savings in case of LED lighting application. Moreover, it turns out that customers are more encouraged to buy products illuminated with LED lighting than traditional one [19].

1.2. Problem description

Large number of supermarkets in today's world and complexity of hydrothermal processes occurring inside them lead to creating numerical models of supermarkets. They help in design process and improvement of energy efficiency. The recent development in technologies applied in supermarkets has led to decrease of energy use and changed its structure. Lack of computer models describing modern supermarkets is a reason to conduct this work.

1.3. Purpose of the study

This work aims to create and verify a computer model of transient heat and moisture flows in a real supermarket, which is designed according to modern energy demand reducing trends (space heating energy demand of 15 kWh/m^2 per year for a passive house without refrigeration). It could help in the process of designing supermarkets or serve as a basis for further development of supermarket's computer models. The presented model might be in the future developed either in terms of current heat and moisture flows, e.g. through increasing number of zones, or in terms of adding electrical energy calculations, which lead to operation cost estimation.

1.4. Method and limitations

At first important energy demand components of a retail food store are determined with the degree of importance. Articles and books on topics of building energy performance, air conditioning and refrigeration are used to express physical heat and mass transfer phenomena in a mathematical way.

To create a computer model of energy flows in the supermarket its design and technical documentation, data from online system monitoring of its performance and weather data are needed. Because of transient nature of the process and for decent fidelity to reality this is going to be a multi-zone lumped model created in MatLab Simulink. The complexity of the model will be increased to a level corresponding to an acceptable error. The program calculates heat transfer and moisture flow in order to evaluate conditions of inside environment and some other parameters.

Limited information about ventilation control system and energy components parameters (e.g. heat exchangers) extorts a need for numerous assumptions and leads to considering different scenarios of system work. Some more uncertainties including e.g. unknown detailed schedule of staff work and deliveries, may lead to inaccuracies in results.

1.5. Outline of the report

Section 2 introduces the analysed supermarket. Section 3 presents components of heat and moisture balance inside a general store developing each of them to sufficient level. Section 4 presents the way

of modelling considered supermarket and presents details about computer program structure. Section 5 presents steps of developing computer program and results of the simulations. Section 6 presents a few tests carried out under imposed conditions to verify the model. Section 7 ends the report with conclusions about created computer program.

2. Description of considered supermarket

The supermarket is located in Hannover, Germany, and was built in 2012. It is a part of supermarket chain REWE. The supermarket has a certificate of a passive house and represents newest trends in building design.

Hannover is located in north-central part of Germany. It is dwelled by 523000 people with average population density of 2565 people per km^2 [22]. The city experiences a mild humid temperature climate with warm summers and no dry season [23].

The supermarket is located in the part of town called Wettbergen, in residential area as appears from author's observation. It is a free-standing facility designed only for purposes of the supermarket.

Plan of the supermarket divided into zones with respect to function is presented in figure 2.

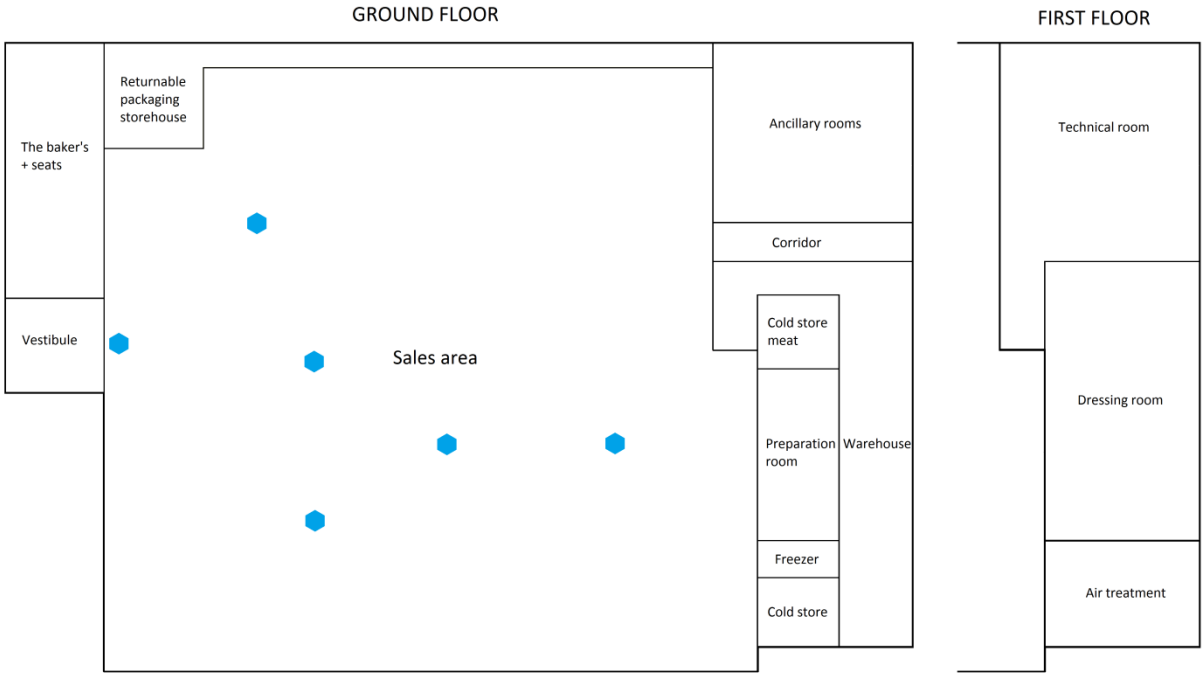

Figure 2. Plan of the supermarket with marked heat exchangers/air suppliers (blue hexagons)[30].

Areas of these zones are presented in table 1.

Zone	Sales area	Vestibule	Bakery + seats	Returnable	Ancillary	Corridor
Area [m^2]	1311,5	26	82	71	94	28,5

Zone	Warehouse	Cold store meat	Preparation	Freezer	Cold store	Technical
Area [m^2]	114,5	18,5	38,5	11	19,5	134,5

Zone	Dressing room	Air treatment
Area [m^2]	149	59

Table 1. Areas of supermarket's zones [30]

The height of sales area is about 6 metres and other zones are about 3 m high either due to presence of first floor or suspended ceiling.

Construction of building envelope is presented in table 2. The roof is corrugated and therefore its area is bigger than floor's one. Over the shopping trolleys box located outside the facility there is a top floor extension and most of the windows are situated on the entrance surface. They reach the height of about 3 metres and are shadowed by an overhang.

Element of the building	Area [m^2]	Thickness [m]	Thermal resistance [m^2K/W]
Outside wall	1212	0,395	3,58
Roof	1934	0,26	6,49
Floor	1854	0,4	3,33
Ceiling over shopping trolleys	95,5	0,2	4,74
Windows west	58,8	-	0,78
Windows roof	30,6	-	0,46

Table 2. List of elements of the envelope [30]

Table 3 describes properties of materials used to build the external partitions. This data is utilized in section 3.1. In the top there are listed materials for outside surface and going down for inside.

Element	Material	Thickness [mm]	Heat transfer coefficient [W/(mK)]	Density [kg/m^3]	Specific heat capacity [J/(kgK)]
Wall	Lathing (pine)	60	0,16	550	2510
	Thermal insulation	80	0,04	100	750
	Aerated concrete	240	0,21	600	840
	Plaster	15	0,21	1000	840
Floor	Thermal insulation	120	0,04	100	750
	Reinforced concrete	180	2,1	2500	840
	Screed	80	1,4	1900	840
	Tiles	20	1	2000	920
Roof	Tar paper	4	0,18	1000	1460
	Insulation board	260	0,04	100	750
	Metal trapezium sheet	1,5	50	7800	450

Table 3. External walls' materials and their properties [30] [29].

Thermal resistances between air and inner surface of partitions are presented in table 4. They are utilized for calculations of heat gains from the structure. Thermal resistance between outer surfaces and ambient air is assumed to depend neither on the speed and direction of wind nor on the temperature. It is equal to a standard value $R_{out} = 0{,}04\ \frac{m^2K}{W}$.

Element	Wall	Floor	Roof
$R_{in}\ \left[\frac{m^2K}{W}\right]$	0,13	0,17	0,1

Table 4. Thermal resistances between air and inner surfaces of the building envelope [30]

The HVAC system applied in the supermarket is a constant air volume (CAV) system. The fresh air, which amount can be adjusted thanks to dampers, after heat recovery in a rotating heat recovery unit is mixed with the recirculating air, heated or cooled and then supplied to the supermarket. That air is distributed to three air blowers. Because air conditioning in the supermarket occurs only

through ventilation, another three fan coils are installed in the supermarket. One is an air curtain at the main entrance and other two are spread in the sales area (all six air suppliers are shown in fig. 2 above). Moreover, the ventilation system comprises decentralized extraction fans for purposes of kitchen (bakery), returnable packaging storehouse, warehouse and technical room. The fans extract air directly outside in order to avoid contamination within rotary heat exchanger or to cool the space as it happens in the technical (machinery) room.

The refrigeration system applied to the supermarket is a compressor-based direct system. It consist of refrigeration system for display cabinets, cold rooms and air conditioning and a heat pump, used during seasons of increased heating need. The refrigeration system comprises medium temperature cycle, evaporation temperature -4 ^{o}C, working with R134a and one low-temperature cycle (evaporation at -30 ^{o}C) working with R744. The heat pump works with R134a.

3. Energy performance of the supermarket

Creating a computer model of a real system is a multi-step and complex process. It requires observation and measurements of the real system in order to choose important phenomena and determine their physical model. The number of parameters describing heat and moisture flow processes in buildings with varying material structure of the partitions and different equipment is so large, that it forces utilization of multiple simplifications. Among them are:

- Constant surface thermal resistances
- Uniform temperature and humidity of air in a zone
- Diffusion of moisture in partition walls is skipped (i.e. vapor tight walls are assumed)
- One dimensional heat transfer in external walls, roof and floor is assumed.

Figure 3 presents components of energy balance of the supermarket and relations between them. Because subject of this work concerns heat and moisture flows, a boundary excluding electrical energy is set. Moreover refrigeration system (meaning roof top unit and processes occurring there apart from exchanging heat with interior of the supermarket) is out of concern too.

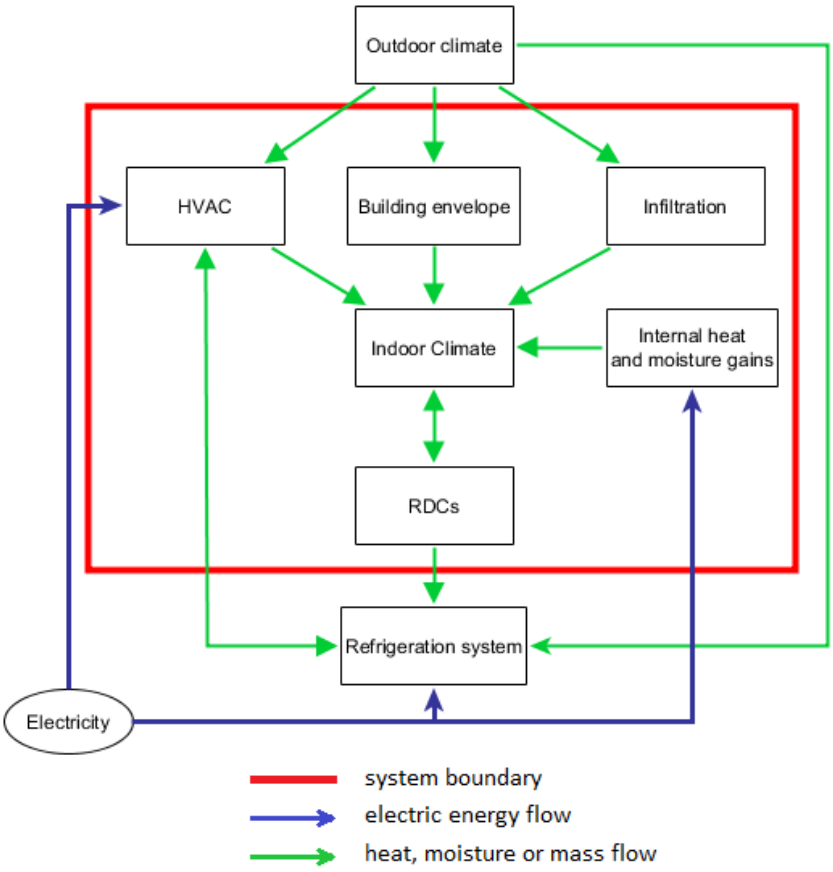

Figure 3. Energy flows between components of the supermarket with marked boundary defining field of interest.

Analysis of heat and moisture flows in a retail store conducted by Dong et al. [15] is a basis for model's development. It is however modified so that total enthalpy of air, and not just sensible part of it, is considered in order to eliminate some uncertainties, for instance human heat rejection is

difficult to express in sensible heat. Moreover total enthalpy better reflects close relation between temperature and humidity ratio as presented in equation (A5) in the appendix. Each component is then described in a way based on standards [29] [6], other researchers works [18] [12] or author's reasoning.

Air heat balance is reduced to "lumps" representing zones of the supermarket i.e. spaces of similar temperatures and energy use profiles, characterized by their structure, installed equipment or function. The assumption is that air is well mixed and each lump represents uniform conditions – one temperature and one humidity node. These parameters lack spatial variation and change only with time. Basing on that, the heat balance of one zone's air including heat transferred with interior walls as well as through windows and heat fluxes due to HVAC, infiltration, mixing of air between zones due to infiltration, people's presence, refrigerated display cabinets, artificial lighting and thermal capacity is introduced:

$$m_{air}\frac{dh_{zone}}{d\tau} = \dot{Q}_{structure} + \dot{Q}_{HVAC} + \dot{Q}_{inf} + \dot{Q}_{mix} + \dot{Q}_{people} + \dot{Q}_{RDC} + \dot{Q}_{LED} + \dot{Q}_{tc} \quad (1)$$

The mass balance of vapour in the air includes water vapour transfer through infiltration and ventilation, air mixing between zones, humidity removed by refrigerated display cabinets and humidity generated by people and equipment.

$$m_{air}\frac{dx_{zone}}{d\tau} = \dot{m}_{inf}(x_{amb} - x_{zone}) + \sum_{i}^{N_{adj}} \dot{m}_{mix\_i}(x_{zonei} - x_{zone}) + \dot{m}_{RDC} + \dot{m}_{people} \quad (2)$$

Then knowing h_{zone} and x_{zone} the calculation of temperature in the zone (t_{zone}) is possible (converting eq. (A5) from appendix).

Heat and moisture balances of air are the core of this model, however they must be supplemented with heat balance over the building's envelope. Due to transient nature of considered processes, heat capacities must be taken into account. Heat balance equations for the outside and inside layers of walls are given by:

$$C\frac{dT_{osurf}}{d\tau} = \frac{T_{amb}-T_{osurf}}{R_{out}} + \frac{T_{isurf}-T_{osurf}}{R_{wall}} + \dot{Q}_{osurf\_sol} \quad (3)$$

$$C\frac{dT_{isurf}}{d\tau} = \frac{T_{zone}-T_{isurf}}{R_{in}} + \frac{T_{osurf}-T_{isurf}}{R_{wall}} + \dot{Q}_{isurf\_sol} \quad (4)$$

3.1. Heat transfer through building envelope

Transmission heat transfer occurs through outside walls, roof, windows and floor. Because of the fact that floor and walls are insulated from outside and built with heat capacious materials from inside, their ability to accumulate heat must be considered. Roof's ability to accumulate heat is lower but must be taken into account in order to calculate properly its heat load influenced to a large extent by solar radiation. Windows represent a complex process combining heat conduction, solar radiation transmission and absorbency. Figure 4 shows a general reduced order model of thermal network for one piece of external wall.

Equations (3) and (4) allow to calculate temperature of the inside surface of the envelope. Then the heat is transferred through convection to the air in the supermarket. The total heat load from the building structure is given by:

$$\dot{Q}_{structure} = \frac{T_{isurf} - T_{zone}}{R_{in}} + \frac{T_{amb} - T_{zone}}{R_{win}} + \dot{Q}_{win\_sol} \quad (5)$$

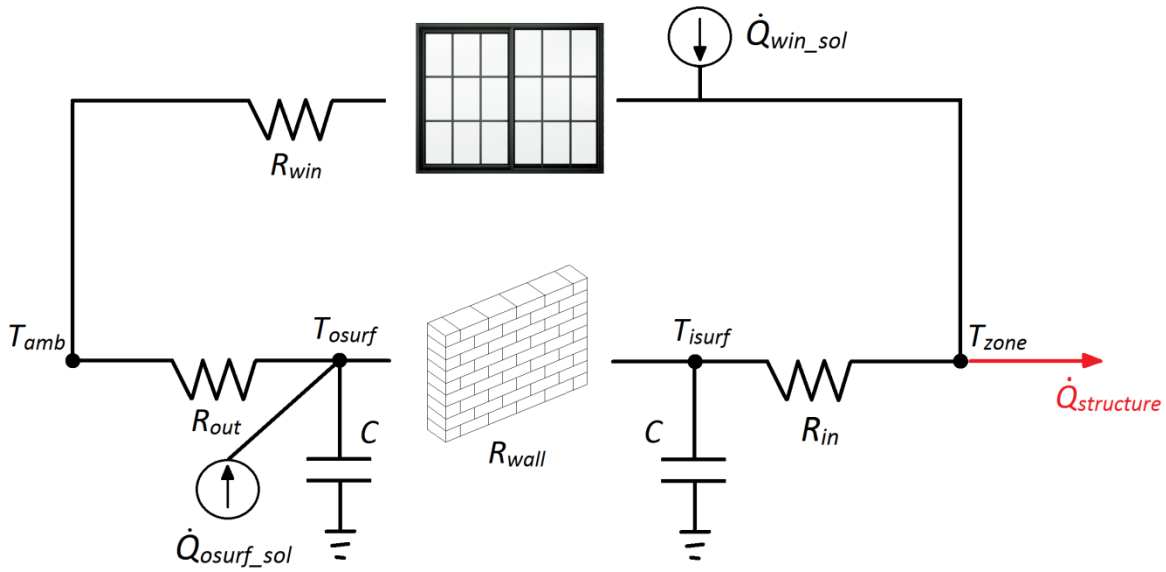

Figure 4. External wall thermal network model.

3.1.1. External walls heat balance

External walls of a zone are divided with regard to their cardinal direction. This is because of solar radiation influence. For instance the eastern wall will be more heated through radiation than the northern wall. A shaded wall lacks solar radiation heat gain component.

Estimation of heat capacity is done based on the periodic penetration depth (d_p) for diurnal (t_p=24 h) temperature variations. Penetration depth is calculated from the equation [20]:

$$d_p = \sqrt{\frac{a\tau_p}{\pi}} \quad (6)$$

where *a* is thermal diffusivity [m^2/s].

Heat capacity per m^2 of wall's inner or outer layer is calculated according to equation:

$$C = c\rho d_p \quad (7)$$

The inside layer of the wall is built from aerated concrete whose a=4,16*10^{-7} m^2/s. Its periodic penetration depth d_p=10,7 cm. Then the heat capacity per m^2 of the wall inner layer equals to:

$$C_{wall\_in} = 55440 \frac{J}{m^2 K}$$

Thermal diffusivity of pine lathing equals 1,159*10^{-7} m^2/s and its penetration depth is 5,65 cm. The heat capacity per m^2 of the outside surface of the wall is:

$$C_{wall\_out} = 48000 \frac{J}{m^2 K}$$

The absorptance factor for the radiation incident on the outside surface and normal to it is estimated at $\alpha = 0{,}75$ – it is the same value as determined for wood [27]. Then the solar heat gain on the considered surface is given by:

$$\dot{Q}_{osurf\_sol} = \alpha A E_t \; [W] \tag{8}$$

Where A is the area of considered surface and E_t is the total solar irradiance on considered surface described in a detailed way in chapter 3.1.5.

Knowing above, relations (3) and (4) are applied in order to determine temperatures of inside wall surfaces which in turn influence inside air according to eq. (5).

3.1.2. Roof heat balance

The roof's heat balance is influenced to a great extent by solar radiation. The roof is built from "strips" each tilted 7° to the horizontal surface in the east-west direction, however it is assumed to be fully horizontal because of its low inclination degree and simplification of solar radiation calculations (figure 5).

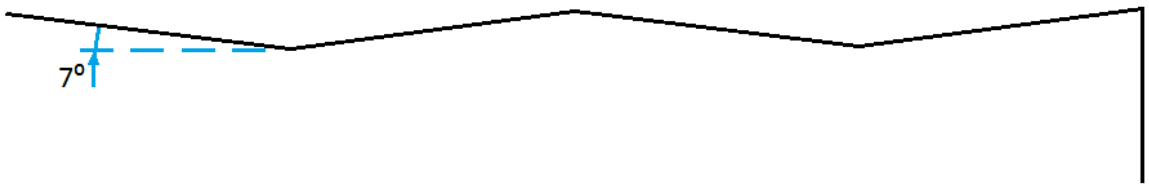

Figure 5. Side view of a part of supermarket's roof. In the model roof is assumed to be horizontal.

The roof consists of a thick layer of insulation accompanied by thin steel sheet, which holds the roof from inside, and tar paper, which serves as mechanical and hydro-insulation from outside. The roof is fixed on wooden beams.

Heat capacity of the inside surface is calculated for the steel sheet layer and equals to:

$$C_{roof\_in} = 5265 \frac{J}{m^2 K}$$

And outside heat capacious surface is assumed to be the tar paper layer:

$$C_{roof\_out} = 5840 \frac{J}{m^2 K}$$

These two heat capacities are one order smaller than heat capacity of walls and therefore their influence on heat transfer is negligible.

The absorptance factor for the radiation incident on the outside surface and normal to it is estimated at 0,975 – it is the same value as determined for black paint [27].

3.1.3. Floor heat balance

The procedure for calculating floor heat balance is adapted from [13]. It is based on a standardized method, however simplified by author of that work.

The floor area is divided into two areas: first one is the 1 metre wide edge of the floor, second one is the rest. Ground temperature for the first area is assumed the same as outdoor temperature, while temperature for the second area is constant and equal to 9,9 ^{o}C, which is the average temperature of the ground for Hannover region [30].

The thermal network model of the floor (figure 6) is different from the one introduced for external walls and roof, because it does not consider heat capacity of external surface. The heat capacity of a 15,5 cm deep top inside layer taking part in heat accumulation (according to eq. 6) amounts to:

$$C_{floor} = 247380 \frac{J}{m^2 K}$$

It is expressed in Joules per Kelvin per square metre of floor area.

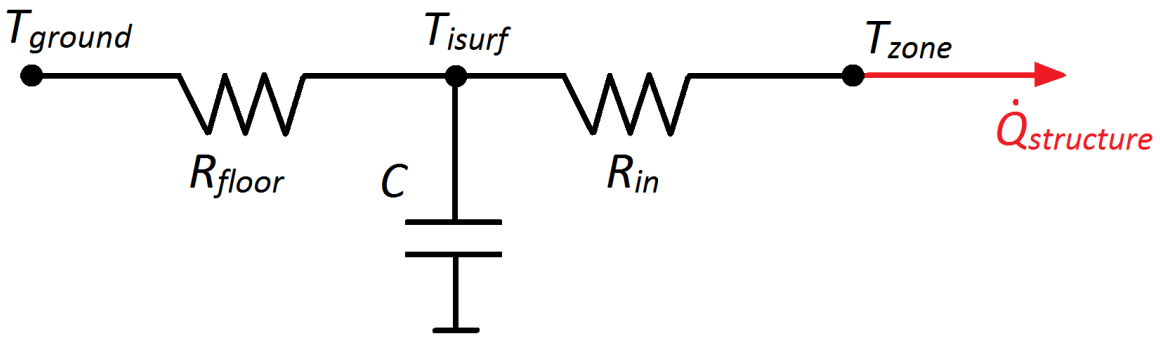

Figure 6. Supermarket's floor thermal network model.

3.1.4. Solar radiation

Solar radiation provides heat gains for walls, roof, windows and directly interior of the supermarket (radiation transmitted through glazing). In this section general information about method adapted for solar radiation calculations is presented.

Solar radiation reaching horizontal surface of earth has two components: beam (direct) and diffuse. The first one describes a part of solar radiation emanating in a straight line from the sun disc. Diffuse radiation comes from different directions [14]. Solar radiation reaching a non-horizontal surface, must be increased by the ground-reflected irradiance component [3].

The value of solar radiation heat gain at a specific time of the day depends on the angle Σ between the considered surface and the horizontal plane, direction of the world this surface is facing called surface azimuth ψ, its absorptance α, solar altitude β and solar azimuth ϕ (figure 7).

The data about solar radiation was generated by program Meteonorm and it provides averaged hourly values of global horizontal radiation and diffuse horizontal irradiance together with solar azimuth and altitude for Hannover for the whole year. Diffuse horizontal irradiance deducted from global horizontal irradiance gives direct normal irradiance. The averaging over a few years results in some differences in comparison to the specific year 2015 considered in the simulation, however it should give better accuracy than monthly averaged values, which were an alternative. An excerpt from the data generated by Meteonorm is presented in table 5.

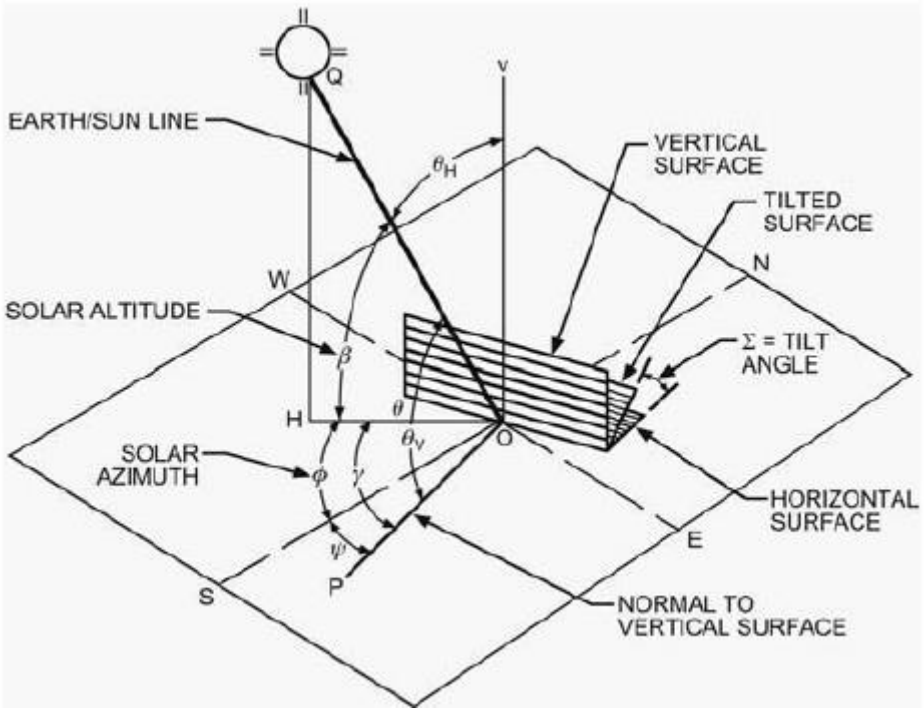

Figure 7. Surface and solar angles (source: [3])

Month	Day month	Hour	Solar azimuth [°]	Solar altitude [°]	GHI [W/m^2]	DHI [W/m^2]
8	6	12	-22,6	52,9	565	338
8	6	13	1,1	54,6	721	278
8	6	14	25,2	52,5	634	326
8	6	15	46	47,1	651	222

Table 5. An excerpt from Meteonorm data for Hannover. GHI – Global Horizontal Irradiance; DHI – Diffuse Horizontal Irradiance.

In order to estimate solar irradiance on an arbitrary oriented surface the surface-solar azimuth angle γ is introduced. Its value ranges from -180° to 180° and values less than -90° and greater than 90° mean that the surface is in shade:

$$\gamma = \phi - \psi \ [°] \tag{9}$$

The angle of incidence θ influences the amount of direct beam solar radiation reaching the surface. It also affects ability of the surface to absorb and transmit solar radiation. In the created model, surfaces exposed to solar radiation are either horizontal (roof) or vertical (external walls, windows). For horizontal surfaces (Σ=0°) the angle of incidence is given by [3]

$$\cos\theta = 90 - \beta \ [°] \tag{10}$$

whereas for vertical surfaces (Σ=90°) its value is given by [3]

$$\cos\theta = \cos\beta \cos\gamma \ [°] \tag{11}$$

The total solar radiation incident on a surface is then described by the sum:

$$E_t = E_{t,b} + E_{t,d} + E_{t,r} \tag{12}$$

where: E_t – total clear-sky irradiance reaching the surface $\left[\frac{W}{m^2}\right]$,
$E_{t,b}$ – direct beam irradiance $\left[\frac{W}{m^2}\right]$,
$E_{t,d}$ – diffuse irradiance $\left[\frac{W}{m^2}\right]$,
$E_{t,r}$ – ground-reflected irradiance $\left[\frac{W}{m^2}\right]$.

The beam component is given by [3]:

$$E_{t,b} = E_b \cos\theta \tag{13}$$

where E_b is the direct (beam) normal irradiance obtained from Meteonorm. $E_{t,b}$ cannot be negative, therefore it equals 0 for $\cos\theta < 0$.

Nature of diffuse radiation is quite complex. It comprises radiation emanating evenly from the sky dome, circumsolar disc radiation and horizon radiation [14]. To estimate the value of diffuse component incident on a vertical surface, a relationship suggested by ASHRAE [3] is used:

$$E_{t,d} = E_d Y \tag{14}$$

where E_d is the diffuse horizontal irradiance obtained from Meteonorm and

$$Y = \max(0{,}45;\ 0{,}55 + 0{,}437\cos\theta + 0{,}313\cos^2\theta) \tag{15}$$

Ground-reflected irradiance originates from the ground in front of the considered surface. It is given by [3]:

$$E_{t,r} = (E_b \sin\beta + E_d)\rho_g \frac{1-\cos\Sigma}{2} \tag{16}$$

where ρ_g is ground reflectance. Its value is 0,2 for concrete sett of the car park present in front of the western façade and 0,2 for grass adjacent to northern and eastern walls of the supermarket.

3.1.5. Heat balance for windows

From energy balancing point of view, windows are quite complex systems. They combine heat conduction, solar radiation absorptance and transmission.

Heat conduction is not uniform over the surface of a window. There might be distinguished central transparent part of the glazing, transparent edge of glass and opaque frame [4]. The central part of the glazing is most predictable and can be modelled as one-dimensional. The frame is characterised by worse insulation capacity. The edge-of-glass area is a zone of significant influence between frame and glazing. It includes area up to 0,063 m from the frame, regardless of the window size [14]. Heat flow in the edge-of-glass should be considered two-dimensional.

This complicated heat conduction process through windows is, however, simplified in this work by using uniform and constant heat transfer coefficient for the window area provided by the window producer. Thermal resistances of installed windows were presented in table 2. Conductive heat gain through windows is given by:

$$\dot{Q}_c = A_{win} \frac{T_{amb} - T_{in}}{R_{win}} [W] \tag{17}$$

The solar radiation influences both the glazing and the frame. However only glazing system will be taken into consideration because of low share of the frame in total area of windows.

Fenestration solar heat gain includes directly transmitted solar radiation and inward flowing fraction of absorbed solar radiation. The first component describes amount of solar radiation that enters the building through fenestration and is restrained by the solar transmittance of the glazing system. The second component describes radiation that is absorbed in the glazing and then transferred to the interior of the building by convection or radiation. As a result the solar heat gain is higher than just the quantity of transmitted radiation and it is described by the Solar Heat Gain Coefficient (SHGC). SHGC is determined for the particular window and depends on the angle of incidence (the angle between the line normal to the irradiated surface and the earth-sun line). Knowing the main transmission factor for western wall windows g=0,46 the SHGC is determined basing on data presented in [4], which was collected for different types of windows. The SHGC for direct beam radiation is a function of angle of incidence θ (figure 8) and for the range 0° to 90° it can be approximated as:

$$SHGC = -10^{-6}\theta^3 + 6 \cdot 10^{-5}\theta^2 - 7 \cdot 10^{-4}\theta + 0{,}571 \quad (18)$$

The SHGC for diffuse solar radiation can be assumed constant [4]:

$$SHGC_D = 0{,}48$$

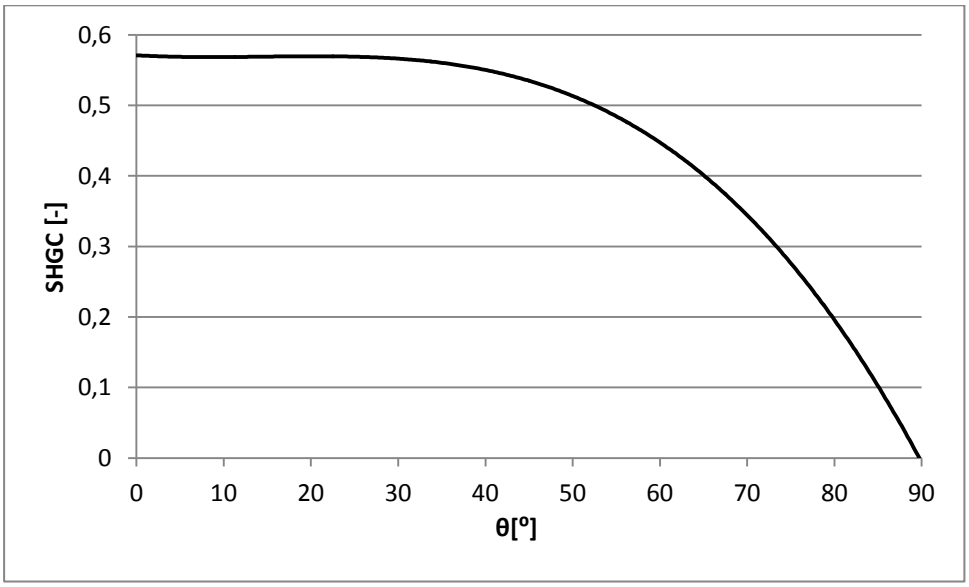

Figure 8. Direct beam SHGC for western façade windows.

Another factor influencing fenestration solar heat gain is the shadowing. Over western windows there is an overhang, 1,7 metre deep, which blocks some part of the direct beam radiation that would otherwise be incident on the surface of windows. To estimate the impact of the shadowing system, indoor solar attenuation coefficient (IAC) is introduced. Influence of the overhang on the direct beam radiation is defined as the relation of non-shaded (sun-lit) surface to the total area of windows [4]:

$$IAC_b = \frac{A_{SL}}{A_{win}} \quad (19)$$

To calculate the sun-lit area, first the shadow height must be determined. It depends on the depth of overhang $d_{OH} = 1{,}7$m, solar altitude angle β and azimuth γ [4]:

$$S_H = d_{OH}\frac{tan\beta}{cos\gamma} \tag{20}$$

Then knowing that the overhang shadows windows evenly, IAC_b equals:

$$IAC_b = \frac{(S_{win}-S_H)\cdot L_{win}}{S_{win}\cdot L_{win}} = \frac{S_{win}-S_H}{S_{win}} \tag{21}$$

Moreover some of the windows are darkened with a sticker stuck on their surface. Its indoor solar attenuation coefficient value is estimated to be the same as grey roller blind that is:

$$IAC_s = 0{,}7$$

For the windows without stickers IAC_s equals 1.

Therefore the fenestration heat gain can be described by the following sum:

$$\dot{Q}_{win} = A_{win}E_{t,b}SHGC\cdot IAC_bIAC_s + A_{win}E_{t,d}SHGC_DIAC_s + \dot{Q}_c \tag{22}$$

The first term of this expression describes direct beam solar heat gain, the second one diffuse solar heat gain and the third one conductive heat gain.

Windows in the supermarket's roof are surrounded by opaque enclosure which should effectively prevent it from most of solar radiation influence, therefore it is assumed to transfer heat only through conduction.

3.2. Ventilation

Stages of ventilation system model development are described in chapter 5. Here are presented some general information about this system and air mass balancing principles.

The ventilation flow in the supermarket is a combination of two streams of different temperatures and humidity ratios: fresh air stream and recirculation air stream. Three of air suppliers operate only locally meaning they heat or cool recirculating air. The remaining three are connected with fresh air supply (figure 9). They mix streams of fresh air and remaining part of recirculation air making their temperature and humidity ratio uniform. After mixing they are either heated or cooled in heat exchangers at supply air outlets. It is assumed that each of six air suppliers supplies the same amount of air. Rotary heat exchanger is not considered in the model.

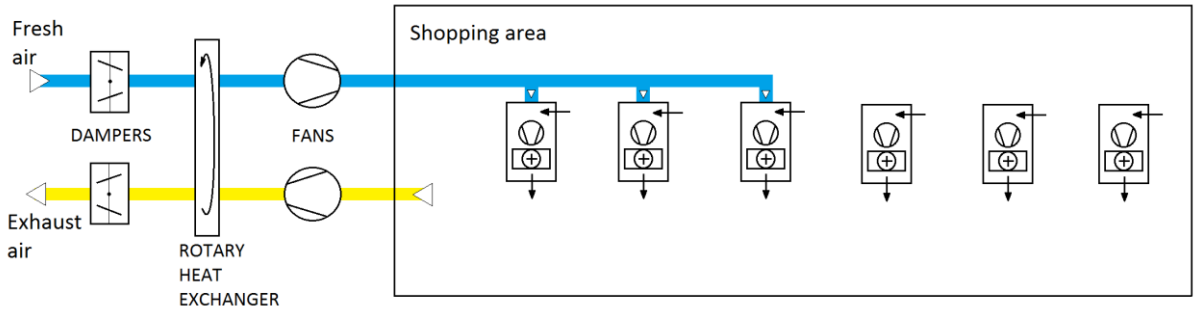

Figure 9. Ventilation system of the supermarket.

Air is the only controllable source of heat or cool used for needs of building air conditioning. The required volume flow of ventilation air for selling halls in self-service shops is estimated for 10 ÷ 12 m^3/h per m^2 of floor area [21]. This means total air flow of about 18560 ÷ 22270 m^3h^{-1} in the considered supermarket. Value of volumetric air flow chosen for the simulation is:

$$\dot{V}_{sa} = 22270\frac{m^3}{h} \approx 6{,}19\frac{m^3}{s}$$

The need for fresh air may be estimated assuming the need of 30 m^3/h per person [28]. Because the store is located in a moderate climate area, the air density is assumed constant $\rho = 1{,}2\frac{kg}{m^3}$. Such practice is approved by ASHRAE [6].

In general the total heat load generated by ventilation is given by:

$$\dot{Q}_{HVAC} = \dot{V}_{sa}\rho(h_{sa} - h_{zone}) \tag{23}$$

Moisture transfer is given by:

$$\dot{m}_{HVAC} = \dot{V}_{sa}\rho(x_{sa} - x_{zone}) \tag{24}$$

The volumetric stream of air conditioned by the ventilation system consists of three components: recirculating air, fresh air stream and dehumidification stream. Recirculating air can be heated and its stream decreases when fresh air stream increases or mechanical dehumidification need appears. An adjustable fresh air algorithm is introduced in section 5.2 meaning that amount of fresh air supplied may vary. Mechanical dehumidification is introduced in section 5.4, where it is described in detail, but looking ahead: in this mode one of air suppliers is adapted into dehumidifier and in fact recirculates cooled and dehumidified air without possibility for further heating it. This air stream is separated for clarity of mass flows deliberations (identical with volumetric flows because of constant density assumption). The following equation describes share of particular streams in the total air stream, which is constant due to application of CAV system:

$$\dot{V}_{sa} = \dot{V}_{rec} + \dot{V}_{fa} + \dot{V}_{dehum} \tag{25}$$

3.3. Infiltration

Infiltration in the supermarket occurs through automatic main door and other auxiliary exterior doors: in the bistro, in the warehouse, etc. It must offset air removed in bathrooms, rubbish disposal room, warehouse and kitchen. That air is removed directly outside skipping air handling unit to avoid contamination or bad smell penetrating to supply air.

The volume flow of infiltration stream through an automatic door with vestibule (as installed in the supermarket) may be approximated with the equation [5]:

$$\dot{V}_{inf} = C_A A R_p \left[\frac{l}{s}\right] \tag{26}$$

where:
A – door area [m^2],
$R_p \approx 4{,}5$ [$Pa^{0,5}$]– pressure factor estimated for ambient temperature -10 ÷ 30 °C,
$C_A = \frac{2}{3}n_p$ – airflow coefficient [L/(sm^2 $Pa^{0,5}$)],

n_p – number of people.

Heat load from infiltration is estimated in the following way:

$$\dot{Q}_{inf} = \dot{V}_{inf}\rho(h_{amb} - h_{zone}) \quad (27)$$

And moisture transfer is described by following equation:

$$\dot{m}_{inf} = \dot{V}_{inf}\rho(x_{amb} - x_{zone}) \quad (28)$$

Infiltration air stream is assumed to balance other air mass losses, or in fact cause air mass exchange, at each moment and not influence ventilation system operation.

3.4. Air mixing

Heat and moisture transfer between zones is assumed to occur through air mass movement. The amount of air exchanged between zones is described in section 4. Temperatures between zone do not differ much (up to 3 ^{o}C), so the density is assumed constant. Total heat load due to air mixing is given by equation:

$$\dot{Q}_{mix} = \dot{V}_{mix}\rho(h_{zonei} - h_{zone}) \quad (29)$$

Moisture transfer is described in the following way:

$$\dot{m}_{mix} = \dot{V}_{mix}\rho(x_{zonei} - x_{zone}) \quad (30)$$

3.5. People

Maximum simultaneous number of people occupying supermarket determined in the passive house approval documentation is 49. As results from author's observation and reasoning, the profile of number of people staying in the supermarket depends on two factors:

1. Time of week. The supermarket is open from 7 to 22 every day excluding Sundays. During working days it is occupied in a similar way, although on Friday evenings more people tend to do shopping. The profile changes significantly on Saturdays as it is a day free from work.
2. Location. The supermarket is located in a residential part of the town, therefore during working days there are two peaks in its occupation – one in the morning and another one in the evening (before and after work). The third common peak – during lunch time – is not present.

It is assumed that shop staff appears at 6 in number of 6 people and after closing the store for customers at 22 there is still 6 people who go home at 23. The average predicted number of customers is presented in figure 10.

The process of heat rejection by people is quite complex, because rejected heat consists of both sensible and latent components, which vary with changing ambient conditions, i.e. when ambient temperature increases, the sensible heat load decreases and amount of moisture given off increases [21]. However, as suggested by ASHRAE [6], the total heat load from humans can be considered constant for particular activity (shopping here) throughout time and ambient conditions and it is assumed:

$$\dot{Q}_{1person} = 130 \left[\frac{W}{person}\right]$$

Because of the fact that the applied method of energy and mass balancing uses total heat load (enthalpy) and vapour mass balance, only a relation for the second component has to be determined. The mass flow of moisture given off by one person to ambient air is approximated by linear equation [21]:

$$\dot{m}_v = 8{,}3324t - 67{,}258 \left[\frac{g}{h \cdot person}\right] \quad (31)$$

where t is ambient temperature in degree Celsius.

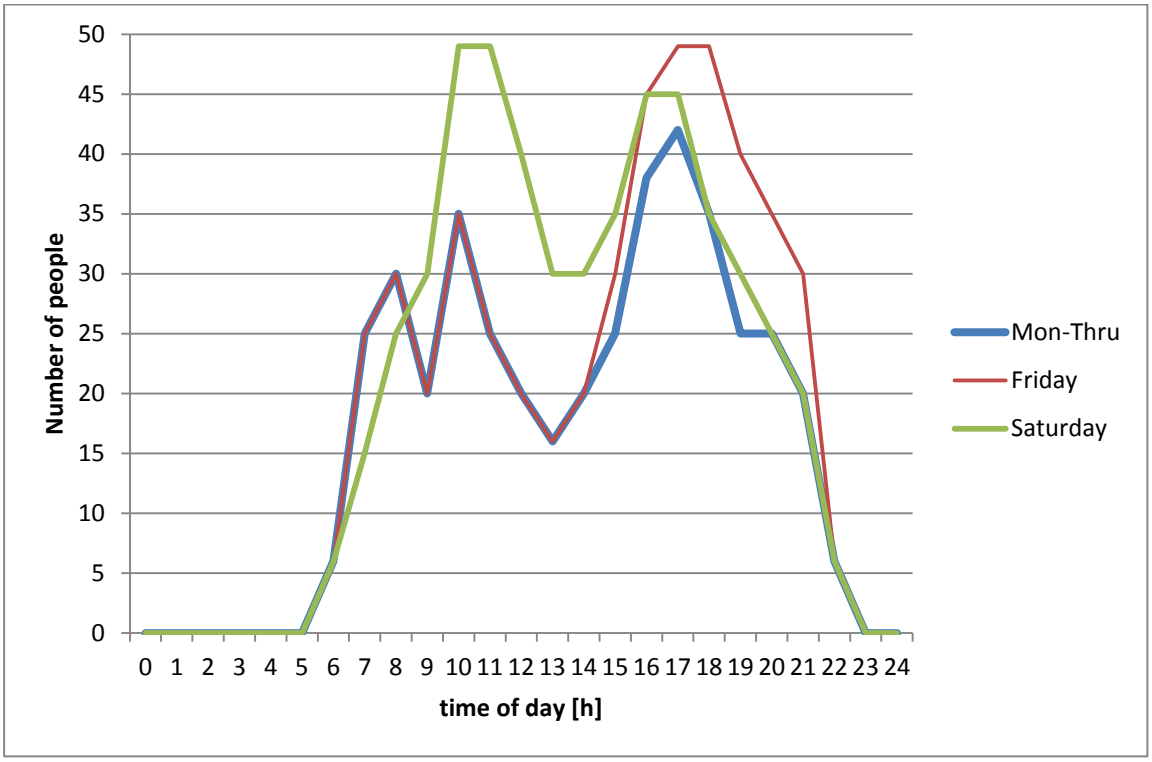

Figure 10. Number of people in function of time of the day and with regard to the day of week.

3.6. Refrigeration

Refrigeration load is supposed to be the biggest contributor to supermarkets' electric energy use. It consists both of a sensible load and latent load which are closely connected and form a rather complicated process.

Refrigerated display cabinets (RDCs) play a vital role in supermarket's energy system and impact a lot inside environment. They may vary a lot depending on temperature levels, type of opening, loading of goods, accessibility, cooling distribution, type of refrigeration system, etc.

Because of modern design of the considered supermarket, refrigerated display cabinets are energy efficient thanks to use of glassed doors, LED lighting and electronically commutated (EC) fans. RDCs may be divided into vertical and horizontal ones. Their profile of energy use is different, because infiltration plays a greater role in vertical cabinets and radiation in horizontal ones [8]. Moreover vertical cabinets may expose a lot of commodities in a little floor area. The RDC's heat balance in a steady state looks as follows [17]:

$$\dot{Q}_{rc} = \dot{Q}_{cw} + \dot{Q}_{Rinf} + \dot{Q}_{rad} + \dot{Q}_{light} + \dot{Q}_{fans} + \dot{Q}_{defrost} + \dot{Q}_{ASH} \quad (32)$$

Considered RDCs are connected to a centralized refrigeration system, so they do not reject heat from condensation of refrigerant or compressor operation directly to air inside the supermarket.

Determining cooling load of real refrigerated display cabinets in the supermarket is difficult, because of two reasons:

1. Producers do not provide exact data about all parameters of RDCs
2. Cooling load changes depending on ambient temperature and humidity ratio.

The first problem can be solved thanks to experiments carried out with RDCs, which determined cooling load of a specific type of RDC in particular ambient conditions. Then, after some corrections, cooling load may be expressed by a set of physical equations making it dependent on ambient conditions.

3.6.1. Vertical medium-temperature glassed display cabinets

Faramarzi et al. [18] determined in an experiment values of particular loads contributing to the total cooling load of a medium temperature (chilled food) vertical cabinet retrofitted with glass doors for constant ambient conditions 24°C dry bulb and 55% relative humidity (figure 11). These results are considered valid for vertical medium-temperature glassed RDCs mounted in the considered supermarket, because of presence of doors. However internal heat gains must be corrected (reduced) due to application of more energy-efficient equipment.

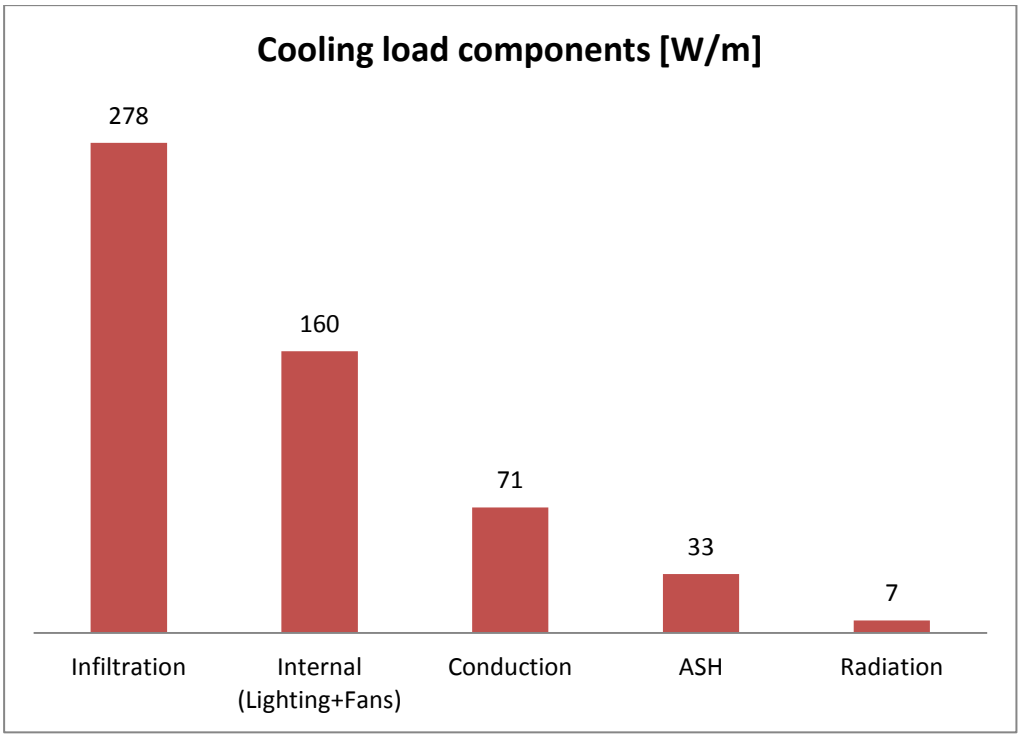

Figure 11. Components of heat load in a medium-temperature RDC retrofitted with glass doors in Watts per metre of length of cabinet for ambient conditions 24°C dry bulb and 55% relative humidity (ASH – anti sweat heaters).

These internal gains come from artificial lighting and EC fans. Vertical medium-temperature RDCs in the supermarket are equipped with energy-efficient lighting and EC fans, whose rejected heat is assumed constant in time and equals:

$$\dot{Q}_{int1} = \dot{Q}_{light} + \dot{Q}_{fans} = 70\ \frac{W}{m}$$

All cooling loads determined in the Faramarzi's experiment and corrected by the new value of internal heat gains give:

$$\dot{Q}_{C-mtv1} = 459\left[\frac{W}{m}\right]$$

This is the total cooling load of a vertical medium-temperature glassed RDC in Watts per metre of length for ambient conditions 24°C dry bulb and 55% relative humidity. Now particular elements of heat balance will be described in order to express their dependence on ambient conditions.

Infiltration heat load consists of latent heat transfer due to cooling, condensation and freezing of vapour present in air and sensible infiltration heat load caused by a need to cool dry infiltration air. Values of these loads can be estimated basing on average mass flow of condensate (water):

$$\dot{m}_{w1} = 2{,}15 \cdot 10^{-5}\ \left[\frac{kg}{s \cdot m}\right]$$

obtained through dividing mass of condensate collected during Faramarzi's experiment by time and length of the cabinet. In fact, vapour from air was almost completely frozen on the surface of evaporator and then liquefied during defrost cycle. Therefore latent heat consists of 3 components:

heat of decreasing vapour temperature, heat of condensation and heat of freezing. However, the first component is much smaller than condensation heat (e.g. for temperature difference 25°C it is just 46 kJ/kg) and it is neglected. Then:

$$\dot{Q}_{latent1} = \dot{m}_{w1}(r_0 + l) = 61\frac{W}{m}$$

where $r_0 = 2501{,}6\frac{kJ}{kg}$ – heat of condensation of water at 0°C,

$l = 334\frac{kJ}{kg}$ – heat of freezing of water.

Now the mass flow of condensate depending on ambient conditions will be determined. The condensation rate is influenced by three factors:

1. Ambient air conditions - its temperature and humidity [17],
2. Refrigerant evaporation temperature,
3. Air temperature in an RDC.

Assuming constant evaporation temperature $t_{evap1} = -4$°C and constant air temperature in the RDC $t_{case1} = 4$°C dry bulb, the condensation process may be approximated in the way presented in figure 12. Points X', X'' and X''' are different conditions of supermarket's ambient air. Point Y expresses extreme conditions of air passing through the evaporator close to the tubes and fins – it is the saturation point at -4°C dry bulb. Points Z are the general conditions inside the RDC. They are determined as the intersection of line X-Y, reflecting condensation process, with the line of constant temperature t_{case1}. However, if the supermarket's air is very dry, RDCs will not humidify ambient air, so the humidity ratio inside an RDC is then equal to the one of ambient air. Line X'-Z'-Y reflects normal condensation. Line X''-Z''-Y reflects condensation if ambient air is very humid. Air conditions cannot cross the curve of 100% relative humidity, therefore X''-Z''-Y slides down that curve. Line X'''-Z'''-Y' reflects lack of condensation if ambient air is very dry – air does not change its humidity ratio.

Assuming that dry bulb temperature lines are perpendicular to the humidity ratio lines, the humidity ratio inside a medium-temperature doored RDC is given by:

$$x_Z = \frac{x_X - x_{evap1}}{t_X - t_{evap1}}\left(t_{case1} - t_{evap1}\right) + x_{evap1}\ \left[\frac{kg}{kg}\right] \qquad (33)$$

However x_Z cannot exceed saturation humidity ratio at t_{case1} equal to $x_{Z''} = 0{,}005\frac{kg}{kg}$. The equation is valid unless ambient air humidity ratio (x_X) is below saturation humidity $x_Y = x_{evap1} = 0{,}0027\frac{kg}{kg}$ at t_{evap1}. Then $x_{case} = x_X$, however this occurs only for very low humidity ratio values.

Getting back to Faramarzi's experiment, where ambient conditions were: $t_{amb1} = 24$°C dry bulb and $\varphi_{amb1} = 55\%$, so using eq. (A3) $x_{amb1} = 0{,}0104\ \frac{kg\,w}{kg\,da}$ the humidity ratio inside the RDC calculated from eq. (33) equals:

$$x_{case1} = \frac{0{,}0104 - 0{,}0027}{24 - (-4)}\left(4 - (-4)\right) + 0{,}0027 = 0{,}0049\left[\frac{kg}{kg}\right]$$

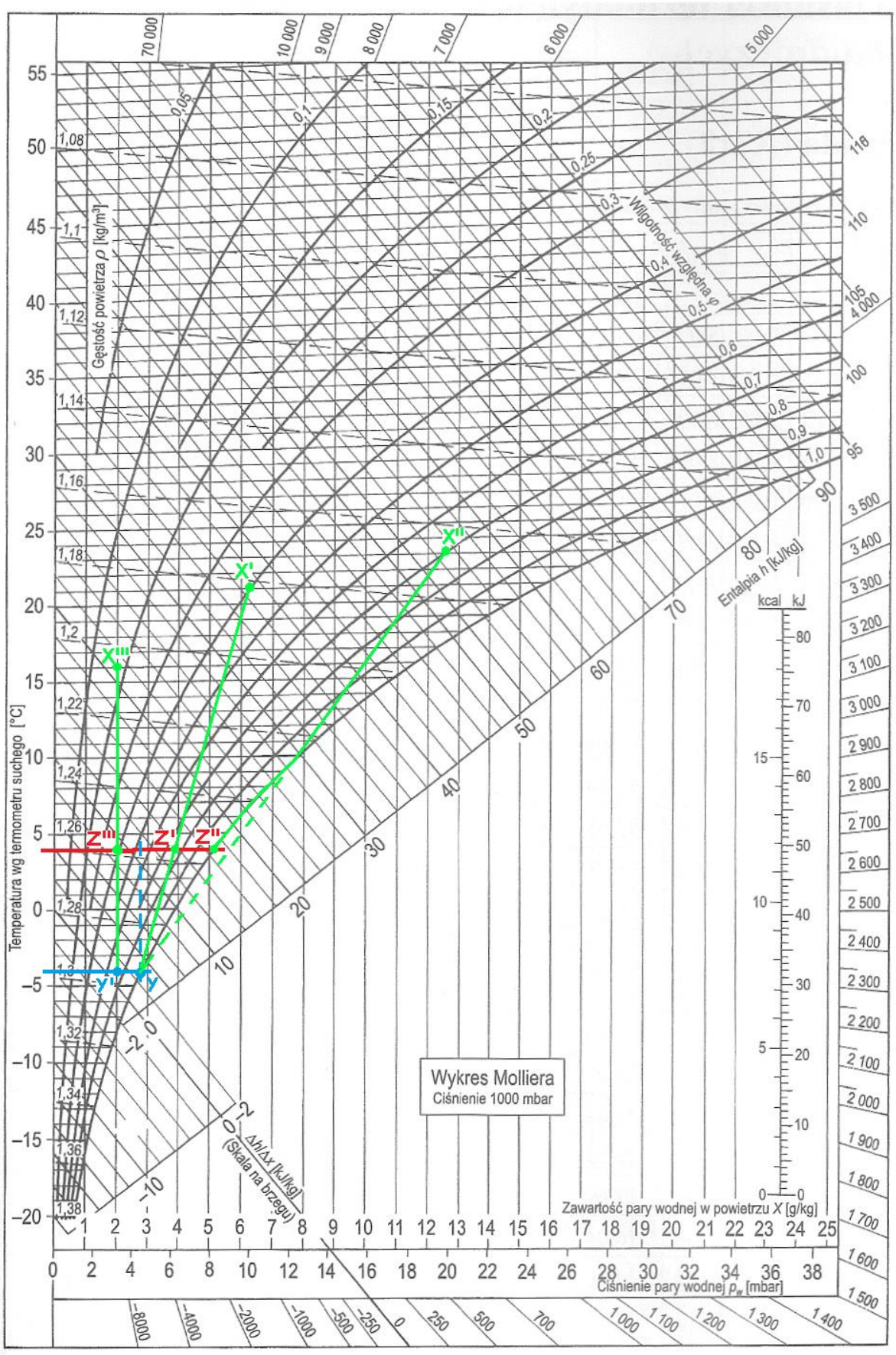

Figure 12. Condensation process in medium-temperature RDCs.

Determining the base air infiltration rate $\dot{m}_{da1}$ is now possible. Knowing that for normal store application there is no distinct correlation between electrical energy use of doored RDCs and door open duration [15], the infiltration rate may be assumed constant throughout time. Mass flow of the condensate is given by:

$$\dot{m}_{w1} = \dot{m}_{da1}(x_{amb1} - x_{case1}) \tag{34}$$

So the mass flow of infiltration air in the vertical medium-temperature RDC equals to:

$$\dot{m}_{da1} = 3{,}9 \cdot 10^{-3} \frac{kg}{s \cdot m}$$

This allows to express relation for latent heat load of vertical doored medium-temperature RDC as a function of moisture content in air inside the supermarket:

$$\dot{Q}_{l-mtv} = \dot{m}_{da1}(x_{amb} - x_Z)(r_0 + l)\frac{W}{m} \tag{35}$$

And mass flow of condensed vapour:

$$\dot{m}_{w-mtv} = \dot{m}_{da1}(x_{amb} - x_{case})\frac{kg}{s \cdot m} \tag{36}$$

It depends both on ambient air humidity ratio and humidity ratio of air inside a cabinet calculated according to eq. (33).

The sensible infiltration heat load from Faramarzi's experiment equals to:

$$\dot{Q}_{s-inf1} = \dot{Q}_{Rinf1} - \dot{Q}_{latent1} = 278 - 61 = 217\frac{W}{m}$$

In general it can be expressed as a function of supermarket's air temperature:

$$\dot{Q}_{s-inf} = \dot{m}_{da} c_p (t_{amb} - t_{case}) \tag{37}$$

where c_p is specific heat of dry air [J/(kgK)].

The conduction cooling load is caused by heat transfer through cabinet's envelope. It can be described by equation:

$$\dot{Q}_{cw} = UA(t_{amb} - t_{case}) \tag{38}$$

where: A – area of conduction heat transfer [m^2],

U – heat transfer coefficient [$W/(m^2K)$].

In Faramarzi's experiment, carried out at $t_{amb1} = 24$°C dry bulb, conduction cooling load was:

$$\dot{Q}_{cw1} = UA(t_{amb1} - t_{case}) = 71\frac{W}{m}$$

Both $\dot{Q}_{s-inf}$ and $\dot{Q}_{cw}$ depend only on ambient temperature. Eventually the total cooling load of a vertical glassed medium-temperature RDC may be expressed as:

$$\dot{Q}_{C-mtv} = \frac{t_{amb}-t_{case1}}{\Delta t_1}\left(\dot{Q}_{s-inf1} + \dot{Q}_{cw1}\right) + \dot{m}_{da1}(x_{amb} - x_{case1})(r_0 + l) + \dot{Q}_{int1} + \dot{Q}_{ASH1} + \dot{Q}_{rad1} \quad (39)$$

Where $\Delta t_1 = t_{amb1} - t_{case1} = 24 - 4 = 20$°C.

And, what's more important, the heat sink for supermarket's environment, comprising infiltration, conduction and radiation heat transfer, is given by:

$$\dot{Q}_{hs-mtv} = \frac{t_{amb}-t_{case1}}{\Delta t_1}\left(\dot{Q}_{s-inf1} + \dot{Q}_{cw1}\right) + \dot{m}_{da1}(x_{amb} - x_{case1})(r_0 + l) + \dot{Q}_{rad1} \quad (40)$$

where t_{amb} and x_{amb} are variables – parameters of supermarket's air. This heat sink depends now on the temperature and humidity ratio inside the supermarket and humidity ratio of air inside a cabinet.

3.6.2. Vertical low-temperature glassed display cabinets

These type of cabinets is much more susceptible to infiltration than medium-temperature cabinets. Therefore better sealing between door and frame is needed, which should in fact decrease infiltration rate below the value for vertical doored medium-temperature RDCs. Triple glazing should effectively reduce radiation cooling load, which is therefore skipped.

Kosar [25] presented in his work data for a closed vertical low-temperature RDC. It will be a base for determining loads of this type of RDC in the considered supermarket. Its total cooling load in ambient conditions 24°C dry bulb and 55% RH was $577\frac{W}{m}$. Internal heat gains accounted for $228\frac{W}{m}$ and anti-sweat heaters rejected $213\frac{W}{m}$. Another research [8] showed that latent cooling load in vertical closed low-temperature RDCs constituted 12% of total cooling load, which means $\dot{Q}_{latent2} = 69\frac{W}{m}$.

However vertical closed low-temperature RDCs applied in the supermarket have a lower internal heat gain (from lighting and fans) that equals:

$$\dot{Q}_{int2} = 145\frac{W}{m}$$

Furthermore, anti-sweat system combines "no-heat" glazing, where no electric heaters are used, and conventional electric heaters in frames. They do not cover such big area as in vertical chilled food cabinets from previous section, however they have to deal with lower temperature inside cabinets and prevent doors from freezing to the frame. Therefore their cooling load is assumed to be the same as for chilled food RDCs [24].

$$\dot{Q}_{ASH2} = 33\ \frac{W}{m}$$

Now the total cooling load may be determined by correcting total cooling load from Kosar's research with lower internal and anti-sweat heaters heat gains. Then the total cooling load at ambient conditions 24°C dry bulb and 55% RH equals:

$$\dot{Q}_{C-ltv1} = 345\frac{W}{m}$$

This value is lower than cooling load of vertical close medium-temperature RDCs. Justification for that may be lower rate of infiltration (due to better sealing) which was responsible for highest cooling load.

To estimate the shift in latent cooling load and mass flow of condensate (dehumidification rate) depending on supermarket's air conditions the procedure described in section 3.6.1 is applied (see figure 12). Assuming constant temperature of refrigerant evaporation $t_{evap2} = -30$℃ and constant air temperature retained in the RDC $t_{case2} = -21$℃ dry bulb, the humidity ratio of air inside a vertical low-temperature RDC is given by:

$$x_{case} = \frac{x - x_{evap2}}{t - t_{evap2}}\left(t_{case2} - t_{evap2}\right) + x_{evap2}\ \left[\frac{kg}{kg}\right] \tag{41}$$

It cannot exceed the value of saturation humidity ratio at t_{case2}, which is $x_{Z''} = 0{,}00058\frac{kg}{kg}$ and in case of very dry air it will be equal to humidity ratio of supermarket's air x.

For the supermarket's air conditions $t_{amb1} = 24$℃ dry bulb, $\varphi_{amb1} = 55\%$ $x_{amb1} = 0{,}0104\ \frac{kg\,w}{kg\,da}$ and knowing that saturation humidity at t_{evap2} is $x_{evap2} = 0{,}00029\frac{kg}{kg}$, the humidity ratio inside the case equals:

$$x_{case2} = 0{,}00058\frac{kg}{kg}$$

Now the average amount of dry air infiltrated into the cabinet can be estimated. It will serve as a basis for calculating amount of condensed vapour and latent cooling load.

$$\dot{Q}_{latent2} = \dot{m}_{da2}(x_{amb1} - x_{case2})(r_0 + l) \tag{42}$$

So the mass flow of infiltrated air (constant over time) is:

$$\dot{m}_{da2} = 2{,}48 \cdot 10^{-3}\,\frac{kg}{s \cdot m}$$

This allows to express relation for latent cooling load of doored vertical low temperature RDC as a function of moisture content of air inside the supermarket:

$$\dot{Q}_{l-ltv} = \dot{m}_{da2}(x_{amb} - x_{case})(r_0 + l)\left[\frac{W}{m}\right] \tag{43}$$

And mass flow of condensed vapour:

$$\dot{m}_{w-ltv} = \dot{m}_{da2}(x_{in} - x_{case})\left[\frac{kg}{s \cdot m}\right] \tag{44}$$

The remaining part of cooling load is caused by sensible part of infiltration load and conduction through walls:

$$\dot{Q}_{s-inf2} + \dot{Q}_{cw2} = \dot{Q}_{C-ltv1} - \dot{Q}_{int2} - \dot{Q}_{latent2} - \dot{Q}_{ASH2} = 98\frac{W}{m}$$

As described before, these two heat fluxes depend on ambient air temperature, therefore total cooling load of the vertical doored low-temperature display cabinets can be estimated as follows:

$$\dot{Q}_{C-ltv} = \frac{t_{amb} - t_{case2}}{\Delta t_2}\left(\dot{Q}_{s-inf2} + \dot{Q}_{cw2}\right) + \dot{m}_{da2}(x_{amb} - x_{case2})(r_0 + l) + \dot{Q}_{int2} + \dot{Q}_{ASH2} \tag{45}$$

For $\Delta t_2 = t_{in1} - t_{case2} = 24 - (-21) = 45$℃.

And the heat sink for supermarket environment is:

$$\dot{Q}_{hs-ltv} = \frac{t_{amb} - t_{case2}}{\Delta t_2}\left(\dot{Q}_{s-inf2} + \dot{Q}_{cw2}\right) + \dot{m}_{da2}(x_{amb} - x_{case2})(r_0 + l) \quad (46)$$

3.6.3. Horizontal low-temperature glassed display cabinets

Horizontal RDCs display less commodities per unit of cabinet length than vertical RDCs which may be seen as a disadvantage, however they create impression of more space in a shop due to their low height. The horizontal opening makes them less vulnerable to infiltration and more to radiation [8]. Another research presented in Kosar's work [25] has shown that closed horizontal low-temperature RDCs consume about 442 W/m with internal gains amounting for 107 W/m and anti-sweat heaters 122 W/m. In the new generation of RDCs these internal gains would be lowered to:

$$\dot{Q}_{int3} = 68\frac{W}{m}$$

Assuming anti-sweat heaters cooling load the same as for vertical medium-temperature RDCs:

$$\dot{Q}_{ASH3} = 33\ \frac{W}{m}$$

the cooling load of horizontal low-temperature glassed RDCs at reference conditions $t_{amb1} = 24$℃ dry bulb and $\varphi_{amb1} = 55\%$ is then lowered to:

$$\dot{Q}_{C-lth1} = 314\frac{W}{m}$$

Mass flow of condensate is about 3 times lower than in vertical closed low-temperature RDCs [8]. Therefore the latent heat load is 3 times smaller too and equals $\dot{Q}_{latent3} = 23\frac{W}{m}$.

Conditions present in horizontal closed low-temperature RDCs are the same as in vertical ones i.e. refrigerant evaporation temperature $t_{evap3} = -30$℃ and saturation humidity ratio at this temperature $x_{evap3} = 0{,}00029\frac{kg}{kg}$, air temperature inside the RDC $t_{case3} = -21$℃ and saturation humidity ratio at that point $x_{Z''} = 0{,}00058\frac{kg}{kg}$.

For estimating shift in latent cooling load and mass flow of condensate depending on supermarket's air conditions the procedure described in section 3.6.1 is applied. The absolute humidity of air inside the RDC is given by:

$$x_{case} = \frac{x - x_{evap3}}{t - t_{evap3}}\left(t_{case3} - t_{evap3}\right) + x_{evap3}\ \left[\frac{kg}{kg}\right] \quad (47)$$

It cannot exceed $x_{Z''}$ and in case of very dry air it will equal humidity ratio of supermarket's air x.

For the supermarket's air conditions $t_{amb1} = 24$℃ dry bulb, $\varphi_{amb1} = 55\%$ $x_{amb1} = 0{,}0104\ \frac{kg\ w}{kg\ da}$ and knowing that saturation humidity at t_{evap3} is $x_{evap3} = 0{,}00029\frac{kg}{kg}$, the humidity ratio inside the case equals:

$$x_{case3} = 0{,}00058\frac{kg}{kg}$$

Now the average amount of dry air infiltrated into the cabinet can be estimated. It will serve as a basis for calculating amount of condensed vapour and latent cooling load.

$$\dot{Q}_{latent3} = \dot{m}_{da3}(x_{amb1} - x_{case2})(r_0 + l) \quad (48)$$

So

$$\dot{m}_{da3} = 0{,}83 \cdot 10^{-3} \frac{kg}{s \cdot m}$$

This allows to express relation for latent cooling load of closed horizontal low-temperature RDC as a function of moisture content of air inside the supermarket:

$$\dot{Q}_{l-lth} = \dot{m}_{da3}(x_{amb} - x_{case})(r_0 + l) \left[\frac{W}{m}\right] \quad (49)$$

And mass flow of condensed vapour:

$$\dot{m}_{w-lth} = \dot{m}_{da3}(x_{amb} - x_{case}) \left[\frac{kg}{s \cdot m}\right] \quad (50)$$

The radiation cooling load in horizontal cabinets may account for as much as 43% of the total cooling load. At the reference conditions it equals:

$$\dot{Q}_{rad3} = 135 \left[\frac{W}{m}\right]$$

Then the conduction and sensible part of infiltration are responsible for

$$\dot{Q}_{cw3} + \dot{Q}_{s-inf3} = 55 \left[\frac{W}{m}\right]$$

of the cabinets cooling load.

The total cooling load of horizontal closed low-temperature display cabinets is given by:

$$\dot{Q}_{C-lth} = \frac{t_{amb} - t_{case3}}{\Delta t_3}\left(\dot{Q}_{s-inf3} + \dot{Q}_{cw3}\right) + \dot{m}_{da3}(x_{amb} - x_{case3})(r_0 + l) + \dot{Q}_{int3} + \dot{Q}_{ASH3} + \dot{Q}_{rad3} \quad (51)$$

For $\Delta t_3 = \Delta t_2 = 45$°C.

And the heat sink for supermarket environment is:

$$\dot{Q}_{hs-lth} = \frac{t_{amb} - t_{case3}}{\Delta t_3}\left(\dot{Q}_{s-inf3} + \dot{Q}_{cw3}\right) + \dot{m}_{da3}(x_{amb} - x_{case3})(r_0 + l) + \dot{Q}_{rad3} \quad (52)$$

3.6.4. Horizontal closed medium-temperature refrigerated display cabinets

These RDCs are modelled in a similar way to horizontal closed low-temperature RDCs. Huge glassed display surface results in a quite high radiation cooling load. The producer of the cabinets claims that these cabinets generate cooling load of 195 W/m at reference conditions $t_{amb1} = 24$°C dry bulb, $\varphi_{amb1} = 55\%$ $x_{amb1} = 0{,}0104$ $\frac{kg\,w}{kg\,da}$.

$$\dot{Q}_{C-mth1} = 195 \frac{W}{m}$$

The internal heat gains and latent cooling load are assumed to be the same as for horizontal low-temperature RDCs:

$\dot{Q}_{int4} = 68\frac{W}{m}$

$\dot{Q}_{latent4} = 23\frac{W}{m}$

The change in latent cooling load may be estimated in the same way as in section 3.5.2 for cabinet conditions $t_{evap4} = -4$℃, $x_{evap4} = 0{,}0027\frac{kg}{kg}$, $t_{case4} = 4$℃ and $x_{3,,} = 0{,}005\frac{kg}{kg}$. Same as in section 3.6.1 the humidity ratio inside the cabinet at reference conditions equals $x_{case4} = 0{,}0049\left[\frac{kg}{kg}\right]$. Equation (33) allows to calculate humidity ratio inside the cabinet.

The latent cooling load is given by:

$$\dot{Q}_{latent4} = \dot{m}_{da4}(x_{amb1} - x_{case4})(r_0 + l) \quad (53)$$

So the average infiltration ratio equals to:

$\dot{m}_{da4} = 1{,}47 \cdot 10^{-3}\frac{kg}{s \cdot m}$

This allows to express relation for latent cooling load of closed horizontal medium-temperature RDC as a function of moisture content of air inside the supermarket:

$$\dot{Q}_{l-mth} = \dot{m}_{da4}(x_{amb} - x_{case})(r_0 + l)\left[\frac{W}{m}\right] \quad (54)$$

And mass flow of condensed vapour:

$$\dot{m}_{w-mth} = \dot{m}_{da4}(x_{amb} - x_{case})\left[\frac{kg}{s \cdot m}\right] \quad (55)$$

Assuming $\dot{Q}_{rad4} = 50\ \frac{W}{m}$, the conduction and sensible infiltration cooling loads equal to

$\dot{Q}_{s-inf4} + \dot{Q}_{cw4} = 54\frac{W}{m}$

The total cooling load of horizontal closed medium-temperature display cabinets is given by:

$$\dot{Q}_{C-mth} = \frac{t_{amb} - t_{case4}}{\Delta t_4}\left(\dot{Q}_{s-inf4} + \dot{Q}_{cw4}\right) + \dot{m}_{da4}(x_{amb} - x_{case4})(r_0 + l) + \dot{Q}_{int4} + \dot{Q}_{rad4} \quad (56)$$

For $\Delta t_4 = \Delta t_1 = 20$℃.

And the heat sink for supermarket environment is:

$$\dot{Q}_{hs-mth} = \frac{t_{amb} - t_{case4}}{\Delta t_4}\left(\dot{Q}_{s-inf4} + \dot{Q}_{cw4}\right) + \dot{m}_{da4}(x_{amb} - x_{case4})(r_0 + l) + \dot{Q}_{rad4} \quad (57)$$

3.7. Lighting

In the supermarket LED lighting is applied. Different from incandescent and fluorescent lighting, LED emits only convective heat [12]. It is assumed to reject constant stream of heat convected to supermarkets air [12]:

$$\dot{Q}_{LED} = 8\ \frac{W}{m^2}$$

Lighting heat gain is expressed in Watts per square metre of floor area. The supermarket is equipped in outside lighting illuminating car park and advertisements. It does not influence supermarket's thermal and moisture conditions, however it affects electrical energy use. A sensor turns on outside lighting automatically when brightness falls below certain value.

3.8. Thermal capacity

Apart from thermal capacities of external walls, floor and roof, a thermal capacity of stored products, furniture, internal partitions and wooden beams supporting the roof in the supermarket must be considered. Value of thermal resistance is assumed equal to the one of inside surface of the wall – air convection and amounts 0,13 m^2K/W. Problems arise when it comes to determining area of heat exchange, because of developed surface of stored products, and thermal capacity, because of different materials forming considered elements. Therefore some simplifications and approximations have to be made. Side area of furniture storing products and wooden beams is estimated about 920 m^2, however it is doubled because of developed surfaces of stored products. Then the UA factor is:

$$UA = \frac{A}{R} = \frac{1840}{0{,}13} = 14154\ \left[\frac{W}{K}\right]$$

Volume of considered elements is approximated to 250 m^3. Because of presence of wooden beams and diverse composition of sold products with particular attention drawn to water content, which influences thermal capacity the most, wood is considered as a uniform substitute for heat capacious elements in the supermarket. Average content of water in wood helps to approximate well both low- and high-water content products. Its specific heat and density is taken from [29]. Then the average thermal capacity equals to:

$$C = Vc\rho = 250 \cdot 1500 \cdot 700 = 262500000\ \left[\frac{J}{K}\right]$$

Heat is absorbed by heat capacious elements by means of convection between an element and inside air, and radiation entering the room. It is assumed that such solar radiation first hits the floor where 50% is absorbed and the rest is reflected reaching surrounding objects: furniture, products, internal walls etc. that means elements described above. It happens close to side windows located at the bakery and main entrance. Heat capacity of refrigerated display cabinets and products inside of them is not taken into account as it is a part of deliberations on RDCs.

The temperature of heat capacious elements is assumed uniform due to their small depth. Then the heat transfer from thermal capacious elements is given by:

$$\dot{Q}_{tc} = UA(t_{tc} - t_{zone}) \tag{58}$$

And the temperature of heat capacious elements is determined from the following equation:

$$C\frac{dt_{tc}}{d\tau} = \dot{Q}_{tc} \tag{59}$$

meaning that it is calculated as an integral. The initial condition for t_{tc} is temperature the same as ambient air meaning no heat flow.

4. Numerical thermal and humidity model of the supermarket

This section aims to present general modeling strategy and further components' and subsystems' modeling methods.

The introduced model represents forward (classical) approach [7], where output variables are predicted based on specific input variables and known modelled object's structure and parameters. These input variables are outside temperature, outside relative humidity, number of people in the supermarket and solar data for Hannover: global horizontal radiation, diffuse radiation, solar azimuth and height of sun. Obtained main output variables are: inside temperatures and inside humidities (absolute and relative). During program processing some other useful variables are calculated e.g. particular heat loads, surfaces temperatures, shading efficiency etc.

The time step in which input variables are given is one hour, however these values are interpolated so that the calculations can be executed in smaller time intervals for better accuracy e.g. of ventilation control system. Length of these intervals is adjusted by the program, however e.g. it was 406 seconds on average for the model 5.4 (active dehumidification). And this is the format for output data too. Time over which the simulation is run is one year (365 days) – from January 1st to December 31th 2015. Current computing powers allow to run such simulation with many feedbacks over one year with short time intervals.

The developed model of the supermarket is composed of "lumps" - zones. Each zone must be coherent and represent specific futures that make it different from adjacent zones. The more zones, the more complicated the model gets and only as few as possible "lumps" should be assigned in order to achieve desired accuracy of results. In the considered model two zones were distinguished: (1) the general shopping area, (2) the cold area. Figure 13 presents these zones with marked RDCs.

In the general shopping area there is the entrance and bakery with the whole western glazing, cash registers, dry foods area, all frozen food RDCs, returnable packaging storehouse and ancillary rooms. The machinery room is modelled as a subzone, because of significant waste heat gains. All six exhaust ducts of the ventilation system are located in zone 1 (see also fig. 2). Three of them are very close to the second zone, so it is assumed that half of circulating ventilation air is mixed between zones. Area of this zone is 1196 m^2.

The temperature in machinery room is controlled by individual ventilation system that works in the following way: if the inside temperature exceeds 25 ^{o}C air is discharged directly outside and outside air is supplied. However this may work properly only if outside temperature is below 25 ^{o}C – above this level it is assumed that temperature inside machinery room is kept at the same level as outside temperature. Assuming thickness of partitions separating machinery room from the rest of the supermarket to be d=0,2 m, its material aerated concrete (its properties are presented in table 3: k=0,21 W/(m^{2}K)), thermal resistance of convection between air and wall R_{in}=0,13 m^{2}K/W (as in table 4) and knowing that total area of those partitions equals A=251 m^2, machinery heat transfer to zone 1 is calculated as follows:

$$\dot{Q}_{machinery} = A\frac{\Delta T}{2R_{in}+\frac{d}{k}} = 207 \cdot \Delta T\ [W] \tag{60}$$

where ΔT is a difference between temperature in the machinery and zone 1:

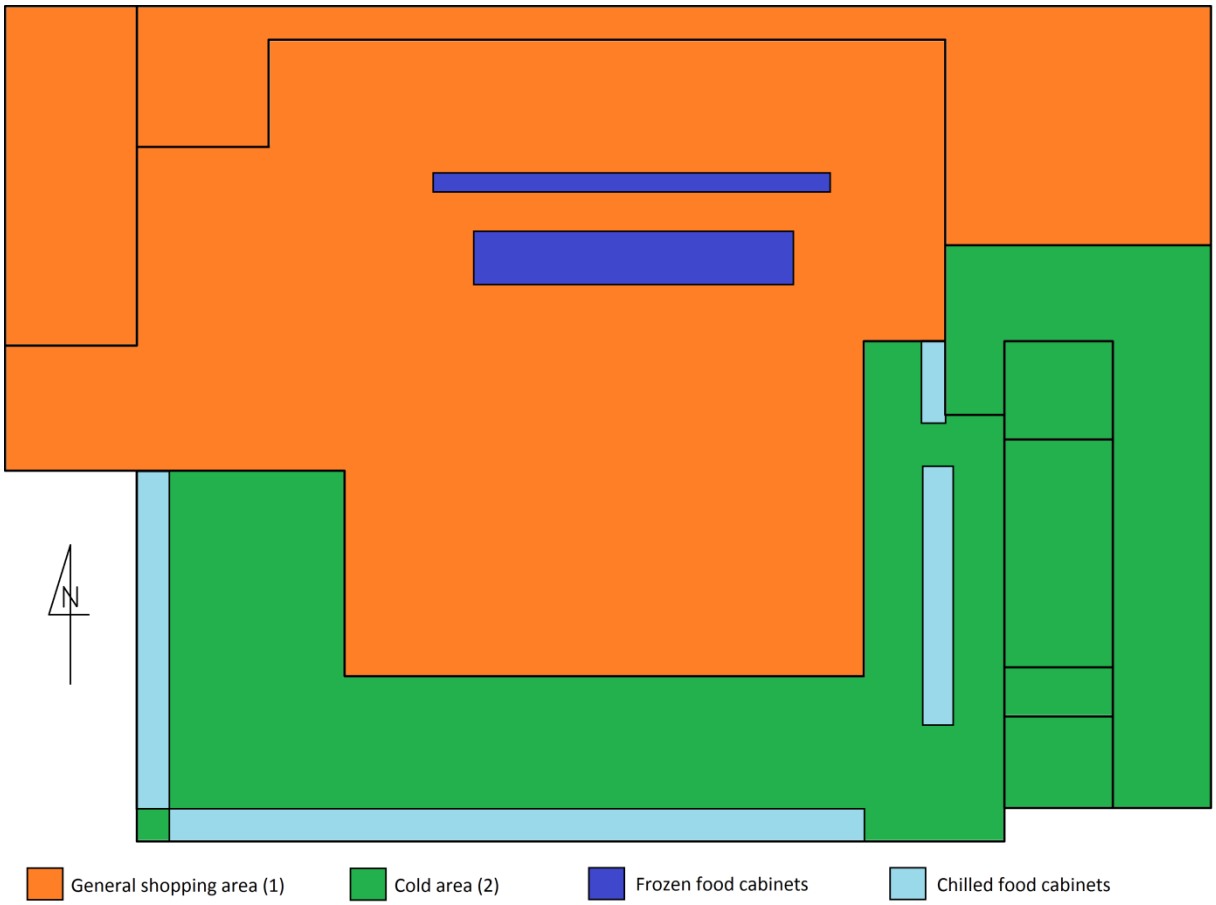

Figure 13. Zones of the supermarket and location of refrigerated display cabinets.

$$\Delta T = \begin{cases} 25 - T_{zone} \; if \; T_{out} \leq 25℃ \\ T_{out} - T_{zone} \; if \; T_{out} > 25℃ \end{cases} \tag{61}$$

Furthermore, the solar heat gain to zone 1 is reduced by the one in machinery room, because it is assumed that heat transfer between zone 1 and machinery room occurs only through conduction.

In the cold area, which temperature is generally lower than in the general shopping area, there is produce area, all chilled food cabinets, cold rooms and warehouse. The influence of cold rooms is neglected due to the fact that transmission losses through well insulated walls of these rooms are very low comparing to other heat sinks. They are assumed to be opened very rarely, so the infiltration loss is low. Moreover it is very hard to determine when these rooms are opened. The southern (bottom) wall is overshadowed by an annex covering the delivery track, so there are no solar heat gains to that wall. It significantly reduces the heat gain to the zone 2. Area of this zone is 660 m^2.

Because both zones include places which particularly attract people and make them stop there, people are assumed to be spread evenly throughout the area of the supermarket.

To visualize structure of the computer model and how the theory is applied into MatLab Simulink, an excerpt from the final version of the program is shown in figure 14. It presents structure of zone 1 modelled in the program. Zone 2 is modelled in analogous way and information is being exchanged between these blocks. In fig. 14 green dots are inputs for calculations: outside temperature (T_out),

outside humidity ratio (x_out), number of people (n_people), humidity ratio in zone 2 (x_zone2), temperature in zone 2 (t_zone2). First three are global inputs (described above) and following two are taken as a feedback from zone 2 calculations (they are determined simultaneously). Input ports are not connected with arrows to appropriate slots for better transparency of the picture, however in reality they send signals to the appropriate slots. Each unconnected slot is marked with a number identical with the number of corresponding input port (names are identical too). Feedback loops and output signals are connected with arrows. Output signals (yellow dots) are forwarded to zone 2 section, in order to execute calculations, or results section, where they are processed into convenient form of data.

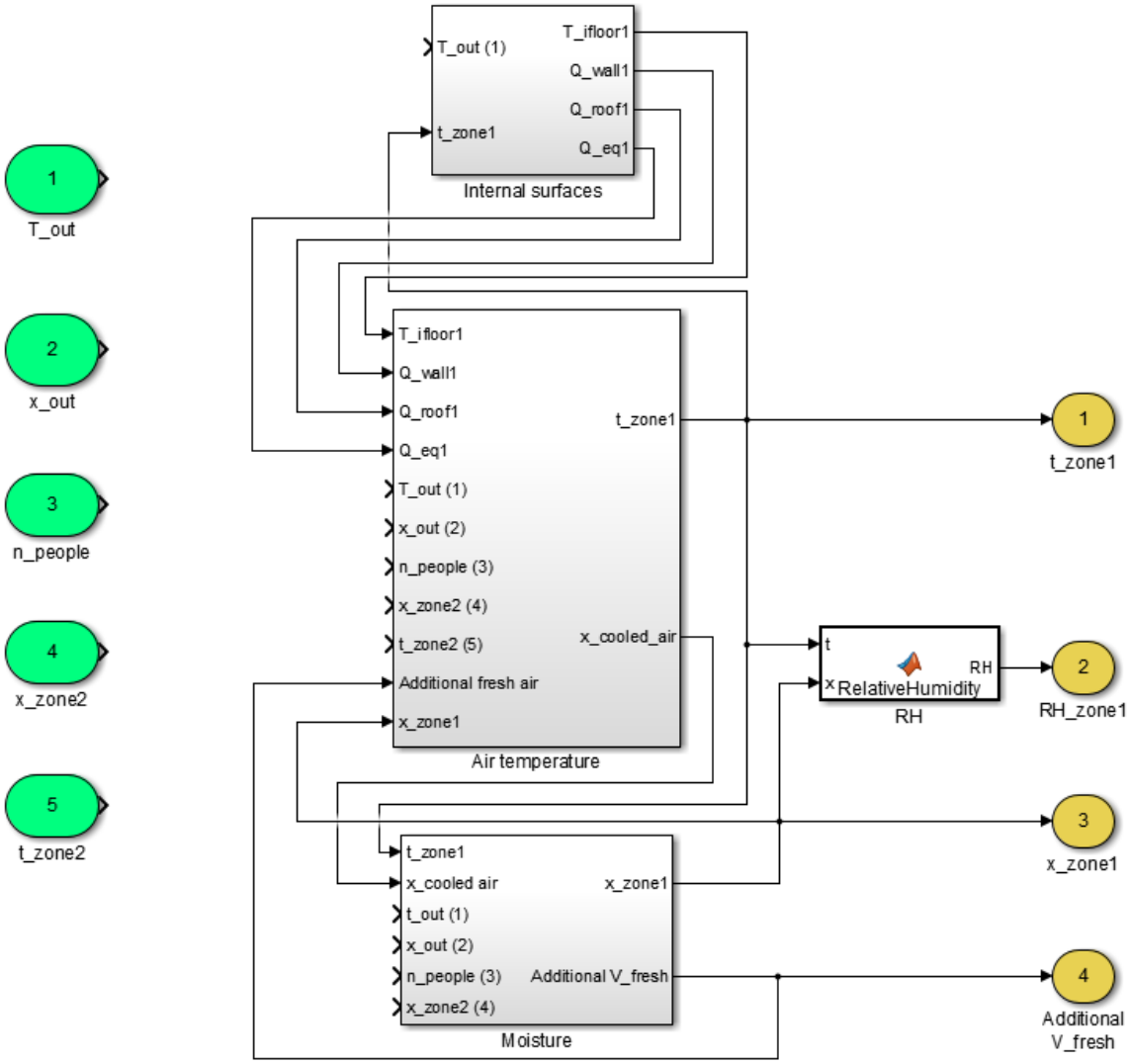

Figure 14. Top level of zone 1 calculation model in MatLab Simulink.

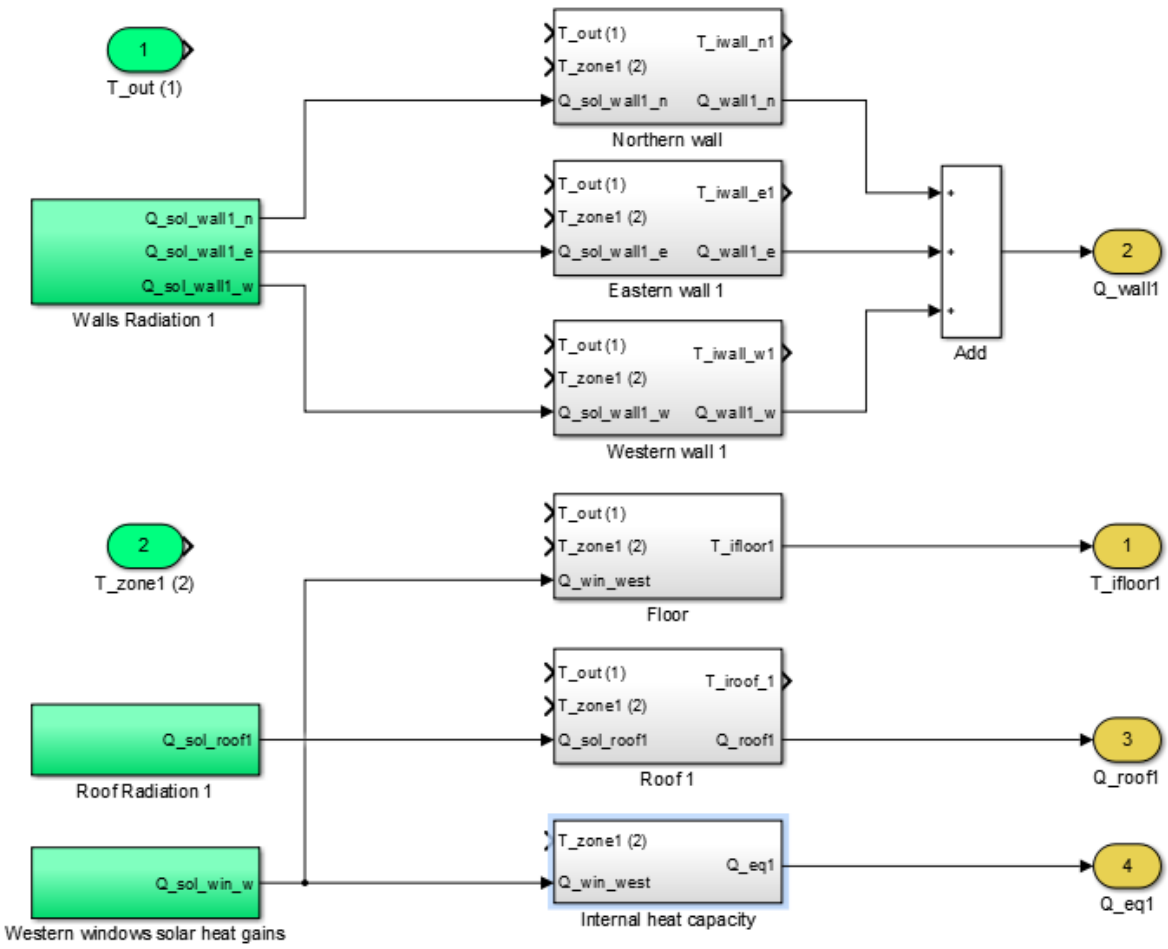

Figure 15. Internal surfaces subsystem in Zone 1 calculations.

Block “Internal surfaces” is responsible for calculating temperatures of internal surfaces exchanging heat with inside air according to equations (3) and (4). The content of this block is shown in figure 15. Subsystems “Walls Radiation 1”, “Roof Radiation 1” and “Western windows solar heat gain” (green boxes) determine solar heat gains incident on particular surfaces basing on solar input data and equations presented in sections 3.1.4. and 3.1.5. In case of zone 1 these are: whole northern wall, parts of eastern and western walls and part of roof. Grey boxes execute equations described in sections 3.1.1, 3.1.2, 3.1.3 and 3.8. If the result is a temperature (in this case only $T_{ifloor1}$ – temperature of inside surface of the floor in zone 1) it is forwarded to “Air temperature” subsystem, where convective heat transfer between floor and air is determined. However because of code simplicity some temperatures are already transformed into heat streams (Q). All calculations in grey boxes take into consideration heat storage in elements of the supermarket. The results are passed for further processing.

Block “Air temperature” executes equation (1) calculating enthalpy in zone 1 and then, knowing humidity ratio, temperature. Structure of this block is presented in figure 16. Sensible and latent heat gains from: building’s structure (section 3.1), refrigerated display cabinets (3.6), artificial lighting (3.7), people (3.5), infiltration (3.3), ventilation (3.2 and calculations described in section 5. Results) and air mixing (3.4) are summed and according to eq. (1) integrated into total enthalpy of air in zone 1. Next transformed equation (A5) from the appendix is used to calculate actual temperature in zone 1. The same procedure is used for zone 2 calculations, however no “Ventilation” subsystem is applied, because of the fact that all six heat exchangers and air suppliers are located in zone 1.

Block “Moisture” (fig. 17) calculates sources and sinks of moisture in zone 1 and eventually humidity ratio according to eq. (2). Algorithm calculating volumetric flow of additional fresh air is also included in that block. It is further sent to the “Air temperature” subsystem.

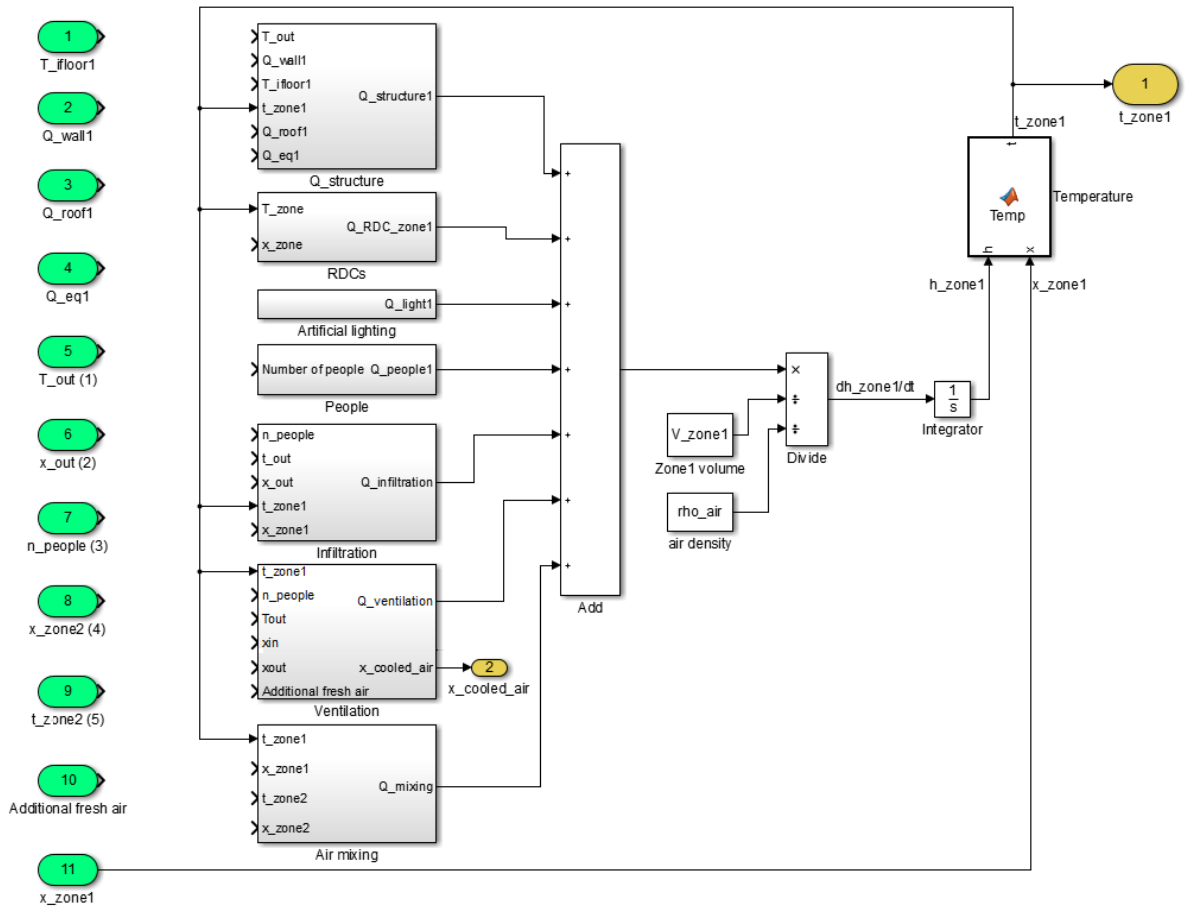

Figure 16. Air temperature subsystem in Zone 1 calculations.

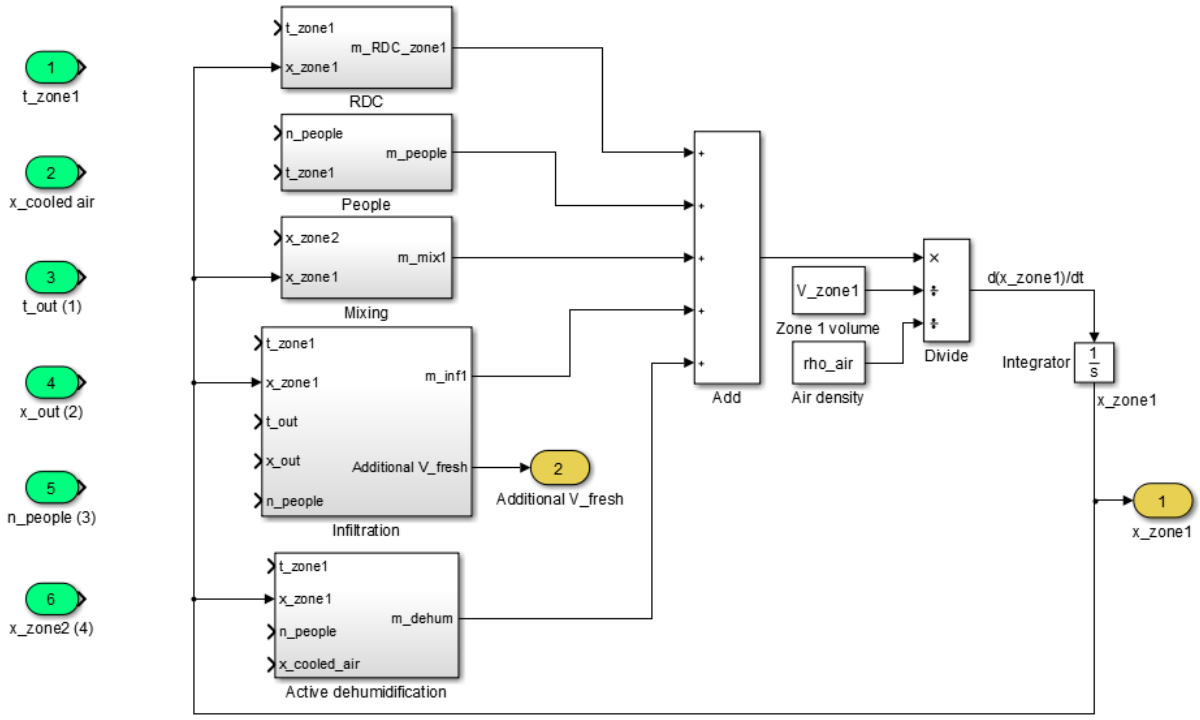

Figure 17. Moisture subsystem in Zone 1 calculations.

5. Model validation and results

This section presents stages of model's thermal and moisture accuracy development. Updates concern the ventilation control algorithm. All results are referred to the known performance of the supermarket: inside and outside temperatures and humidities.

Figure 18 shows real indoor climate of the supermarket over the whole year 2015. This chart shows some general trends. The general shopping area temperature is higher than temperature in the cold area. This temperatures are lower in winter and higher in summer. Relative humidity measured in the general shopping area fluctuates between about 45 and 70%. The outside temperature does not fall below -10 ^{o}C and does not exceed 38 ^{o}C. Table 6 presents statistical data about performance of the supermarket: mean values and standard deviations. It will be useful when comparing results of the simulation with reality.

	Real general shopping area temperature [^{o}C]	Real general shopping area relative humidity [%]	Real general shopping area humidity ratio [g/kg]
Mean value	19,80	57,82	8,32
Standard deviation	1,51	3,64	0,98

Table 6. Statistical data about real performance of the supermarket.

5.1. Simplest ventilation algorithm

The first attempt to simulate conditions in the supermarket was to set two constant temperatures of air over day and night, which the ventilation system tries to keep. The set temperature during day (from 6 am to 11 pm) is 21 ^{o}C and during night 17 ^{o}C. Ventilation system uses proportional algorithm with reinforcement factor 3, so there is a deviation. Heating power is limited by heating capacity of the heat exchangers and the capacity of the refrigeration system and heat pump – it is set to 28 kW. This approach represents low accuracy therefore remarks are made only for two representative weeks of the year – one in winter and one in summer.

Figures 19 and 20 show data for week 7 (from Monday to Sunday). In figure 19 you can see that both temperatures, simulated and real in general shopping zone, do not reach set 21 ^{o}C during the day. Temperature in the cold zone is slightly lower than in zone 1, which is true for the real supermarket's performance. However a rise of calculated temperature in zone 1 after the night mode is more steep as well as its drop after day mode. This could be due to assumption of perfectly mixed air in the whole zone or thermal inertia of heat exchangers in the ventilation system or some specific futures of the ventilation control system or refrigeration system constraints. There are days (during winter) when the simulation follows the real performance strictly. Steep changes of temperature influence the path of relative humidity (figure 20), because relative humidity is a function of both humidity ratio and temperature. Although relative humidity starts from lower value (the program shows dehumidification tendency during winter when supermarket is empty – during nights, on Sundays and holidays, because of supplying dry outside air and moisture sinks in RDCs), after a while it reaches a level very similar to the real performance and peaks occur when the set temperature is 17 ^{o}C. According to the simulation a dehumidification occurs on Sundays while it is not true in the real supermarket. The probable reason for that is the use of spray humidifiers in the fruit & vegetable area, which increase the absolute humidity of supermarket's air. They are applied in order to prevent fruit and vegetables from dehumidification – losing weight and appearance. They are not simulated in the model.

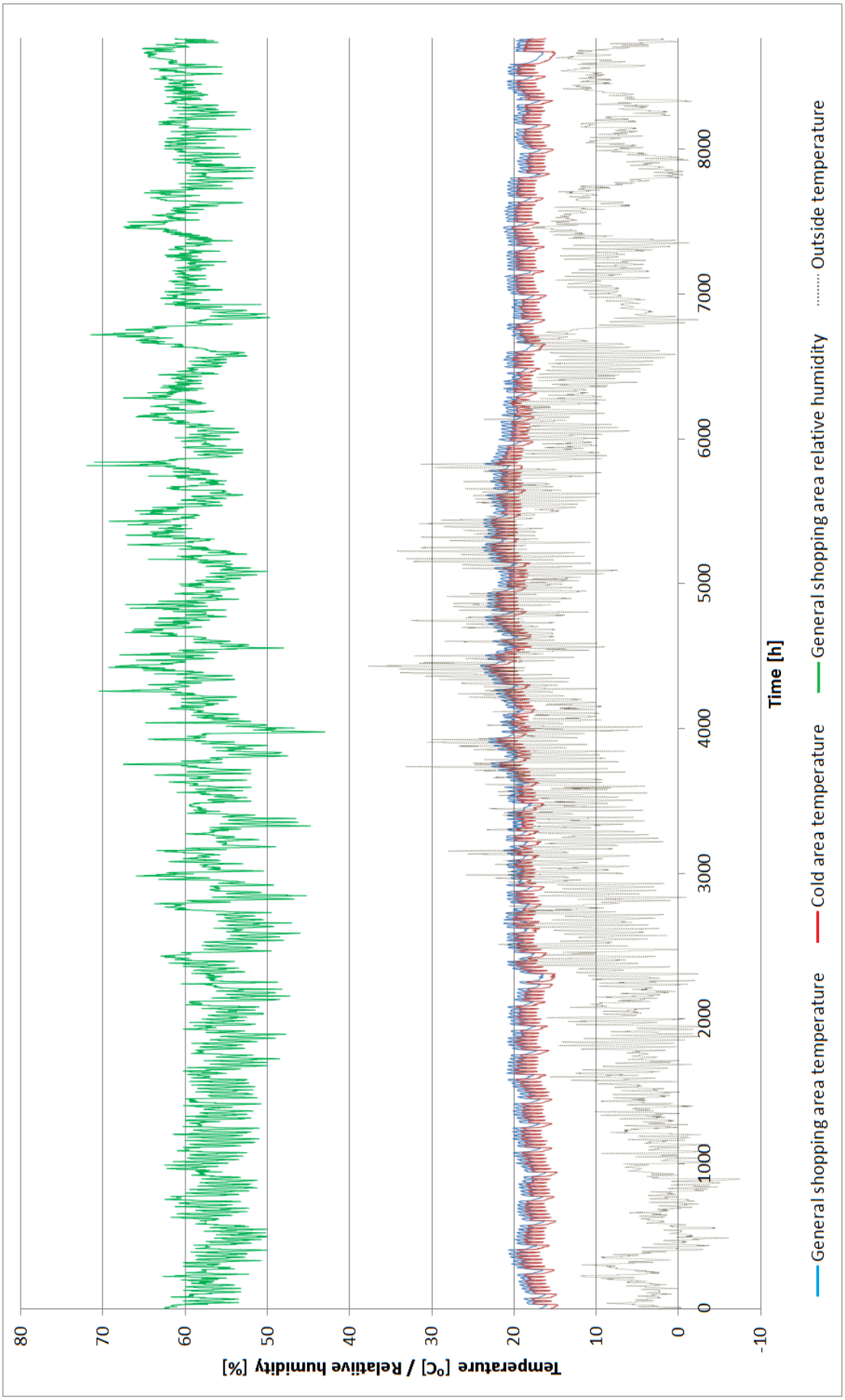

Figure 18. Performance of the real supermarket.

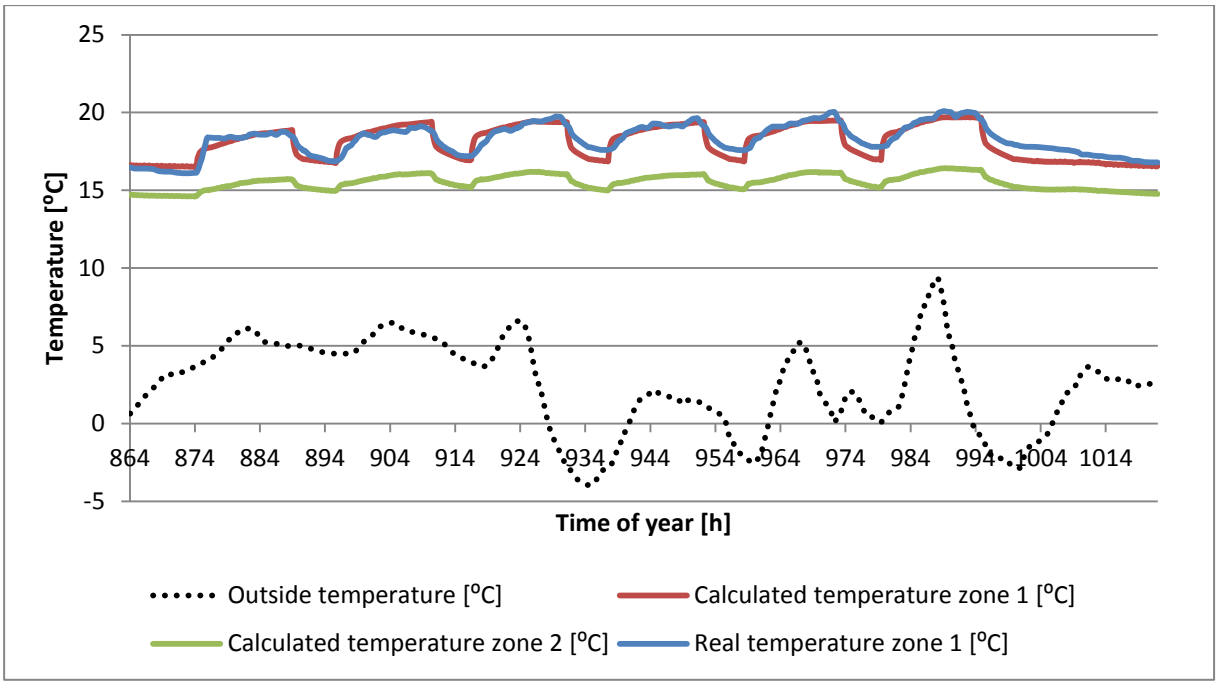

Figure 19. Results of thermal calculations for week 7.

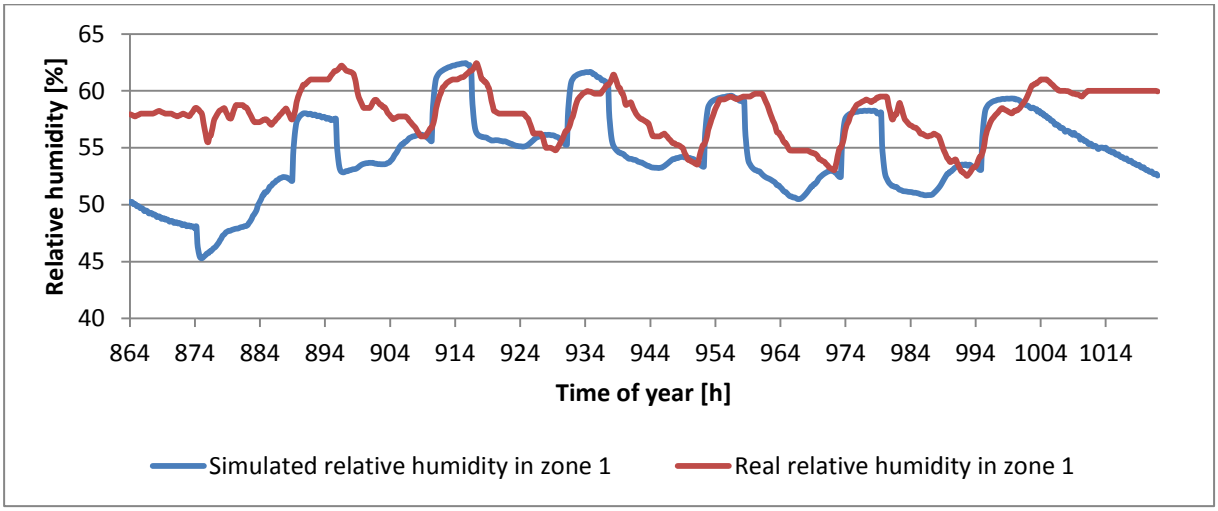

Figure 20. Results of indoor relative humidity calculations for week 7.

Figures 21 and 22 show data for week 28 (from Monday to Sunday). During this week the highest outside temperature in the whole year occurred: 38 °C. It is clear that the simulation and reality do not converge here well. Most obvious difference concerns relative humidity. In the real supermarket it does not exceed 70%, while the simulations shows much higher level of relative humidity fluctuating around 90% during the time from Monday to Friday's morning. Starting from Friday evening it exceeds 100% which is physically impossible and condensation would occur. This must be caused by three factors: more people visiting the shop on Friday and Saturday, high absolute humidity of outside air which is supplied to interior through ventilation or infiltration and lack of dehumidification methods. Another difference concerns temperature of inside air, because it is visibly lower than the real temperature. The real temperature in the supermarket is retained higher than the assumed basic set temperature in order to decrease the relative humidity. The calculated inside temperature in zone 1 resembles the temperature calculated for winter, however it reaches

the set point of 21 °C – it indicates very low or none need for heating at some points of the day. The real temperature in zone 1 increases up to 24 °C. It is remarkable that the simulation has not shown any need for cooling, because the inside temperature does not rise excessively (it does not exceed the real temperature). This remark will be elaborated in section 5.4.

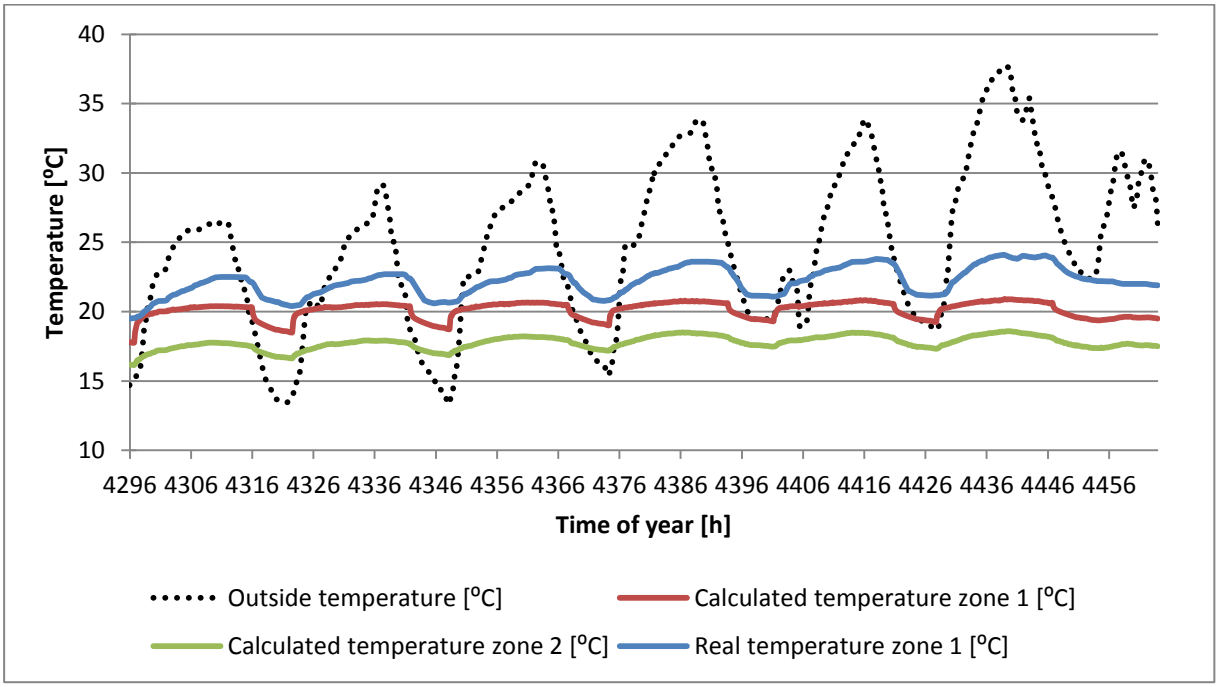

Figure 21. Results of thermal calculations for week 28.

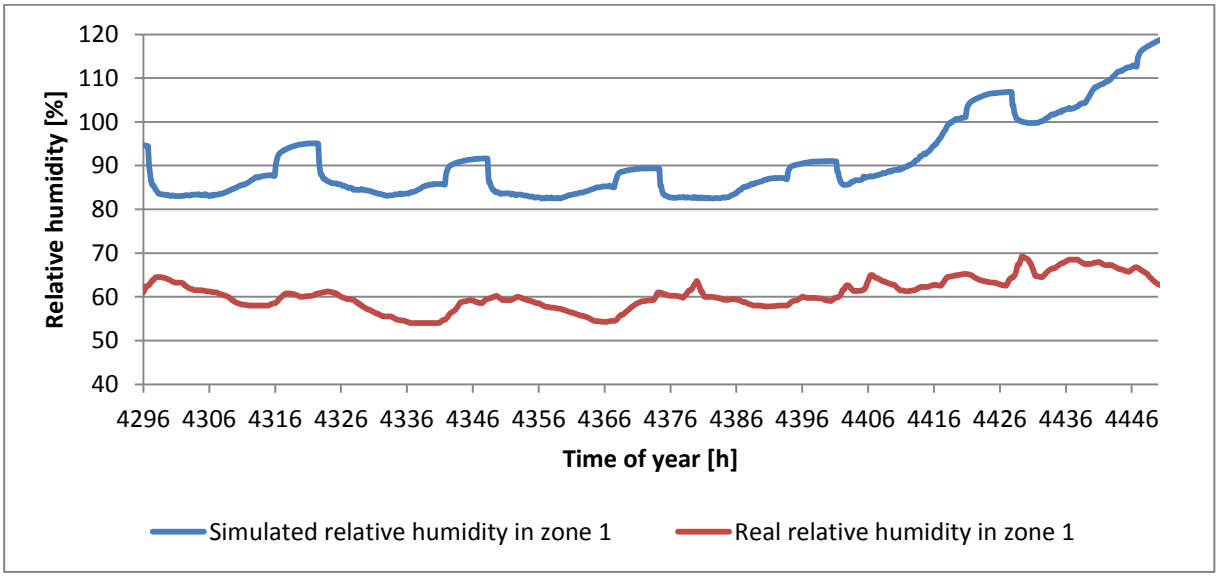

Figure 22. Results of moisture calculations for week 28.

5.2. Passive dehumidification

The ventilation system is able to adjust amount of fresh air supplied to the supermarket depending on the relative humidity and CO_2 concentration inside the supermarket. Figure 23 shows when and how much additional fresh air is supplied in the real supermarket. Additional fresh air means adjustable amount of fresh air, which is supplied apart from basic volume of fresh air. In the figure

value 0 V means closed additional fresh air damper and therefore zero flow. Value 10 V means fully open damper and maximum fresh air flow. Outside temperature is presented for reference as it shows that additional fresh air is mainly supplied during warm season.

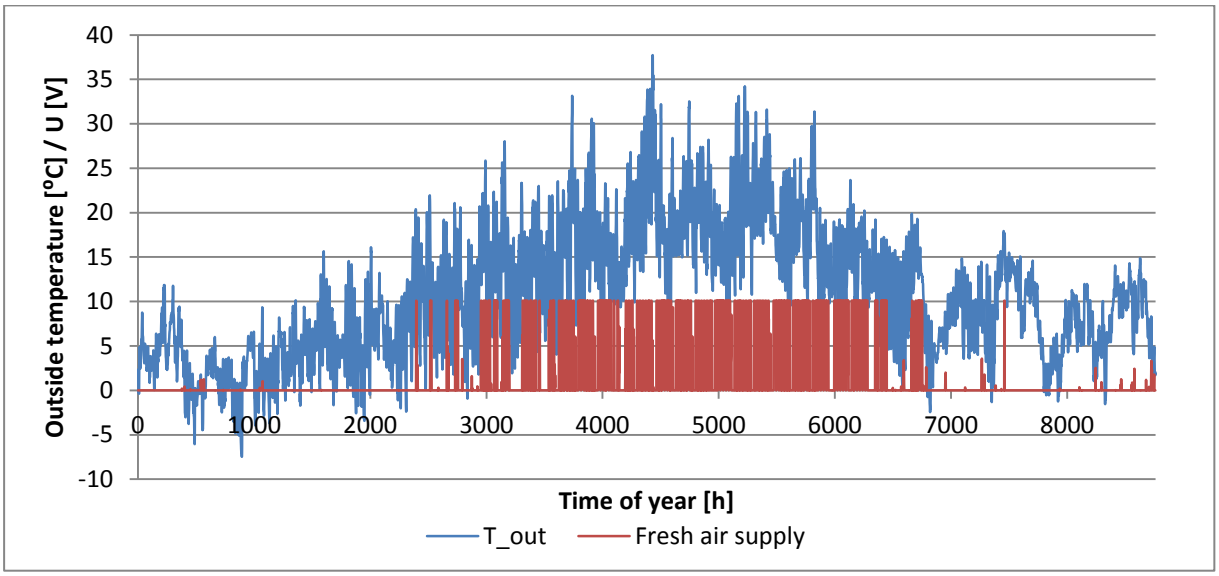

Figure 23. Amount of additional fresh air supplied in the real supermarket.

However CO_2 concentration is not considered in the created model, so the amount of supplied fresh air is controlled by the need to dehumidify inside air. This function of ventilation system is called passive dehumidification. Such fresh air can be of course still heated or cooled, because it passes through heat exchangers.

An algorithm determining additional flow of fresh air is described in the supermarket's documentation and it is presented in figure 24. Maximum volumetric flow of additional fresh air is:

$$\dot{V}_{add\_max} = 0{,}4\frac{m^3}{s} = 1440\frac{m^3}{h}$$

There are some constraints put in the model and limiting additional flow of fresh air in order to perform dehumidification. These are:

1. Inside relative humidity higher than 50%
2. Outside humidity ratio lower than inside humidity ratio: $x_{amb} < x_{zone}$
3. Inside temperature higher than 17 °C

If inside relative humidity exceeds 65%, the control algorithm looks as shown in figure 25, still concerning conditions 2. and 3. described above.

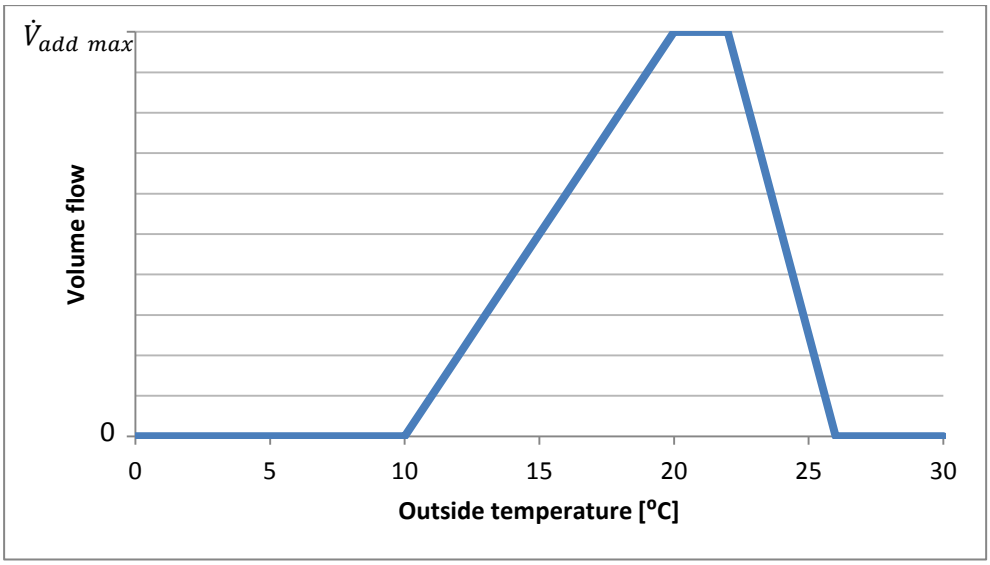

Figure 24. Additional fresh air volumetric flow in function of outside temperature for intermediate inside humidity.

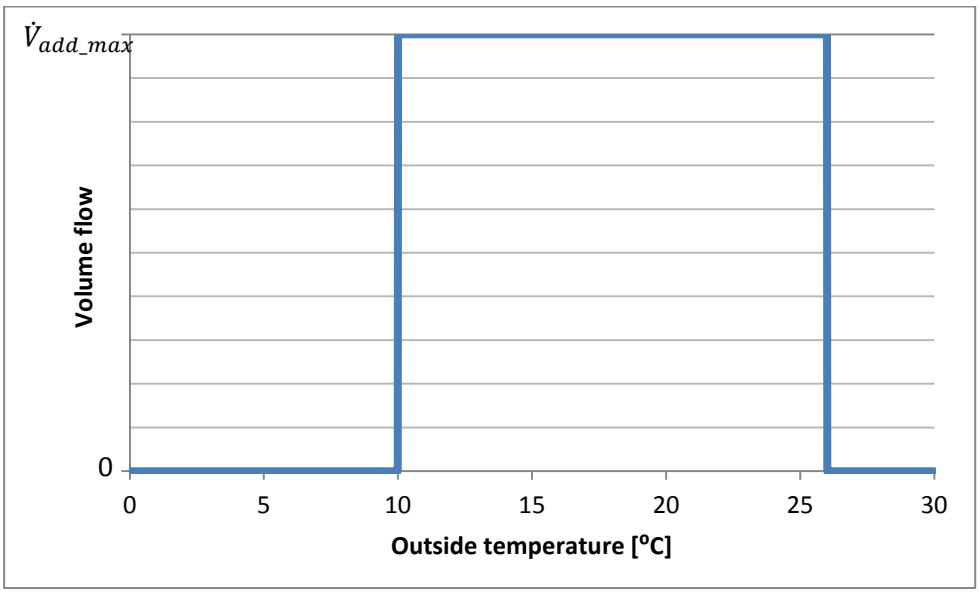

Figure 25. Additional fresh air volumetric flow in function of outside temperature for high inside humidity.

Implementing passive dehumidification into created model allowed to decrease relative humidity inside the supermarket. Instead of 35 days when relative humidity in zone 1 was above an unrealistic value 100% in the previous version of the model, it is reduced to 4 days. Figure 26 presents results of the simulation. Fresh air supply represents amount of additional fresh air supplied to the supermarket and value -10 means zero flow and value 0 means maximum flow (values adapted for clarity). Table 7 presents statistical data about simulated parameters. The general shopping area (zone 1) temperature mean value and standard deviation are lower than the real ones. It proves less diverse profile of simulated temperature (zone 1 temperature fluctuates between 17 and 21 °C). In summer calculated temperature is lower than the measured one, which is discussed in the next

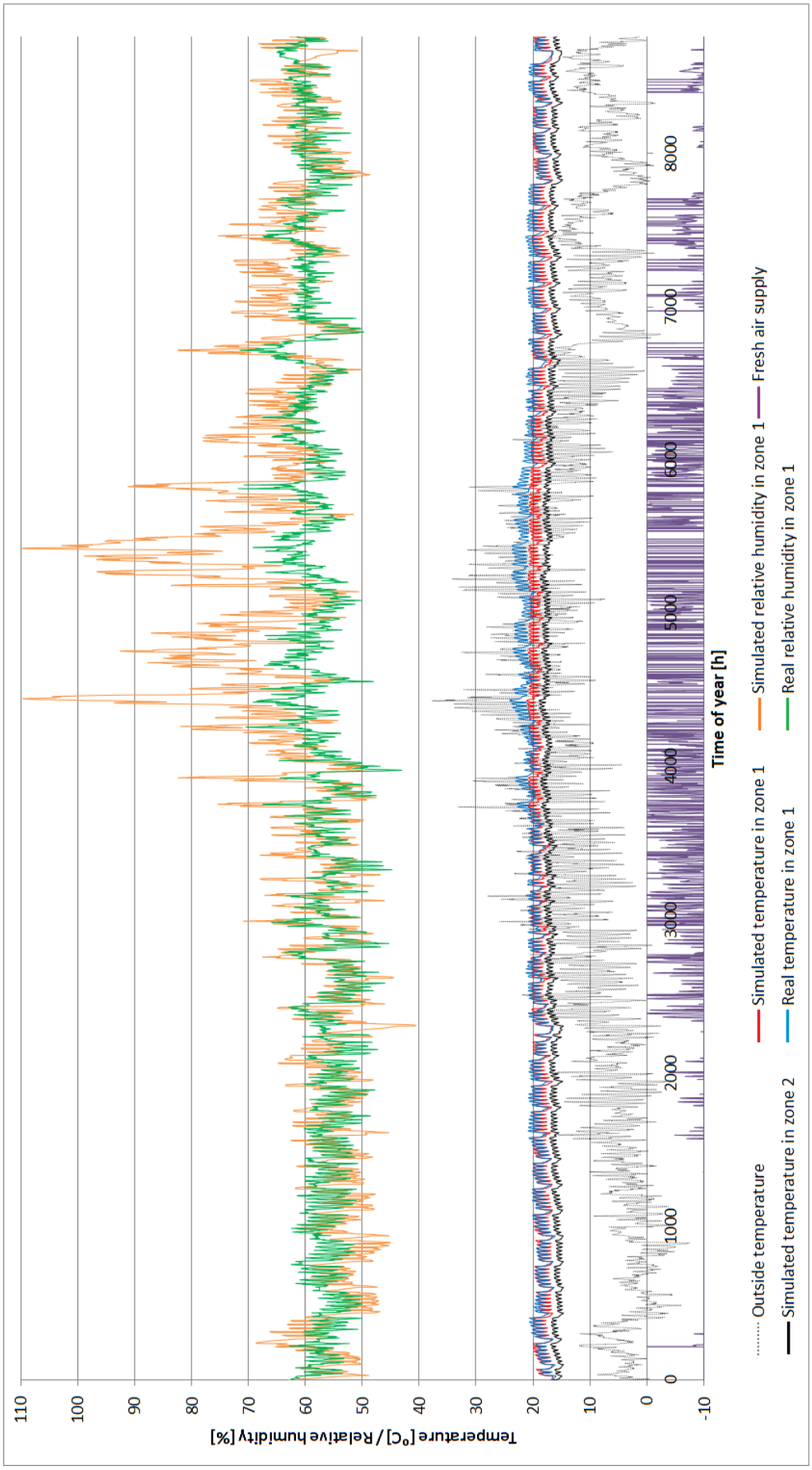

Figure 26. Results of the simulation of passive dehumidification with marked real performance.

section. Mean value and standard deviation of relative humidity in zone 1 are higher than the real values, because relative humidity still reaches much higher values in summer.

Model 5.2.	General shopping area temperature [°C]		General shopping area relative humidity [%]	
	Simulation	Measurement	Simulation	Measurement
Mean value	19,19	19,80	60,95	57,82
Standard deviation	1,12	1,51	9,54	3,64

Table 7. Statistical data about parameters simulated in model 5.2.

5.3. Adjustable temperature

Another feature of the ventilation control system is adjustable temperature. This module modifies the set temperature in order to prevent excessive rise of relative humidity. This is mainly useful during warm and humid seasons. The introduced algorithm adjusts the set temperature depending on inside air absolute humidity [kg/kg] in order to prevent coupling with dehumidification systems (passive and active), which use relative humidity. It could cause an undesirable rise in relative humidity.

The algorithm operates at 3 characteristic points (humidity ratios defined basing on temperature and relative humidity):

1. $x_1(17℃, 60\%) = 0{,}0072 \frac{kg}{kg}$
2. $x_2(21℃, 60\%) = 0{,}0092 \frac{kg}{kg}$
3. $x_3(24℃, 60\%) = 0{,}0111 \frac{kg}{kg}$

Then, similarly to constant temperature set point algorithm from previous sections, different set temperatures for day and night modes are determined. The procedure looks as follows (a subscript 'in' means actual inside air):

- Night mode:
  $t_{set_0} = 17℃;\ t_{set} \in \langle 17; 21 \rangle$
  $x_{in} > x_1 \ \Rightarrow \ t_{set} = t_{set_0} + 4 \frac{x_{in} - x_1}{x_2 - x_1}$ (62)
- Day mode:
  $t_{set_0} = 21℃;\ t_{set} \in \langle 21; 24 \rangle$
  $x_{in} > x_2 \ \Rightarrow \ t_{set} = t_{set_0} + 2{,}9 \cdot \frac{x_{in} - x_2}{x_3 - x_2}$ (63)

Implementation of adjustable set temperature algorithm into the model allowed to decrease peaks of relative humidity to the feasible value of 100% as presented in figure 27. Statistical data about temperature and relative humidity in zone 1 is presented in table 8. In comparison to real performance data, the mean temperature is different by 0,05% and relative humidity by 3,7% of relative error. Difference in standard deviation is 4% for temperature. Standard deviation of relative humidity is almost two times higher than measured value, however a significant drop compared to previous model is observed. Due to inaccuracy in humidity calculations active dehumidification module is applied, which is described in next section.

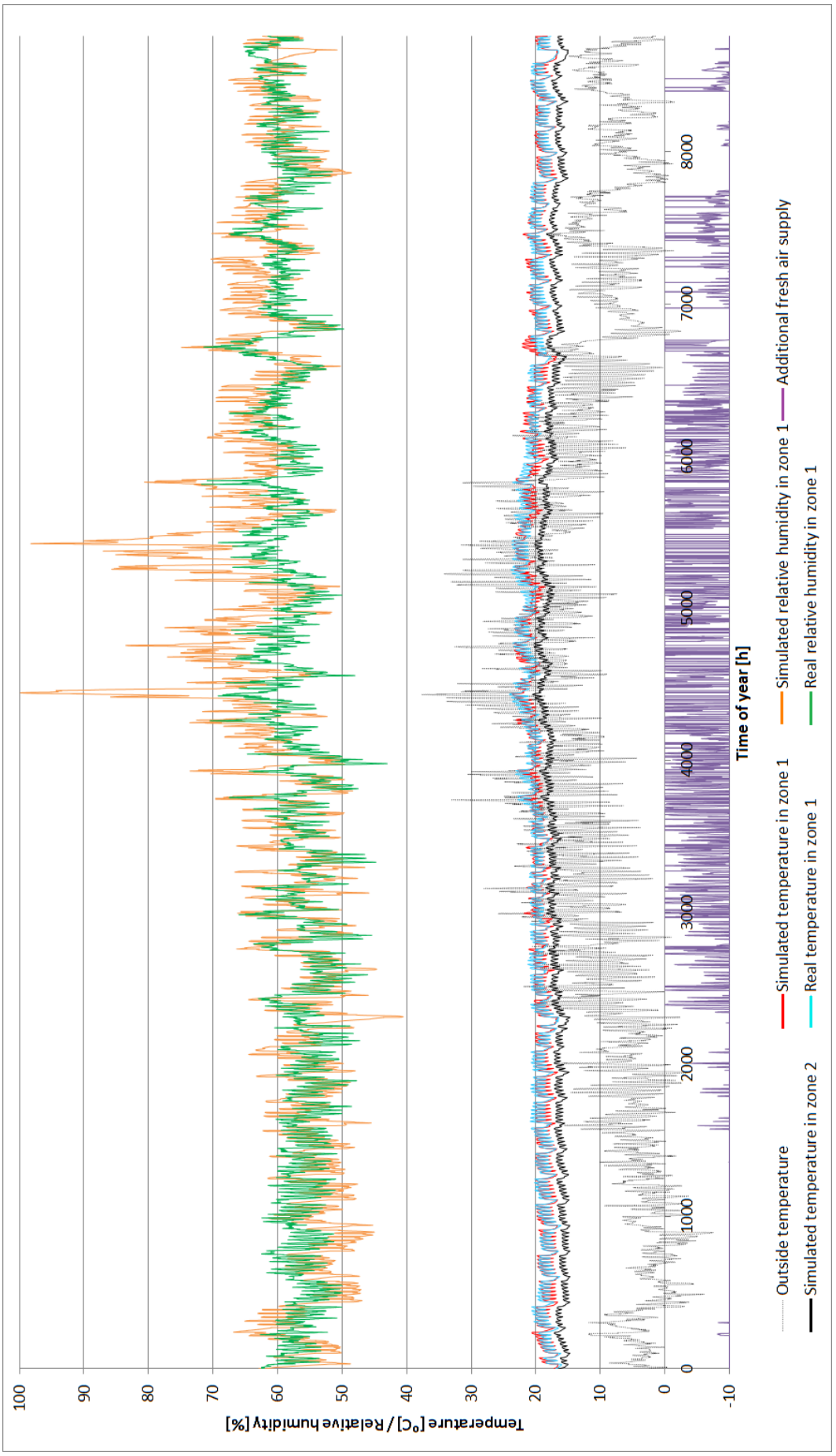

Figure 27. Results of the simulation of adjustable temperature model with marked real performance.

Model 5.3.	General shopping area temperature [°C]		General shopping area relative humidity [%]	
	Simulation	Measurement	Simulation	Measurement
Mean value	19,81	19,80	59,95	57,82
Standard deviation	1,45	1,51	7,1	3,64

Table 8. Statistical data about parameters simulated in model 5.3.

5.4. Active dehumidification

The last method of decreasing relative humidity in the supermarket is active dehumidification. It works in the following way: recirculating air flows through cold heat exchanger and becomes colder and drier, because some part of vapour present in air condenses and then is removed. The same process occurs in RDCs, which also dehumidify supermarket's air.

In the considered supermarket five heat exchangers may work both as heaters and coolers, but each of them can perform only one of these functions at the same time. The sixth heat exchanger – air curtain installed at the main entrance – may only heat air. It happens so, that during ventilation system operation some of heat exchangers may supply cold air and some of them warm air in order to satisfy heat and moisture balances.

An algorithm applied in the model assumes that one heat exchanger may perform as a cooler, which turns out to be enough. Constant air volume (CAV) system is applied in the supermarket, therefore constant amount of air flows through that heat exchanger and equals 1/6 of the total supply air flow. This air stream cannot be heated again. In order to satisfy dehumidification need the temperature of the coil is changing. The assumed cool air volumetric flow is:

$$\dot{V}_{dehum} = \frac{1}{6} \cdot 22270 \approx 3710 \frac{m^3}{h} = 1{,}03 \frac{m^3}{s}$$

Bohdal et al. [10] advice that when cooling air the temperature difference between air at the inlet and evaporating refrigerant should be within range 10 ÷ 15 °C. Therefore maximum temperature for refrigerant evaporation is 13 °C and minimum 4 °C (falling below 0 °C would lead to accumulation of frost). The temperature of air at the outlet will be lower than at the inlet, but higher than refrigerant temperature. It is assumed to be 4 °C higher than the refrigerant temperature.

Active dehumidification is carried out during day mode in order to avoid coupling with passive dehumidification which occurs mostly during nights. Evaporation temperature is set according to equation:

$$t_{evap} = 78 - \varphi_{zone} \ [°C] \tag{64}$$

for $\varphi_{zone} > 65\%$. Moreover $t_{evap} \in \langle 4; 13 \rangle$ and temperature of air leaving heat exchanger equals:

$$t_{air} = t_{evap} + 4 \ [°C] \tag{65}$$

The way of determining mass flow of condensate acquired from supermarket's air is similar to the way presented for RDCs in section 3.6.1, however the temperature of evaporator and air leaving the heat exchanger alters. The dehumidification process is presented in the Mollier diagram in figure 28.

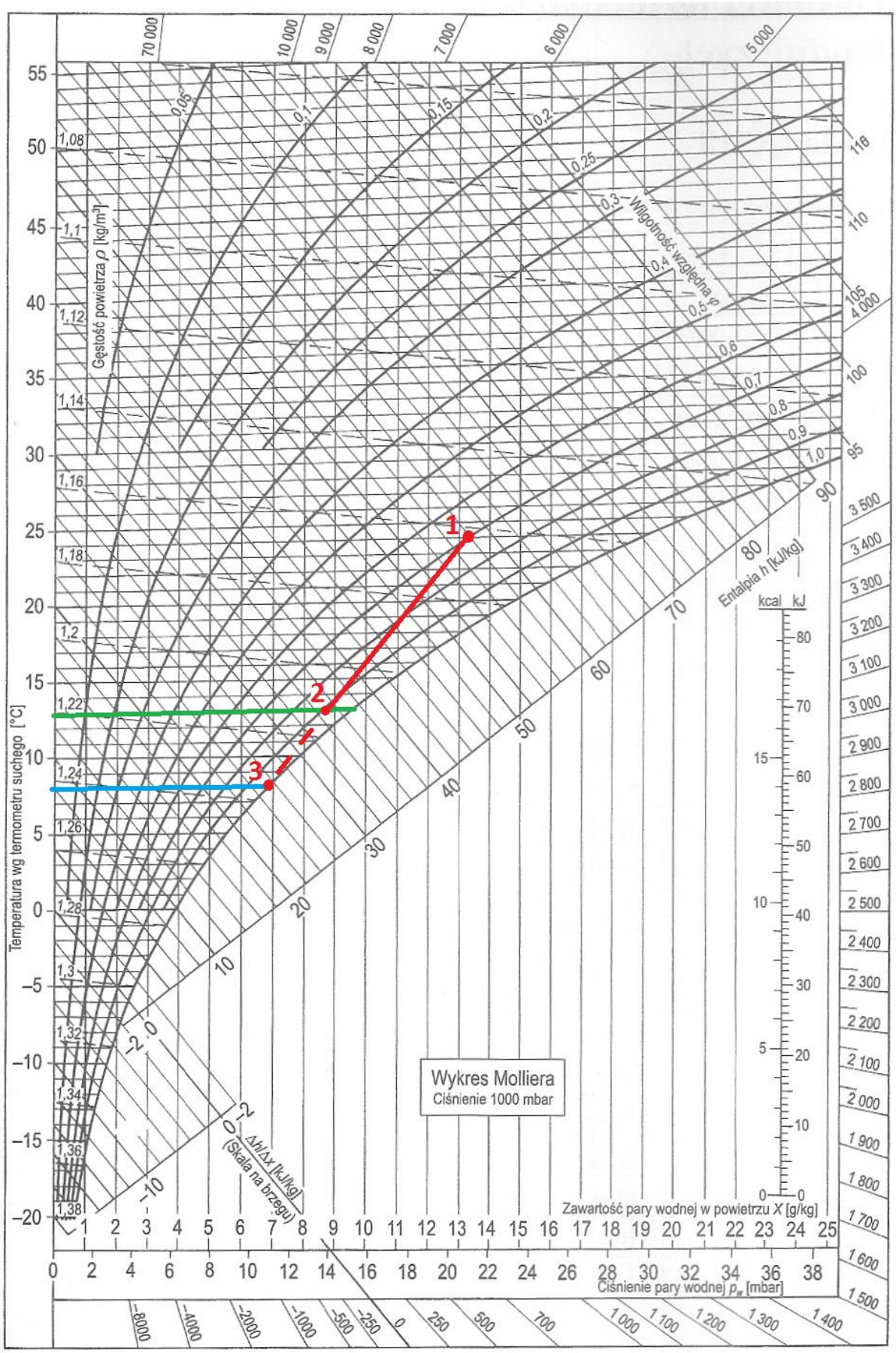

Figure 28. Active dehumidification process in the Mollier diagram.

Assuming that dry bulb temperature lines are perpendicular to the humidity ratio lines in the Mollier diagram, humidity ratio at point 2 (air leaving the heat exchanger) can be calculated. Inside air (point 1) parameters are known as well as conditions very close to the evaporator (point 3), which are always at saturation line. Then:

$$x_2 = x_3 + \frac{x_1 - x_3}{t_1 - t_3}(t_2 - t_3)\left[\frac{kg}{kg}\right] \quad (66)$$

And dehumidified air's humidity ratio x_2 is within range $\langle x_3;\ x_{2_{sat}}\rangle$, where $x_{2_{sat}}$ is humidity ratio at temperature t_2 in saturation conditions (relative humidity 100%). Next the dehumidification rate, meaning mass flow of vapour removed from air, is determined assuming constant air density (subscripts same as in figure 22):

$$\dot{m}_{dehum} = \dot{V}_{dehum} \cdot \rho \cdot (x_2 - x_1)\ \left[\frac{kg}{s}\right] \quad (67)$$

This parameter has a negative value and is added to the right side of vapour mass balance (eq. 2). Heat sink for the supermarket is calculated in the following way (subscripts same as in figure 25):

$$\dot{Q}_{dehum} = \dot{V}_{dehum} \cdot \rho \cdot (h_2 - h_1)\ [W] \quad (68)$$

Above equation takes into consideration sensible and latent heat flux and is added to the right side of supermarket's heat balance (eq. 1). Enthalpies h_1 and h_2 are calculated according to equation A5 from the appendix.

The simulation has shown that active dehumidification occurs during about 248 hours, which is 2,84 % of the whole year. In reality active dehumidification was carried out for 194 hours, which is 2,21 % of the whole year. Although the relative error is 28 %, such result seems to be possible and within acceptable error.

Results of the final model, which comprises passive dehumidification, adjustable amount of fresh air algorithm and active dehumidification, are presented in figures 29-35. Figure 29 presents yearly results of the simulation with marked real performance. In contrary to previous figures of the same type (figures 26 and 27) simulated relative humidity is within a feasible range, because it doesn't exceed 80%. Moreover value of this parameter reaches at most 77,9 %, while maximum real value of relative humidity in zone 1 is 71,8 %. This excessive rise happened due to a gap in work of both passive and active dehumidification system. The first one was turned off, because of too high outside humidity ratio and the second one, because it was night and the introduced algorithm states that active dehumidification occurs only during day mode. Statistical data presented in table 9 shows that annual mean value of the relative humidity is only 0,5 % different from the real value (compare table 6). Standard deviation is higher, but still much lower than for previous versions of the model, e.g. almost two times lower compared to "passive dehumidification" model. It shows that fluctuation of simulated relative humidity was higher than in reality. However relative humidity is a resultant of temperature and absolute humidity, therefore results of absolute humidity are more reliable, although relative humidity counts for the supermarket's environment. The average value of relative humidity is visibly higher in summer than in winter. This is due to higher humidity of outside air.

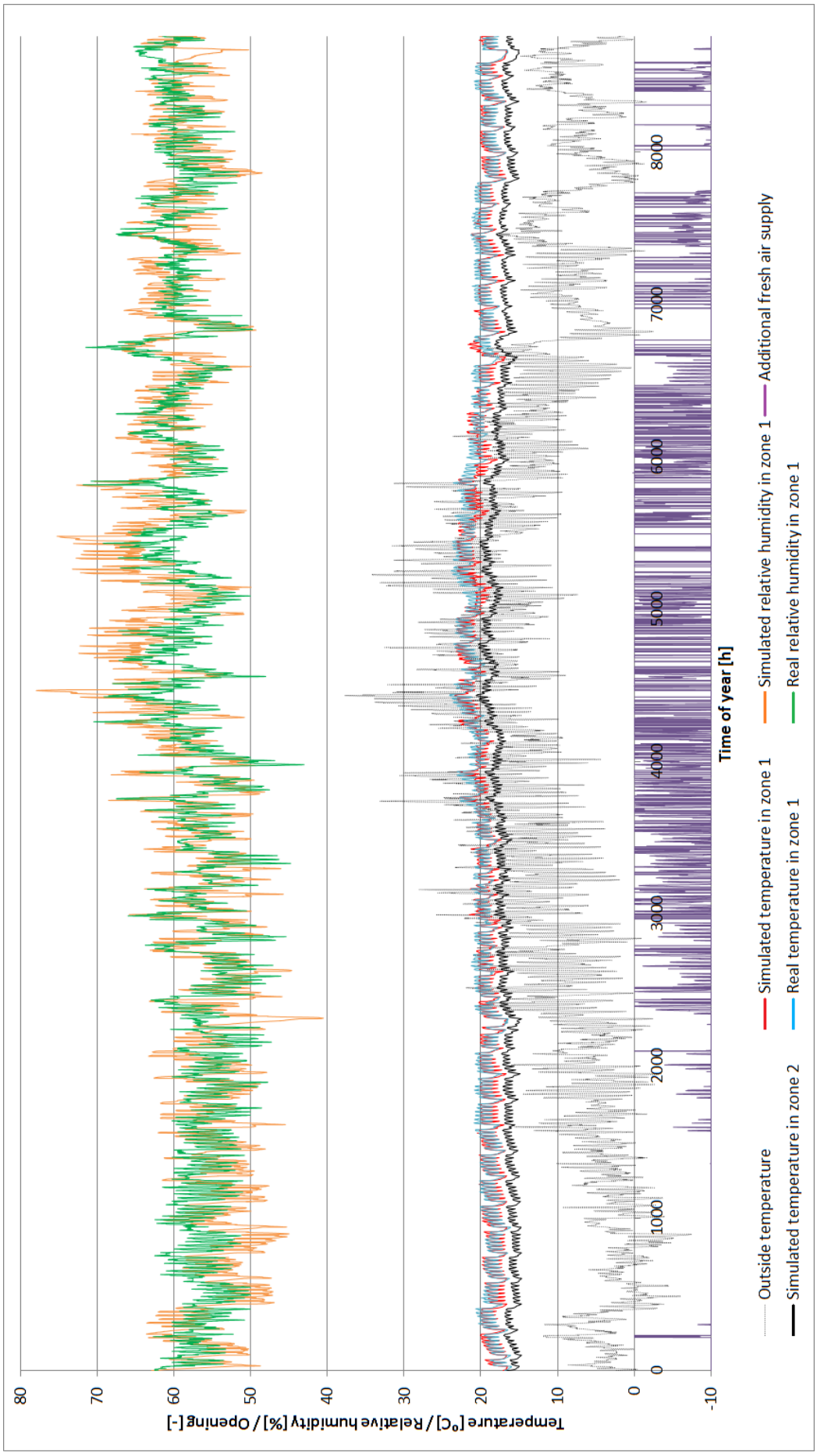

Figure 29. Results of annual simulation of the active dehumidification model with marked real parameters.

Annual mean value of temperature in zone 1 is only 0,8 % different from the real value. Relative error in standard deviation is 8,7 %, which is a low value and could be caused by e.g. a more sophisticated ventilation control algorithm applied in the supermarket.

Model 5.4.	General shopping area temperature [^{o}C]		General shopping area relative humidity [%]		General shopping area humidity ratio [g/kg]	
	Simulation	Measurement	Simulation	Measurement	Simulation	Measurement
Mean value	19,66	19,80	58,09	57,82	8,3	8,32
Standard deviation	1,38	1,51	5,30	3,64	1,27	0,98

Table 9. Annual statistical data about parameters simulated in model 5.4.

As mentioned before, maximum value of simulated relative humidity in zone 1 was higher than the real value, which was not a case for humidity ratio. Simulated humidity ratio reached at most 12,1 g/kg and maximum value of real humidity ratio was 12,7 g/kg. Mean value of the general shopping area humidity ratio is almost the same as real value (table 9), however standard deviation is 30% higher. A reason for that may be determining too high stream of outside air coming into the supermarket through ventilation or infiltration, which led to higher deviations in humidity ratio. What is interesting, simulated humidity ratios in zone 1 and 2 were identical at the chosen rate of mixing air between zones.

In order to show the results in better detail, figures 30 to 35 present two-week long fragments of the simulation results for winter and summer time.

Figures 30, 31 and 32 present data for weeks 5 and 6, when the lowest temperature during the whole year occurred. Figure 30 shows that simulation illustrates well the day and night modes and the calculated temperature reaches the same levels as the real one. Its line is more “smooth” and predictable, because no random events are taken into consideration. Moreover growth and drop of simulated temperature is more steep. This might be due to the assumption of well mixed air in a zone, which is not necessarily truth in the real building, particularly so high.

Figure 31 presents difference between simulated temperature and real one in zone 1. The peaks are connected with mentioned steep changes of temperature. The difference generally does not exceed 1 ^{o}C in absolute units. Moreover, during these two weeks the mean value and standard deviation were 18,2 ^{o}C and 1,06 ^{o}C for simulated temperature in zone 1 and 18,14 ^{o}C and 0,93 ^{o}C for real temperature in zone 1. It shows that the simulation reproduced the temperature well.

Figure 32 presents simulated, real and outside humidity ratio. Outside climate was dry, therefore ventilation and infiltration would have provided only moisture loss. Other significant sources of moisture must have appeared in the supermarket, e.g. humans. Path of the calculated parameter is more smooth than the real one, which may result from considering too few phenomena influencing moisture balance in the supermarket. Peaks are delayed and excessive drop in simulated humidity ratio occurs on Sundays, when the store is closed for longer time. Ranges of fluctuation are similar during the first of presented weeks, however in the second one simulated parameter has slightly lower values – this was caused by excessive humidity ratio drop during preceding Sunday. Interestingly there is no clear correlation between outside humidity ratio and the real one in zone 1.

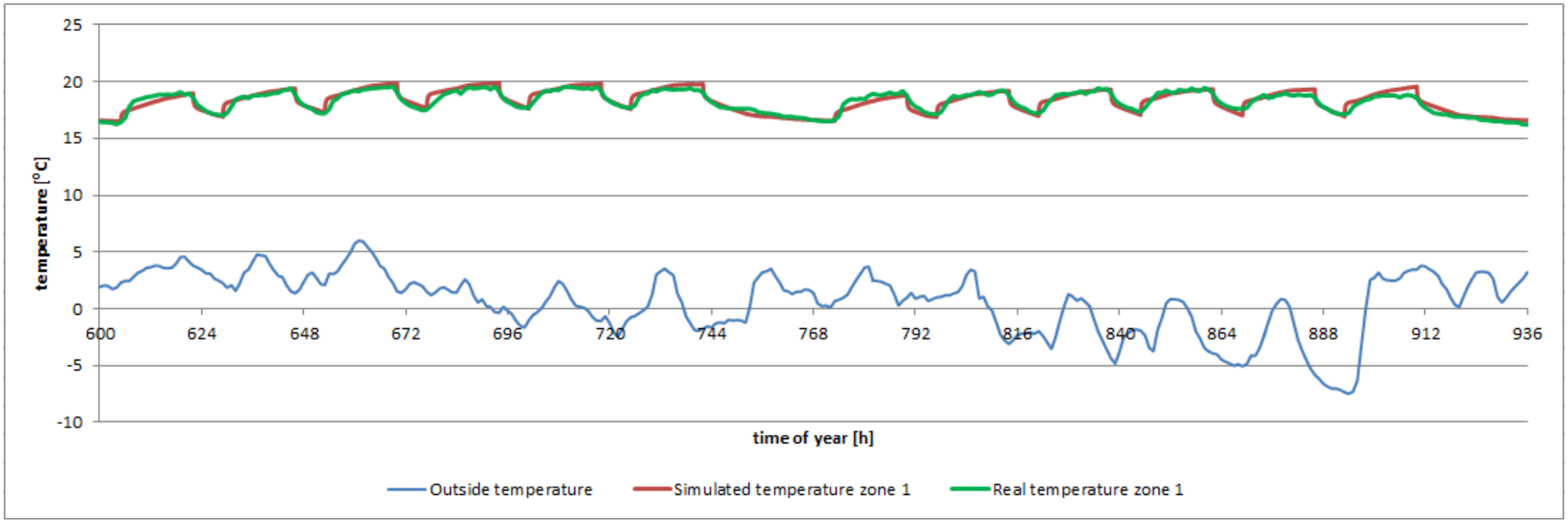

Figure 30. Temperature simulated in the supermarket's zone 1 in weeks 5 and 6

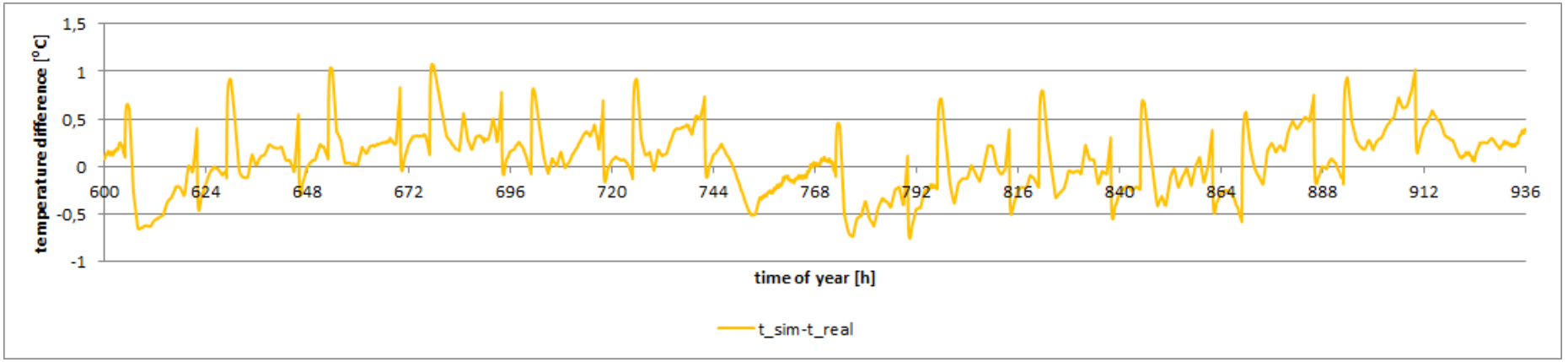

Figure 31. Temperature difference between simulated and real temperature in the supermarket in weeks 5 and 6.

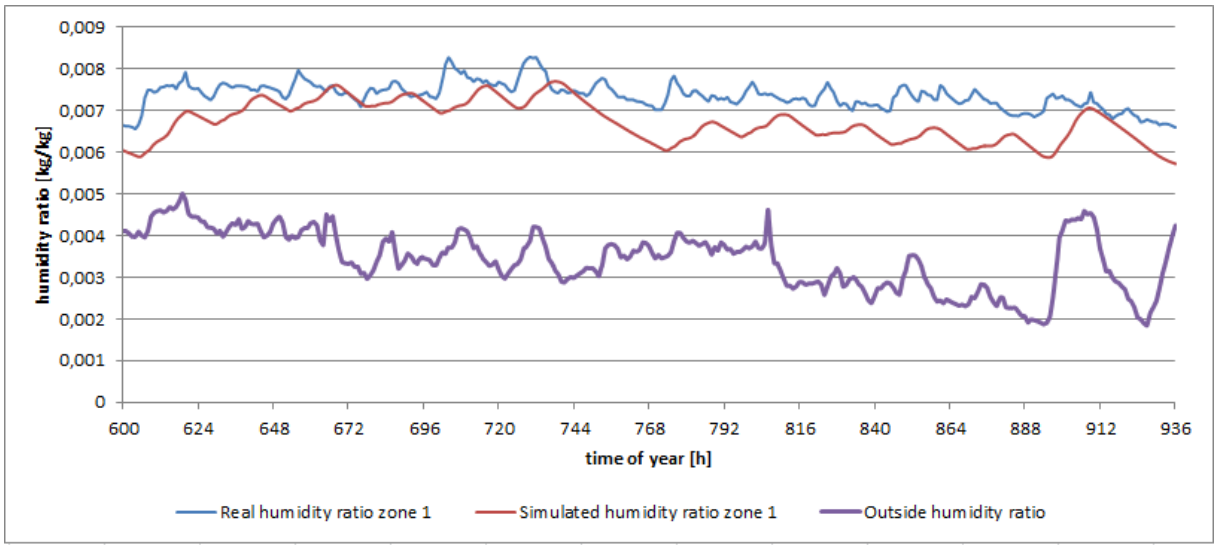

Figure 32. Humidity ratio in the supermarket in weeks 5 and 6.

Figures 33, 34 and 35 present data for weeks 25 and 26, when the highest temperature during the whole year occurred. The temperature inside the supermarket is dynamically adjusted (fig. 33) and the opening of fresh air damper is changing too (purple line) – value 0 V means closed damper and 10 V fully open. Profile of the temperature is irregular and higher values were reached during week 26, when outside temperature was higher and outside humidity ratio was higher too particularly during 3 last days of that period. The mean value of simulated temperature was 21,23 ^{o}C and mean value of real temperature was 21,43 ^{o}C. Difference between simulated and real temperature was within range of 1,5 ^{o}C in absolute numbers (fig. 34). These differences were higher than in winter time (compare fig. 31) because of changing set temperature. The algorithm was not obtained from supermarket's documentation, but created by author of this work, which leads to some uncertainties. Moreover set temperature depends on absolute humidity in the supermarket, which in turn depends on more factors which clearly leads to more uncertainties.

The simulation did not show passive dehumidification during two last days of the presented period, because of high outside humidity. Together with the assumption that active dehumidification occurs only in day mode, it led to excessive rise of humidity on last Sunday of considered period (fig. 35). Mean values of simulated and real humidity ratio were 0,0098 and 0,0096 kg/kg respectively. Their standard deviations were 0,00119 for simulated parameter and 0,00103 for the real one. It shows that simulated humidity ratio was fluctuating more. Peaks were postponed and occurred in the evening while in reality humidity ratio was more or less uniform during day. In both cases humidity ratio decreased during night mode. On the first Saturday and second Friday and Saturday active dehumidification is visible – small fluctuations at a similar level of humidity ratio occur. Generally simulated and real humidity ratio had similar ranges. The biggest difference concerns second Sunday when applied algorithms forbad effective dehumidification of the supermarket.

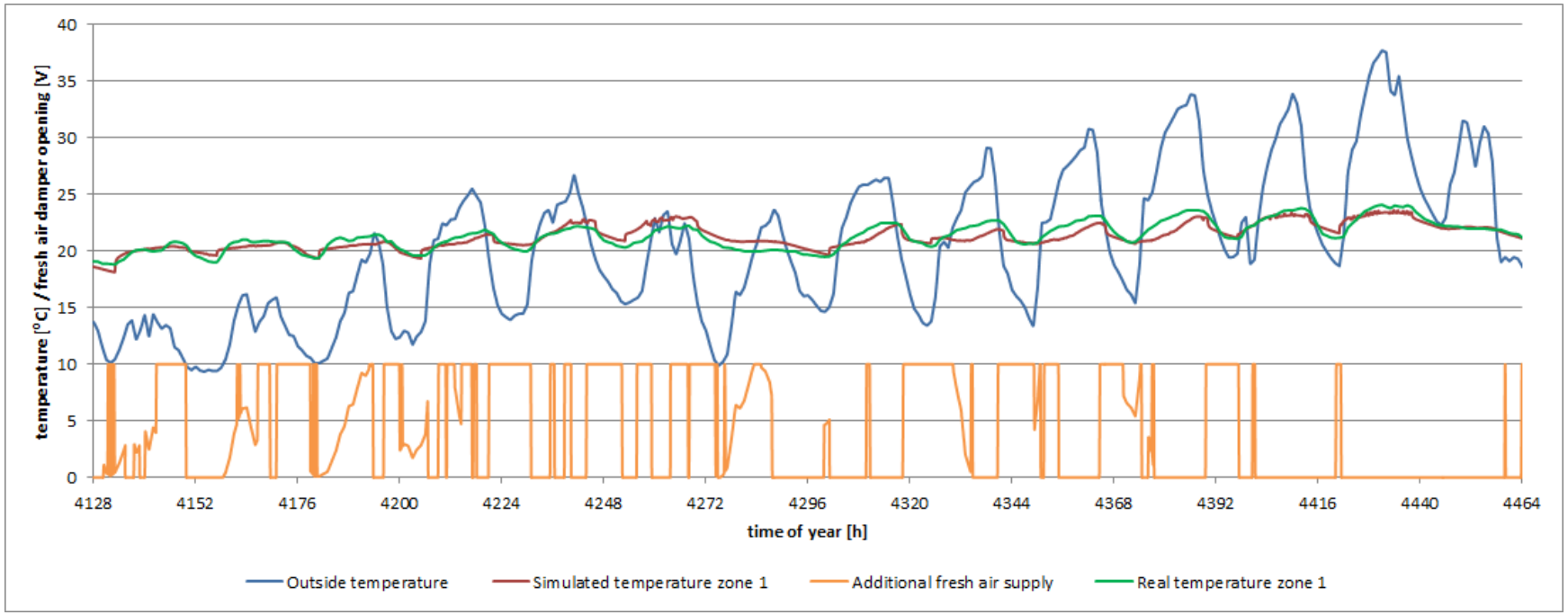

Figure 33. Simulated temperature in the supermarket in weeks 25 and 26.

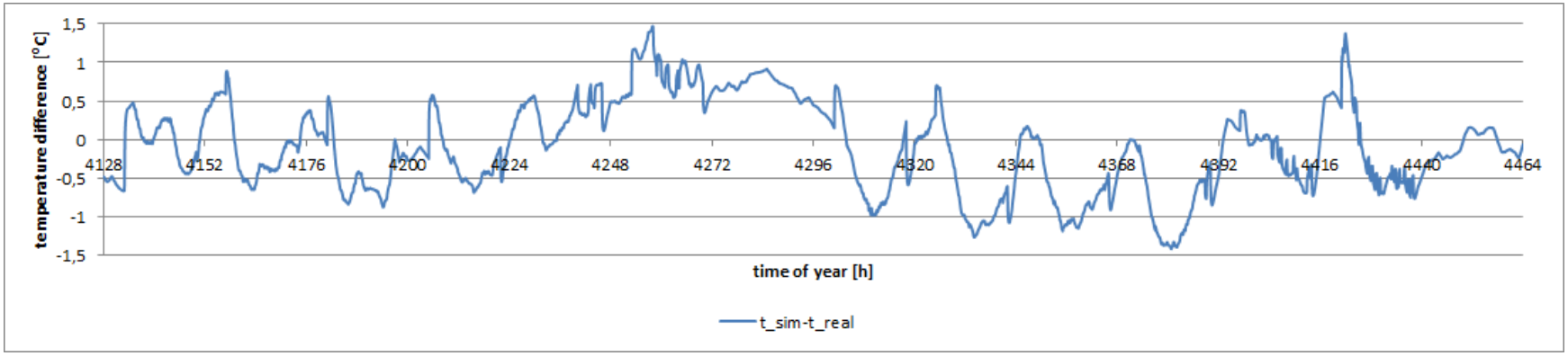

Figure 34. Difference between simulated and real temperature in the supermarket in weeks 25 and 26.

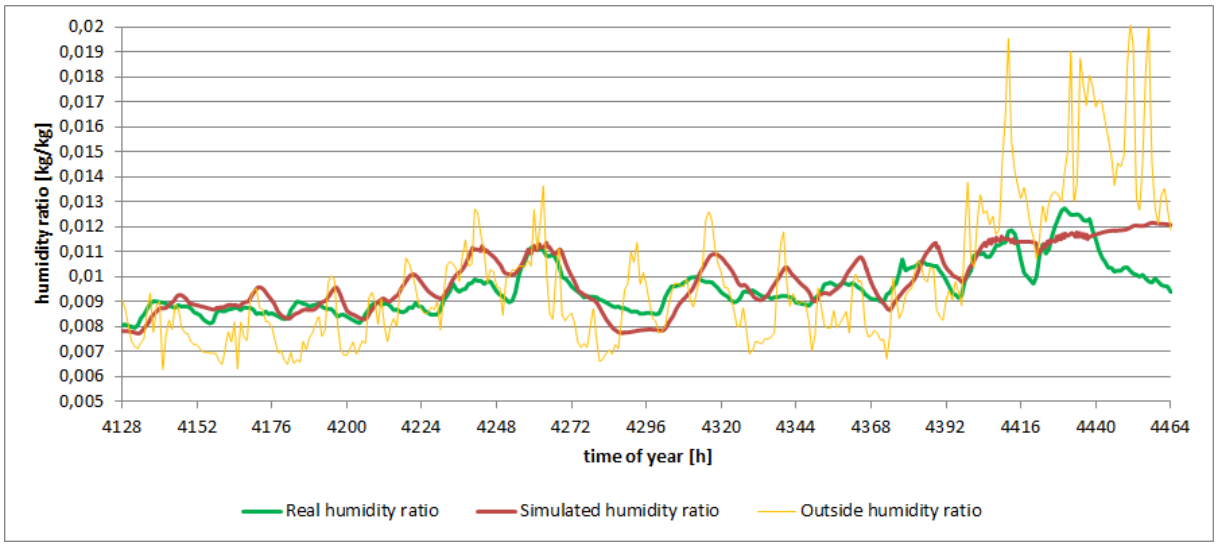

Figure 35. Humidity ratio in the supermarket in weeks 25 and 26.

Figure 36 presents components of energy balance in the supermarket's zone 1 for two times: one in winter at 6 pm, and the second one in summer at 6 pm too. The winter graph shows almost perfect balance between total heat gains and losses. It means that air parameters were kept steady. Ventilation is the biggest heat source, while structure (heat transfer through envelope) is the biggest heat sink. The summer graph shows cooling tendency, which was caused by active dehumidification process – total heat losses exceed gains. The biggest contributor to heat gains is artificial lighting. Structure gives very little heat loss and RDCs together with mixing air with zone 2 provide highest heat sink.

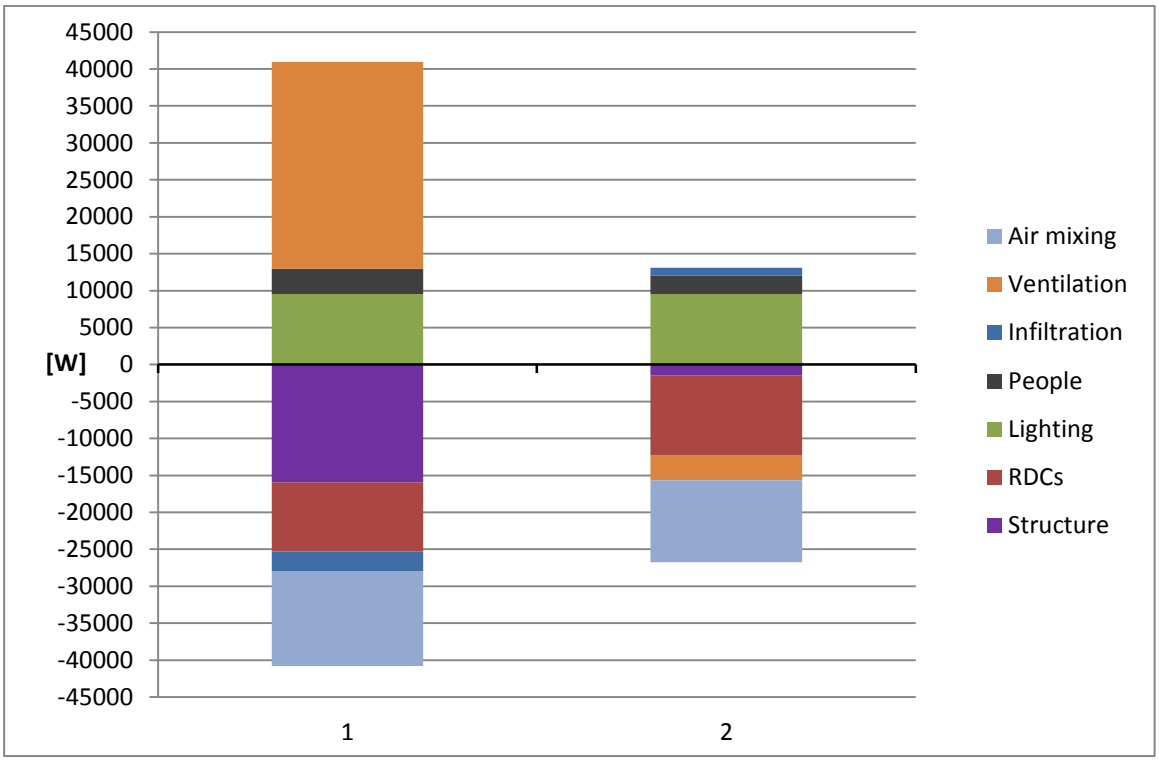

Figure 36. Components of total heat balance in zone 1 on day 36 at 6 pm (time of year = 882 h) (1) and day 184 at 6 pm (time of year = 4434 h) (2).

Figure 37 presents components of moisture balance in zone 1 for the same times as above. The winter graph (left column) shows no active dehumidification. People are responsible for the only and biggest moisture gain, while ventilation and infiltration are the biggest moisture sink. Moisture sink from RDCs and air mixing between zones is negligible. A good balance is kept meaning equilibrium in supermarket's humidity ratio. In the summer graph there is a significant moisture sink caused by active dehumidification. Again people contribute the most to moisture gains but this time ventilation with infiltration provide moisture gain too. RDCs' moisture sink is bigger than in winter, because of higher temperature and humidity ratio in the supermarket, but still negligible.

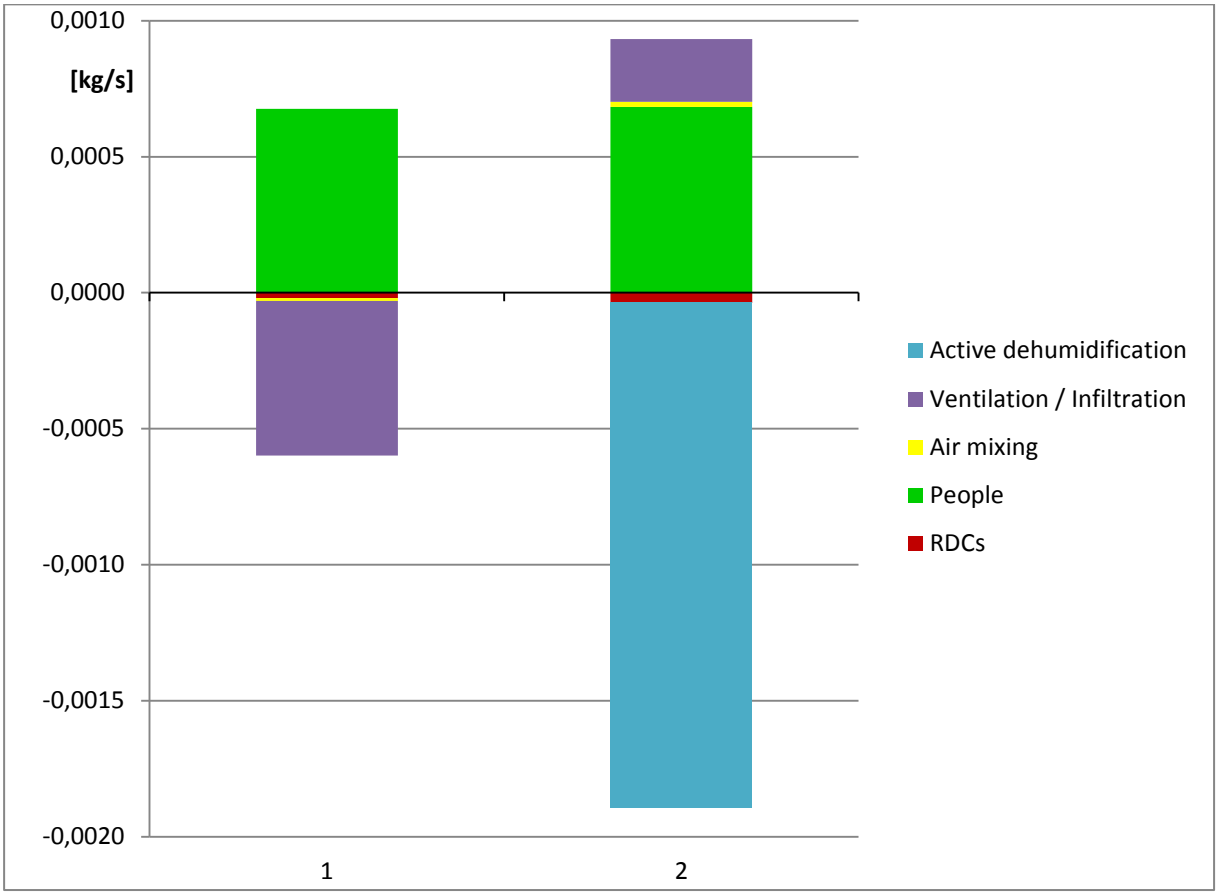

Figure 37. Components of moisture balance in zone 1 on day 36 at 6 pm (time of year = 882 h) (1) and day 184 at 6 pm (time of year = 4434 h) (2).

6. Model testing

In the previous section results from the simulation were compared to monitored data from the real supermarket, which is called *empirical validation*. ASHRAE [7] points out that a good agreement between simulated and real performance may to some extent result from errors offsetting. To eliminate such possibility, a further verification of the applied model is presented in this chapter. At first the model is limited to a very simple one and tested with a given periodic outside temperature profile. Then its complexity will be gradually increased.

The first test checks the thermal performance of supermarket's envelope. Only external walls, roof, windows and thermal mass of the supermarket participate in heat transfer. There is no solar radiation affecting the building, and humidity is not considered. Outside temperature, changing periodically with frequency of 24 hours, amplitude 7 °C and mean value 23 °C, is the only factor influencing inside environment. Floor heat transfer is excluded from the test, because it would provide continuous heat loss for these parameters of outside air (see 3.1.3). Moreover, compared to the final model presented in section 5.4, ventilation, infiltration, people, RDCs and lighting is not considered here. Ventilation provides only mixing of air between zones.

Figure 38 presents results of the test number 1. Initially temperature of air in the supermarket, envelope and thermal mass was uniform and equal 16 °C. Then it gradually rises and asymptotically reaches a periodic steady state with mean value the same as mean value of outside temperature. It proves that equilibrium appears in the model and there are no unexpected heat gains or losses. The phase shift between outside and inside air temperature is 3 hours 48 minutes. Inside air temperature amplitude is 0,27 °C in the periodic steady state and it is significantly lower than outside amplitude because of thermal capacity of the building.

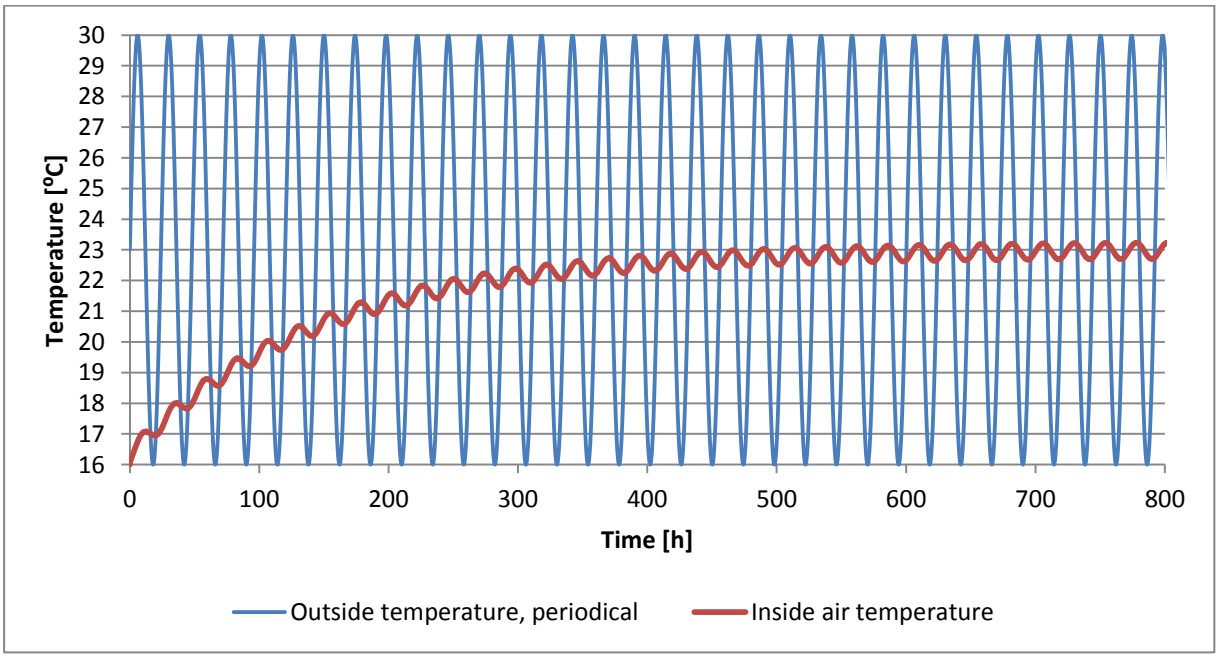

Figure 38. Test number 1.

In the next test (number 2) floor heat transfer is added. Figure 39 shows the results. Profile of inside air temperature is still periodical, however it approaches stable fluctuations faster and then its mean value equals only about 17,5 °C. This is due to continuous heat loss caused by exchanging heat with

ground. Moreover amplitude of inside air temperature is lower and equals 0,17 °C. Reason for that is additional thermal capacity of the floor.

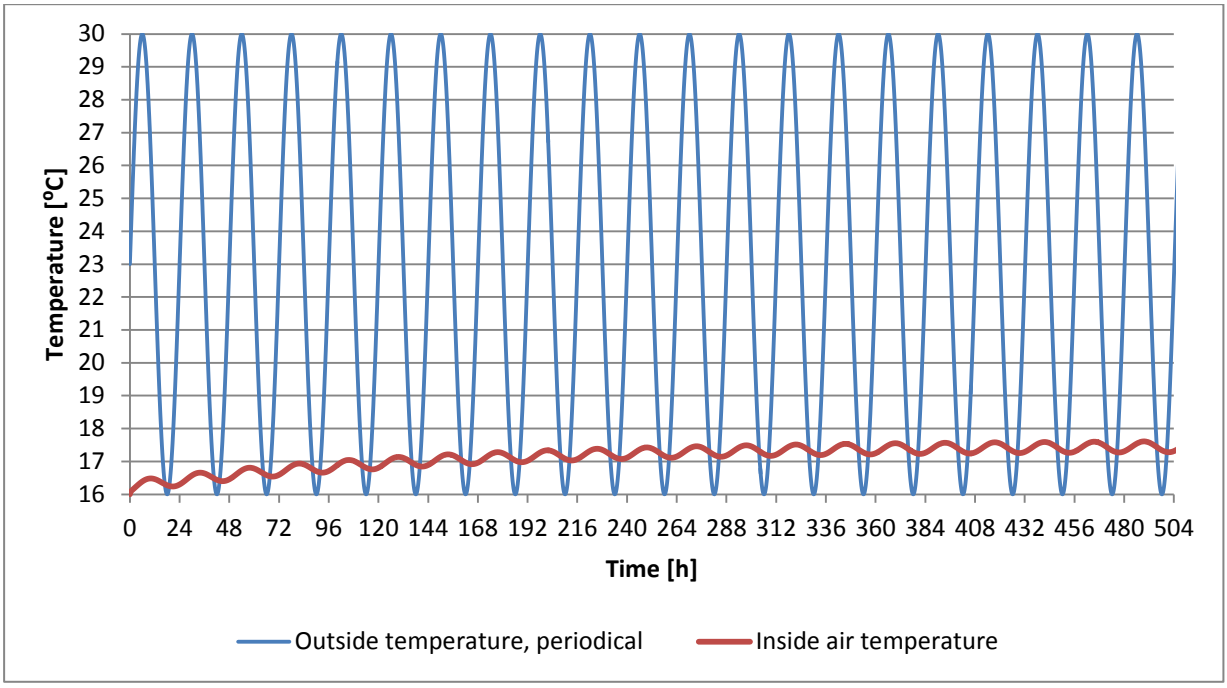

Figure 39. Test number 2 – floor heat transfer is considered.

In the test number 3 artificial lighting heat gain is added to the model. This heat gain is sensible in nature and so significant that inside air temperature, after stabilization (reaching equilibrium), has maximum of 30,1 °C which is above maximum outside temperature (fig. 40). The amplitude is the same as in the previous test.

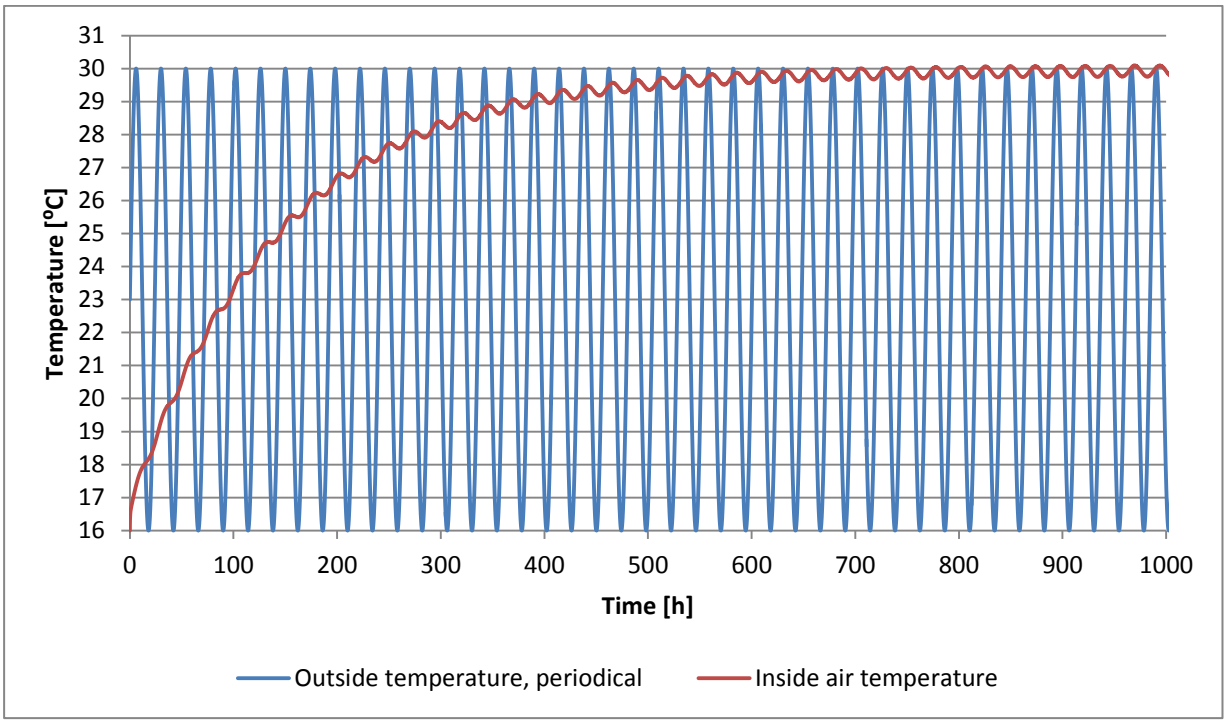

Figure 40. Test number 3 – artificial lighting heat gain is considered.

Test number 4 introduces internal sensible heat gain/sink which comes from machinery room. As described in chapter 4 temperature in machinery room equals 25 °C unless outside temperature is higher. Then such temperature is in the machinery room too. Therefore machinery room may provide heat loss if temperature of inside air exceeds 25 °C and outside temperature is lower than inside. Figure 41 shows that inside air temperature after stabilization is lower than in test 3, which is a proof for heat loss. The difference between temperatures simulated in zone 1 and 2 equals at most 0,07 °C and therefore one uniform temperature is still presented in the figure.

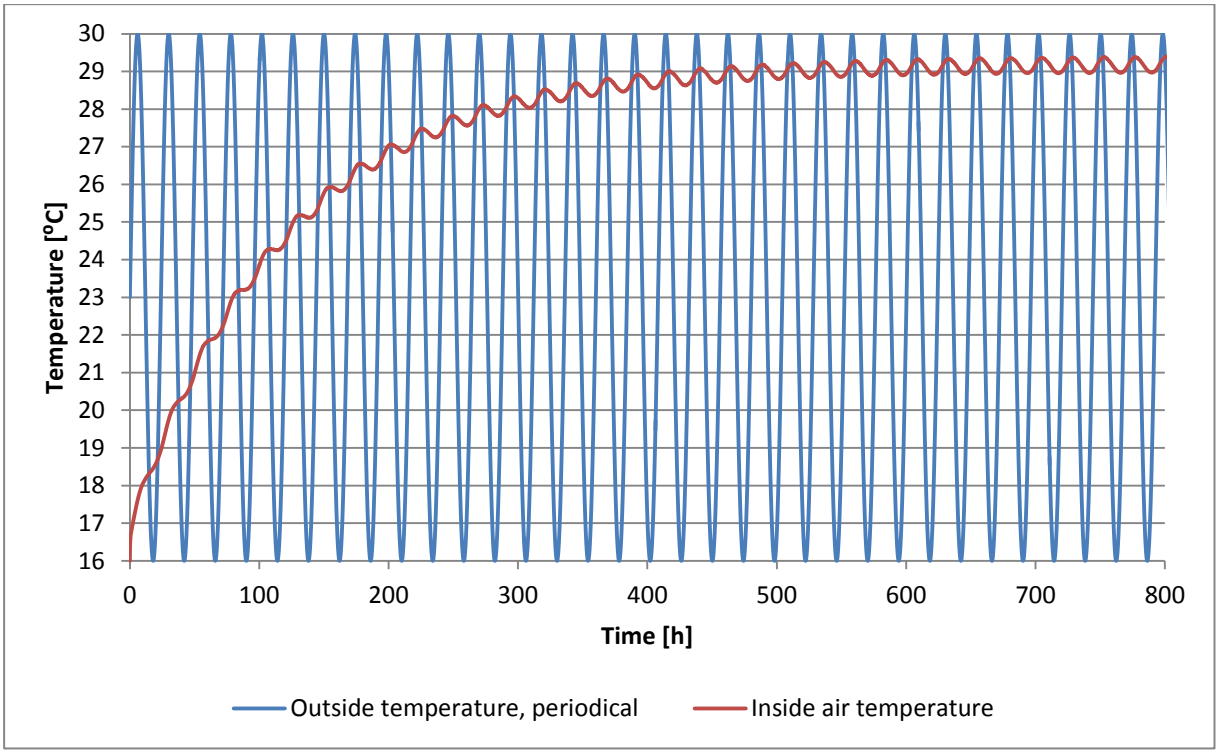

Figure 41. Test number 4 – machinery room heat gain/loss is considered.

Test from 1 to 4 showed thermal behaviour of the supermarket, but did not consider moisture balancing. Next tests are carried out with periodically changing outside humidity ratio – its frequency is 24 hours, amplitude 0,0028 kg/kg and mean value 0,0092 kg/kg, which corresponds to temperature 21 °C and relative humidity 60%. Conditions of supermarket's air start with x=0,0064 kg/kg. In test number 5 (figure 42) only basic ventilation algorithm is applied. It means that constant amount of fresh air is supplied and mixing of air between zones occurs. Graphs for two streams of fresh air are presented. Neither of them reaches amplitude of outside air humidity ratio, because the number of air exchanges they provide is lower than 1 exchange per hour. Both reach periodic steady state with mean value equal to that of outside air.

Test number 6 includes RDCs moisture sink. An assumption is that temperature of air in the supermarket is constant and equals 21 °C. Amount of fresh air supplied is 540 m^3/h. The reader can see in figure 43 that the mean value of inside humidity ratio after stabilization is 0,00894 kg/kg - lower than in test 5. This is due to moisture sink of RDCs.

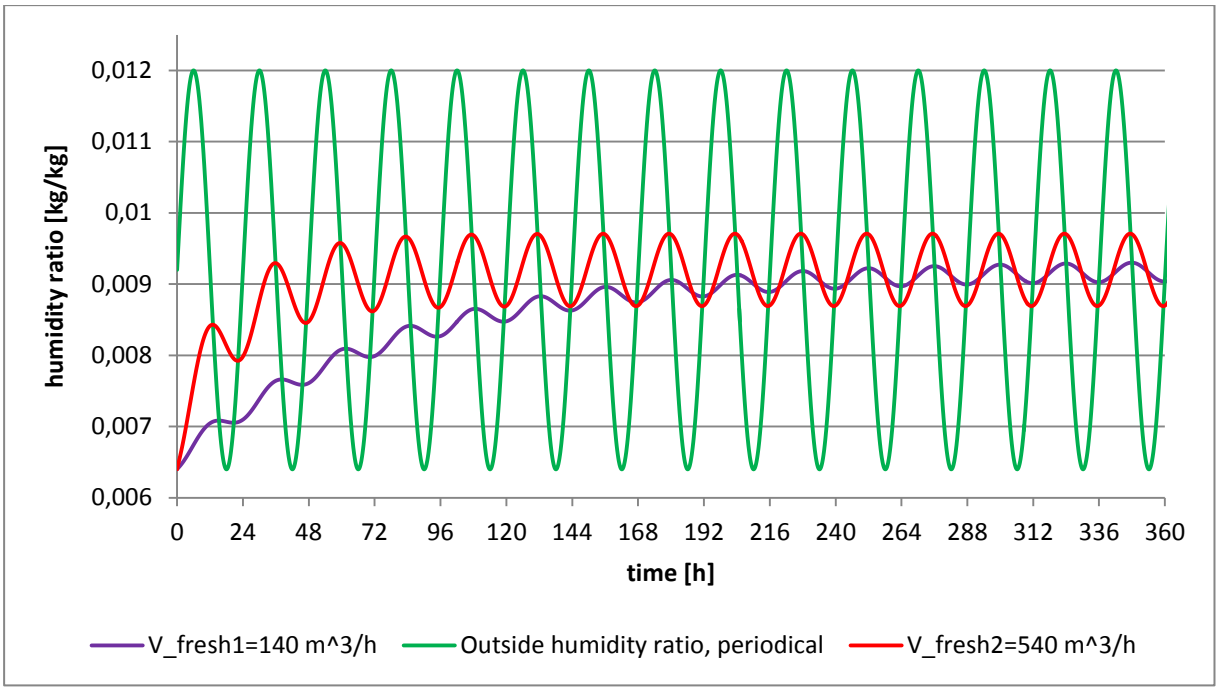

Figure 42. Test number 5 – moisture test.

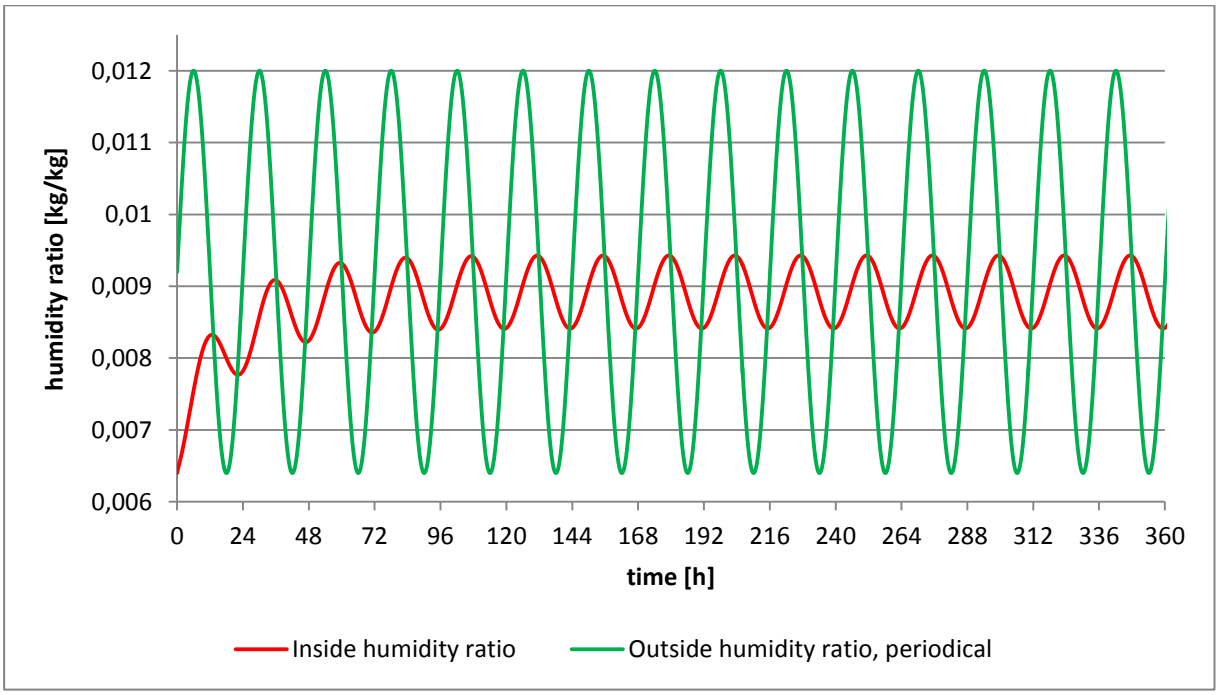

Figure 43. Test number 6 – RDCs' moisture loss is considered.

Further tests could introduce the rest of considered moisture phenomena, but the results are rather predictable. As shown in figure 37, people provide a very significant moisture gain dependent on number of people staying in the supermarket. It would increase inside humidity ratio and perhaps lead to some irregularity if number of people were changing. Infiltration rate is closely connected to the number of people and it may lead both to humidifying or dehumidifying of inside air – depending on outside humidity ratio.

7. Conclusions and discussion

A way of energy balancing in a general supermarket was presented in the report. Total heat (1) and moisture (2) balancing equations were presented and led to essential results: temperature and humidity ratio in the supermarket. The model assumed uniform conditions in each zone, so called lump. Heat and moisture balance components were developed to the complexity level corresponding to real results, however there was a lot of simplifications. Other methods for energy calculations may of course be used, e.g. for heat transfer through building envelope calculations, however one should consider if such methods bring significant improvement in results accuracy and do not complicate the calculations too much.

The most important factor influencing inside climate turns out to be ventilation with its mechanisms of humidity control. Created and introduced algorithms of decreasing inside humidity (supplying fresh air, increasing inside temperature and mechanical dehumidification) allowed to simulate temperature in the supermarket well. The simulated temperature reached values very similar to those of real temperature, however the change in temperature after night mode and after day mode was usually more steep. A reason for that may be the simplification of perfectly mixed air in each lump. It omits the phenomenon of air mass movement due to density difference, which may be significant in such high building and could stabilize temperature.

The program reached worse accuracy in humidity modelling, particularly absolute humidity. Although long-term levels of humidity value reflected real performance, the hourly values were rather inaccurate. This might be due to considering insufficient number of factors influencing humidity. People are responsible for big moisture gains, therefore a more detailed analysis of customers and staff behavior could improve accuracy of results. Moreover considering mechanical devices different than RDCs, e.g. dishwasher, impacting moisture conditions, might improve results. Unfortunately during work on the program schedule of their work was not known. Applied humidity control mechanisms performed well and led to significant improvement of results compared to initial model (5.1), however at one point all of them failed to decrease humidity in the supermarket (fig. 35), which shows that some improvement is desired – a comparison with real algorithms would be helpful.

In the report heat and moisture sinks of refrigerated display cabinets (RDCs) were determined very precisely. They depend on ambient air's temperature and humidity ratio. As it turns out moisture sink of new-generation doored RDCs, as installed in the supermarket, is negligibly small compared to people's and ventilation & infiltration moisture sinks or gains. As presented in figure 34, it rises when humidity ratio inside the supermarket grows, however probably simplified methods of determining this moisture sink would be sufficient. Such complex way of determining moisture sink would more appropriate for open RDCs, which condense about 8 times more moisture from ambient air [18].

Division into two zones is enough for general simulation of conditions in the supermarket. In fact it would not be possible to compare with reality a model divided into more zones, because of lack of sensors in the considered supermarket. However, further improvement of energy calculations accuracy through adding other zones is possible. A suggestion is to distinguish:

- tills, where people wait in queues and mechanical devices generate heat
- bakery, where heat and moisture is generated in order to serve hot meals

- warehouse, where increased infiltration is possible, because of unloading goods.

During nights and on holidays simulated humidity ratio drops excessively. Reasons for that may be: supplying dry outside air, assumed constant infiltration rate of RDCs and no spot spraying humidifiers implemented into the program. The last thing is worth implementing into the program.

The computer model was created in MatLab Simulink. This program allowed to enter energy and mass relations considering division into zones and multiple feedbacks quite easily. Structure of the program consists of subsystems, each reflecting one process, for instance structure heat transfer. Interestingly the assumed amount of air mixed between zones (equal half of whole ventilation air stream) led humidity ratios in both zones to become uniform with some very small exceptions. This means that only one subsystem calculating moisture balance, instead of two (one for each zone), should be enough for accurate results.

8. References

1. Arias, J. (2005). *Energy Usage in Supermarkets – Modelling and Field Measurements [On-line Version].* Stockholm: KTH. Available at: <http://kth.diva-portal.org/smash/record.jsf?pid=diva2%3A7929&dswid=9594>
2. ASHRAE Handbook – Heating, Ventilating and Air-Conditioning Applications. (2007). *Chapter 2: Retail Facilities*.
3. ASHRAE Handbook Fundamentals. (2013). *Chapter 14: Climatic Design Information.*
4. ASHRAE Handbook Fundamentals. (2013). *Chapter 15: Fenestration.*
5. ASHRAE Handbook Fundamentals. (2013). *Chapter 16: Ventilation and Infiltration.* Eq. (51).
6. ASHRAE Handbook Fundamentals. (2013). *Chapter 18: Nonresidential cooling and heating load calculations.*
7. ASHRAE Handbook Fundamentals. (2013). *Chapter 19: Energy Estimating and Modeling Methods*.
8. ASHRAE Handbook Refrigeration. (2014). *Retail Food Store Refrigeration and Equipment.*
9. Banaszek J., J. Bzowski, R. Domański, J. Sado. (2007). *Termodynamika. Przykłady i zadania.* Warszawa: OWPW. ISBN 978-83-7207-666-3
10. Bohdal T., H. Charun, M. Czapp. (2003). *Urządzenia chłodnicze sprężarkowe parowe.* Warszawa: WNT. ISBN 83-204-2845-9
11. Butrymowicz D., K. Gutkowski, (2012). *Chłodnictwo i klimatyzacja.* Warszawa: WNT.
12. Byung-Lip A., J. Cheol-Yong, L. Seung-Bok, Y. Seunghwan, J. Hakgeun. (2013). *Effect of LED lighting on the cooling and heating loads in office buidlings.* Applied Energy 113 (2014), pp. 1484-1489.
13. Bzowska, D. (2007). *Dynamika procesów wymiany ciepła i naturalnej wymiany powietrza w budynkach o różnej strukturze materiałowej przegród.* Warszawa: IPPT PAN. ISBN 978-83-89687-15-9
14. Chwieduk, D. (2006). *Modelowanie i analiza pozyskiwania oraz konwersji termicznej energii promieniowania słonecznego w budynku*. Warszawa: IPPT PAN.
15. Dong, B., M. Gorbounov, S. Yuan, T. Wu, A. Srivastav, T. Bailey, Z. O'Neill. (2013). *Integrated energy performance modelling for a retail store building.* Building Simulation 6 (2013), pp. 283-295.
16. Evans, J. (2014). *Are doors on fridges the best environmental solution for the retail sector?* London: The Institute of Refrigeration.
17. Faramarzi, R. (1999). *Efficient Display Case Refrigeration.* ASHRAE Journal (1999), November, pp. 46.
18. Faramarzi, R.T., B. Coburn, R. Sarhadian. (2002). *Performance and energy impact of installing glass doors on an open vertical deli / dairy display case.* ASHRAE Transactions 108, pp. 673.
19. Goulding, C., R. Kumar, D. Audette. (2011). *LED Building Lighting Drives Supermarket EPAct Tax Deductions.* Corporate Business Taxation Monthly, July.
20. Hagentoft, Carl-Eric, (2005). *Introduction to building physics.* Lund: Studienlitteratur. ISBN 91-44-01896-7
21. Hendiger J., P. Ziętek, M. Chludzińska. (2014). *Wentylacja i Klimatyzacja. Materiały pomocnicze do projektowania.* Warszawa. ISBN 978-83-934024-0-3
22. https://pl.wikipedia.org/wiki/Hanower. Access: 06.05.2016 10:55
23. https://weatherspark.com/averages/28636/Hanover-Niedersachsen-Germany. Access: 06.05.2016 10:57

24. Hussmann Corporation. (2012). *Door Anti-Sweat Heater Control.*
25. Kosar, D. (2005). *Humidity effects on Supermarket Refrigerated Case Energy Performance: A Database Review.* ASHRAE Transactions 111, pp. 1051.
26. Law, J. (2016) . *A Dictionary of Business and Management.* Oxford University Press. ISBN 978-0-1996-8498-4
27. Modest, F. M. (2003). *Radiative heat transfer – appendix B.* Elsevier. Pp. 745-758
28. PN-83/B-03430; Az3:2000
29. *PN-EN ISO 6946:1999*
30. REWE Wettbergen technical documentation
31. Tassou, S. A., Y. Ge, A. Hadawey, D. Marriott. (2011). *Energy consumption and conservation in food retailing.* Applied thermal Engineering vol. 31 (Issues 2-3) 147-156.
32. Tetens, O. (1930). *Über einige meteorilogische Begriffe.* Zeitschrift für Geophysik, Vol 6:297.

Appendix A – Humid Air

In the project different physical equations describing humid air are used. They describe: absolute humidity, relative humidity and enthalpy. However, first the saturation pressure of humid air must be determined. It is a function of temperature only and it is well approximated by empirical equations [32]. The saturation pressure over water ($t \geq 0$℃) is given by equation:

$$p_s = 610{,}78 \cdot exp\left(\frac{t}{t+238{,}3} \cdot 17{,}2694\right)\ [Pa] \qquad \text{(A1)}$$

where *t* is the temperature in degrees Celsius.

The vapour saturation pressure over ice ($t < 0$℃) can be calculated according to formula:

$$p_s = \exp\left(\frac{-6140{,}4}{273+t} + 28{,}916\right)\ [Pa] \qquad \text{(A2)}$$

Humidity ratio (moisture content), which is the ratio of vapour mass to dry air mass, is calculated as follows [11]:

$$x = 0{,}62198\frac{\varphi \cdot p_s}{p - \rho \cdot p_s}\ \left[\frac{kg}{kg}\right] \qquad \text{(A3)}$$

where: φ – relative humidity [-],
p = 101325 Pa – total air pressure.

Converting above equation, relative humidity is obtained:

$$\varphi = \frac{x \cdot p}{p_s(0{,}62198+x)} \qquad \text{(A4)}$$

Specific enthalpy of humid air (without condensation) is a function of both temperature (in degrees Celsius) and humidity ratio [9]:

$$h = 1{,}005t + 2501{,}6x + 1{,}86xt\ \left[\frac{kJ}{kg}\right] \qquad \text{(A5)}$$